Fast Qualification Methods for Microelectronic Packages

Proefschrift

ter verkrijging van de graad van doctor
aan de Technische Universiteit Delft
op gezag van de Rector Magnificus Prof. ir. K.C.A.M. Luyben
voorzitter van het College voor Promoties,
in het openbaar te verdedigen op 10 oktober 2011 om 12:30 uur
door

Xiaosong MA

Master of Science in Engineering at Shanghai University for Science and Technology

Geboren de Qiqihaer, Heilongjiang, China

Dit proefschrift is goedgekeurd door de promotor:
Prof. dr. ir. G.Q. Zhang

Copromotor: Dr. ir. K.M.B. Jansen

Samenstelling Promotiecommissie:

Rector Magnificus, voorzitter
Prof. dr. ir. G.Q. Zhang, Technische Universiteit Delft, promotor
Dr. ir. K.M.B. Jansen, Technische Universiteit Delft, copromotor
Prof. dr. J. Li, Chinese Academy of Science, China
Prof. dr. J.G. Korvink, University of Freiburg, Germany
Prof. dr. C.I.M. Beenakker, Technische Universiteit Delft
Dr. H. Fremont, University Bordeaux, France
Dr. ir. Olaf Van der Sluis, Philips
Prof. dr. P.M. Sarro, Technische Universiteit Delft, (Reserve)

ISBN 978-94-91104-00-8

Cover by Xiaosong MA
Printed by PrintPartners Ipskamp, The Netherlands

To my parents
To my wife: Yun Zhang
To my son: Yukun
To my brothers and sisters

Contents

Abbreviations

2D	Two Dimensions
3D	Three Dimensions
BIM	Bismaleimide
CME	Coefficient of Moisture induced Expansion
CTE	Coefficient of Thermal Expansion
DCB	Double Cantilever Beam
DMA	Dynamic Mechanical Analysis
ELS	End-Loaded Split
EMC	Epoxy Moulding Compound
ENF	End Notched Flexure
FE	Finite Element
FEM	Finite Element Method
HAST	Highly Accelerated temperature and humidity Stress Test
IC	Integrated Circuit
MSLA	Moisture Sensitivity Level Analysis
PCB	Printed Circuit Board
RH	Relative Humidity
QFN	Quad Flat package No lead
SiP	System in Package
TGA	Thermal Gravimetric Analyzer
TMA	Thermal Mechanical Analyzer

Chapter 1

Introduction

1.1 State of the art of reliability qualification

Electronic devices have increasing become an integral part of countless products in the industrial, consumers and even military market. Hence, the failure of these devices in critical application, such as aviation and automotive applications may have detrimental consequence in term of safety or productivity. These failures are mainly related to reliability of electronic packaging. The electronic packaging is a technology that houses the silicon chip in an electronic device so as to provide the necessary protection of the chip from the environment and to ensure their proper functioning of the electronic device. Hence, the reliability of the electronic packaging is critical for the adoption of these products in these engineering applications.

Electronic packages in the industry can be classified under two main types of electronic packages. They are the hermetic packaging type where no moisture can penetrate into the package and the non-hermetic package where moisture can diffuse into the package. Non-hermetic packages are the mostly wide used packaging type in the industry due to their lower price whereas hermetic packages, such as ceramic packages, are mainly used in high reliability and military applications.

The packaging materials for non-hermetic packages are usually epoxy with high content of silica filler. Since these materials are sceptical to moisture absorption, moisture induced failure, such as pop-corn cracking and interface delamination, are common failure phenomena during the reflow soldering process. One of the failure modes, popcorn cracking, is dependent on the moisture concentration in the interface of the package since the increase in moisture concentration at the interface will not only reduce the adhesion strength of the packages, it will also increase the hygro-thermal stress. Therefore, it is necessary to evaluate and predict their moisture diffusion behaviour, and moisture effects on the packaging material properties and packages. In conclusion, the overall reliability of these electronic devices will not only tie to their thermal reliability as in the case of the ceramic packages, it is now also highly sceptical to their moisture induced failure.

To ensure the reliability of any new commercial package, qualification test is needed to be performed as outlined by the industrial standards. An example of such a test is the moisture sensitivity level analysis (MSLA) test outlined by JEDEC industry standard. This test has established the exposure condition of temperature, humidity and duration for which the moisture sensitivity rating are classified. Moisture sensitivity level is often used to identify the floor life of non-hermetic microelectronic packages so that they can be properly packed, stored and handled to avoid damage during solder reflow process. However, the duration of this test procedure is very long. For example, a Level 3 moisture sensitivity test requires 192 hours of moisture pre-conditioning in 30^{o}C/60%RH chamber. Hence, there is a strong drive to reduce this test duration due to the highly dynamics and competitive nature of the electronic packaging industry. Although attempts have been made by some researchers [Fan, 2010, Zhang, 2006] but these remain unsatisfactory.

Accordingly, the main objective of this research is to develop knowledge based fast qualification method that is suitable for the electronic packaging industry. This includes fast moisture sensitivity level qualification test and fast thermal cycling test. The methodology for moisture sensitivity levels outline in the JECDEC standard are divided into two main stages

- The first stage is to perform package moisture diffusion at certain temperature and relative humidity conditions.
- The second stage to subject the packages to solder reflow process.

We will focus only on the first stage in this research due to its long duration requirement for moisture diffusion. For example, in a design cycle for level 2 moisture sensitivity test, package may require a few iterations of 168 hours of exposure to 85ºC/60%RH and solder reflow process before they could finalised the design of the product. Furthermore, in order to ensure the applicability and accuracy of the developed fast qualification test, an in-depth understanding of the package failure will be established in this research. This includes the relationship between moisture weight gain and the pre-conditioning duration for hygro-thermal reliability; and between the interfacial properties and delamination for thermal reliability. With these information, knowledge based fast qualification methodology can be developed and implemented to shorten the design cycle.

Reliability qualifications

Since reliability of the packages is critical for the adoption of these devices for their applications, several reliability qualification methods have already been developed in semiconductor industry to ensure the safety of these devices. Some of the examples included the Moisture/Reflow Sensitivity Classification for Non hermetic Solid State Surface Mount Devices [J-STD-020D, 2007] and the Thermal (Temperature) Cycling test [JESD22-A104C, 2005]. Although there is a large number of test in the literature, all qualification methods can be classify under two main categories and the most representative test of each categories will be discussed in the next section. Furthermore, the limitation of these tests will be addressed.

Moisture related reliability qualifications

Five moisture related reliability qualification tests have been developed for various loading conditions which includes different temperature range, relative humidity and electrical current (bias or unbiased). These qualification methods are summarised below:

Eight classified moisture sensitivity levels with different pre-defined conditions for each moisture sensitivity levels (MSL) are outlined in the standard. “Moisture/Reflow Sensitivity Classification for Non hermetic Solid State Surface Mount Devices” and it is applicable to all package thicknesses from that are below 1.5mm and above 2.5mm. Furthermore, due to the need to shorten the test cycle, acceleration test at the condition of 60ºC/60%RH for certain levels is also included in it. However, the rationale for the applicability of using the same moisture diffusion time for different packages thicknesses is not explained although diffusion is dependent on the thickness of the packages.

The Highly-Accelerated Temperature and Humidity Stress Test HAST [JESD22-A110-B] is another commonly used moisture related fast reliability qualification method. In this test, the sample is continuously subjected to a combination of severe conditions such as temperature, humidity and bias in order to accelerate moisture induced failure. The conditions are as follow:

- temperature range from 110 to 130ºC
- relative humidity around 85%RH
- vapour pressure 122 to 230kPa

The HAST test is supposed to be equivalent to pre-conditioning of at least 1000 hours at 85ºC/85%RH for package that reaches moisture equilibrium in less than 24 hours. However, it is known that moisture may lower the glass transition temperature (T_g) of the moulding compound and this may lead to failure mechanism that is not related to standard 85ºC/85%RH test to be tested instead. Therefore, this HAST test method is not considered in the research.

The Accelerated Moisture Resistance Unbiased Autoclave [JESD22-A102D] is another commonly used reliability test to evaluate packages moisture resistance and their robustness. In this test, samples are subjected to a condensing, high humidity and pressure to detect packages' weaknesses such as delamination and metallization corrosion. This is also a highly accelerated test since the packages is subjected to high pressure, humidity and temperature. Furthermore, the condensing humidity condition will hugely accelerate the moisture penetration through the external protective material or along the interface between the external protective material and conductor. The exact conditions of this test are as follows:

- Temperature of 120ºC
- Relative humidity 100%RH
- Vapour pressure 205kPa.

Due to the severity of the accelerated condition, unrealistic failure mechanisms may be induced. For example, most semiconductor components are not rated for field application conditions exceeding 95%RH. This even includes scenarios with condensing moisture such as rain or fog. The combination of high humidity, high temperature ($>T_g$) and high pressure may produce unrealistic material failures because the absorbed moisture typically decreases the glass transition temperature of polymeric materials. Therefore, this method is also not suitable as acceleration method in this research.

The Accelerated Moisture Resistance Unbiased HAST [JESD22-A118] or HAST is performed to evaluate the reliability of non-hermetic packages in humid environments. This test is similar to the Accelerated Moisture Resistance Unbiased Autoclave test but under non-moisture condensing conditions. Furthermore, electrical bias is not applied in this test to ensure that the failure mechanism is not overshadowed by bias. The conditions are as follow:

- Temperature from 110 to 130ºC

- Relative humidity around 85%RH
- Vapour pressure 122 to 230kPa

Different failure mechanisms can again be expected due to the high temperature and hence, this method is also not considered further in this research.

The Steady State Temperature Humidity Bias Life Test [JESD22-A101C] is the fifth moisture related test. This test is similar to Accelerated Moisture Resistance Unbiased HAST with the exception of 85ºC and vapour pressure of 49.1kPa. Moisture pre-conditioning duration of 1000 hours is used in this test.

In summary, it can be noted from the above discussion that unrealistic failure can be induced at temperature above T_g (typically about 100ºC) and at high vapour pressure. Hence, J-STD-020D has been chosen as our benchmark. Since most humidity testing equipments is equipped to perform 85ºC/85%RH condition, 85ºC/85% RH condition has be selected as the acceleration condition for fast MSL qualification. The rationale of using only one condition as the mean of acceleration is for further reduction of the time and effect needed to perform this test. Since only one condition is needed, only ovens with one condition are needed. This will reduce the number of ovens needed for the qualification test. Since all the test can be perform concurrently instead of waiting for each time with different MSL to conclusion, further reduction of time can be achieved. As with the other qualification test, this qualification is to be used only for non-hermetic electronic packages.

Thermal cycling related reliability qualification

Apart from moisture related reliability qualification test, thermal cycling is another important reliability qualification test to evaluate the thermal reliability of these packages. There are three main reliability qualification methods that are related to temperature cycling. They are Temperature Cycling [JESD22-A104C, 2005], Power and Temperature Cycling [JESD22-A105C, 2004] and Cycled Temperature Humidity Bias Life Test [JESD22-A100C, 2007]. These three temperature cycling tests are summarised below:

Temperature Cycling (thermal cycling) is conducted to determine the ability of components and solder interconnects to withstand mechanical stresses induced by cycling between high and low temperature extremes. In addition, permanent changes in electrical and/or physical characteristics can result from these mechanical stresses and this could have detrimental effect on their functionality. Temperature extremes, ramping speed and holding time are three important variables to be considered in s temperature cycling test. Since it is known that the temperature ramping speed and holding time are not critical for most component tests, the temperature cycling extremes should be the only parameters considers for further study in this research.

The second temperature cycling reliability qualification method is the Power and Temperature Cycling. This test is performed to determine the ability of a device to withstand alternate exposures at high and low temperature extremes while periodically switching the electric biases to a on and off state. The temperature extremes are usually from -40 to 85ºC or -40 to125ºC with a ramp time of 20 to 30 min between the temperature extremes. Furthermore, the dwell time at each temperature extreme has to be at least 10 mins. A device is defined to have failed if parametric limits are exceeded or if functionality cannot be demonstrated under nominal and the worst case specified conditions. This is similar to temperature cycling but with the main difference of applied biased in this test.

The third reliability test is Cycled Temperature Humidity Bias Life Test. This test is performed to evaluate the reliability of non-hermetic, packaged solid state devices in humidity environments where surface condensation is likely to occur. It employs conditions of bias, temperature cycling and high humidity that will cause condensation on the device surface. It is useful to determine the device surface susceptibility to corrosion and dendritic growth. One of the main disadvantages of this test is that it requires a temperature-humidity test chamber capable of maintaining a specified temperature and relative humidity profile, while providing electrical connections to the devices under test in a specified biasing configuration. The temperature range normally used in this test is from 30 to 65ºC and relative humidity is around 90 to 98%RH.

From the above three thermal cycling methods, it can be seen that the cycled temperature humidity tests is a good candidate for fast delamination prediction but the stability of a wide temperature range is difficult to maintain in the presence of high humidity. Furthermore, due to the difficulty in characterize moisture related properties above 100ºC, it will limit the use of simulation, which is a powerful tools, to investigate their reliability. Therefore, the Thermal (Temperature) cycling test is chosen instead for our research for fast qualification and delamination prediction.

The research carrier chosen for this project is a quad flat no lead (QFN) package as shown in Fig. 1.1(a) and with its structure schematically shown in Fig. 1.1(b). The QFN package consists of an active die and a passive die interconnected by small bumps using flip chip technology. In order to enhance their thermal reliability, underfill and die attach, which is a silver particle filled glue dispensed between active die and copper die pad for better thermal interface, is often used. The passive die is then connected to lead frame using solder balls for electric signal transfer. All these components are encapsulated in the epoxy mould compound (EMC).

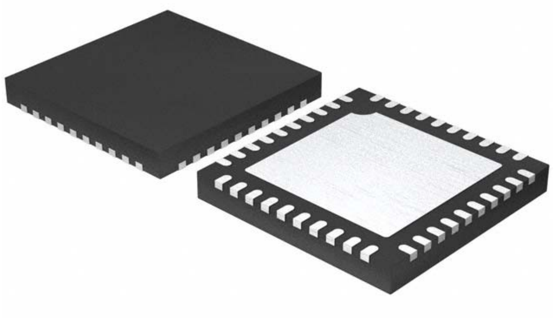

Fig. 1.1(a) QFN package

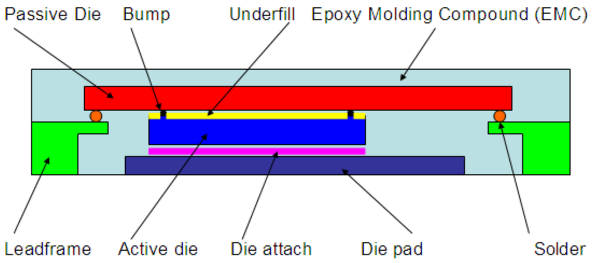

Fig. 1.1(b) Cross section of QFN

As mentioned in the earlier section, 85°C/85%RH was used as the accelerated test condition. Furthermore, since our carrier known to failure by delamination between copper die pad and die attach when it is subjected to thermal cycling condition, another main goal in this research is to find a fast method to predict this delamination.

1.2 Goal and approach

Goal of the research

Accordingly, the goal of this research is to develop knowledge based fast reliability qualification method that ensures similar failure modes to that occur during the operating condition. Moisture sensitivity levels analysis and thermal cycling are chosen as the methods for fast qualification. Last but not least, the relationship between package design and reliability qualification will be addressed in this research.

Approach

The approach for this research is as follows:

1. Setup a framework for knowledge based fast qualification method.
2. Obtain the essential knowledge from both experimental and simulation.

3. Perform fast qualifications and validate with experiments.

In order to accelerate moisture diffusion, a higher test temperature will be employed in this research. However, the accelerated temperature is limited to temperature below the glass transition temperatures of the packaging materials to ensure the correct failure mode in sample. Hence, using this criterion, a means temperature below 90-102ºC is employed in this research. Furthermore, since moisture diffusion rate also is known to be accelerated at higher temperature and higher relative humidity, 85ºC/85%RH is used in this research to accelerate the test.

In order to validate the assumption of equal moisture weight gain between industrial standard and the accelerated test, moisture diffusion analysis, which requires moisture diffusion properties at different conditions, is performed. Since characterization of the moisture diffusion properties and the coefficient of moisture induced expansion of the moulding compound, underfill and die attach are extremely time consuming, a new step relative humidity method is developed in this research to speed up the characterization experiments. It has been found that this new method is not only faster, it is also more reliable as compared to that of traditional method.

Lastly, it has been found from the thermal cycling test that the carrier’s failure mode is the delamination at the interface between the copper die pad and the die attach. Since cohesive zone method has been found to be able to simulate this type of delamination, cohesive zone methods will be used to model the transient delamination of our carrier. Hence, in order to achieve this, the cohesive zone property of interface between copper die pad and die attach are characterised in this research.

1.4 Outline of the thesis

Now that the importance and the context of this research has been established, this section will give a outline of the structure of this thesis

Chapter 2 will focuses on the development and implementation of the fast moisture sensitivity qualification that is based on the criterion of equal moisture weight gain prediction between the different pre-conditioning. This chapter is divided into five sections. The chapter starts by briefly introducing the theory of moisture diffusion whereas the second section presents the results from the moisture diffusion tests of EPN1180 with respect to their different contents filler. Furthermore, the relationship between the moisture saturation, moisture diffusion coefficients at different diffusion conditions and different filler content will be established in this chapter. The third section describes the characterization of the properties of EMC, underfill and die attach using the fast moisture diffusion characterization method whereas the fourth section compares the two characterization methods (naming TGA/TMA and DMA) used in this research for characterizing the packaging materials' coefficient of moisture expansion (CME). The last section of this chapter deals with thermal cycling effects on the mechanical properties of packaging materials.

Chapter 3 presents the methodology for characterizing the interface's cohesive properties between the copper die pad and die attach. This includes the four point bending test setup that is equipped with optical camera system. This will be then followed by describing the methodology for measuring the critical delamination loads at different temperatures and the computation methodology for characterizing the cohesive zone interface toughness and critical opening value. These two parameters are then used the Chapter 5 FE delamination model.

Chapter 4 presents the validation of the moisture diffusion and warpage parameters obtained from Chapter 2. The chapter starts by providing validation for the moisture diffusion properties and ends with the comparison of the CME values measured from DMA and TMA/TGA.

Chapter 5 presents the knowledge based fast qualification method using fast moisture sensitivity level analysis and the delamination prediction from delamination FE models. For the fast moisture diffusion, different moisture sensitivity level analyses are performed using different boundary conditions. The calculated fast moisture diffusion and MSL diffusion are first validated with experiment. The implementation of the delamination simulation performed using calculated interface toughness and critical opening value is then presented and comparison of the results from numerical simulation and cross section characterization are also discussed.

Chapter 6 ends with a review of the research being done, their limitations and suggestions for further research.

References

Fan, Xuejun and Suhir, E, Moisture Sensitivity of Plastic Packages of IC Devices, Springer, 2010.

Zhang, G. Q., van Driel, W.D., and Fan, X.J., Mechanics of Microelectronics, Springer, 2006.

IPC/JEDEC STANDARD J-STD-020D Moisture/Reflow Sensitivity Classification for Non hermetic Solid State Surface Mount Devices, 2007

EIA/JEDEC STANDARD JESD22-A110-B Highly-Accelerated Temperature and Humidity Stress Test HAST, 1999

JEDEC STANDARD JESD22-A102D Accelerated Moisture Resistance Unbiased Autoclave, 2008

JEDEC STANDARD JESD22-A118 Accelerated Moisture Resistance Unbiased HAST, 2008

JEDEC STANDARD JESD22-A101C Steady State Temperature Humidity Bias Life Test, 1997

JEDEC STANDARD JESD22-A104C Temperature Cycling, 2005

JEDEC STANDARD JESD22-A105C Power and Temperature Cycling 2004

JEDEC STANDARD JESD22-A100C Cycled Temperature Humidity Bias Life Test 2007

JEDEC STANDARD JESD22-A120A Test Method for the Measurement of Moisture Diffusivity and Water Solubility in Organic Materials Used in Electronic Devices, 2001

Chapter 2

Characterization of Moisture Related Material Properties

2.1 Introduction

Packaging materials, such as epoxy moulding compound [EMC] and underfill are widely used in electronic packaging for their outstanding properties. The mechanical properties of these packaging materials are, however, strongly influenced by various environmental factors. Moisture penetrating into the polymer induces expansion and results in reliability failure, such as stress cracking [Gils, Zhang, et al., 2004, and Tee, et al., 2004], delamination and pop-corning during reflow [Lee, et al., 2005]. Such moisture and temperature induced failure has long been recognized as an important issue for package reliability but there is often a lack of reliable material data. This includes the moisture diffusion mechanism and moisture related material properties.

In this chapter, the moisture related properties of different packaging materials are studied. They are pure Novolac epoxy (EPN1180) with different silica filler concentration, commercial EMC, underfill and die attach. The diffusion coefficients and saturation levels at different conditions were obtained by regressing the diffusion equation with experimental data from three series of humidity steps at different temperatures. This moisture model of EMC is then used to predict moisture uptake of a bi-material sample in Chapter 4 and to perform fast moisture diffusion in Chapter 5. Moisture induced expansion coefficient (CME) is also studied in this research. Currently, CME is determined by correlating thermal mechanical analyzer (TMA) and thermal gravimetric analyzer (TGA) measurements. However, it has been found in this research that these CME values are largely overestimated and a new moisture expansion measurement method that is more accurate and faster is developed here. The CME value measured by this new method is also verified using warpage measurements in Chapter 4.

In order to perform knowledge-based fast moisture sensitivity level qualification, the characterization of packaging materials' moisture related properties need to be fast and efficient too. Therefore, a fast moisture diffusion properties characterization method and a fast CME characterization method are investigated. The moisture related models, such as moisture diffusion coefficient and moisture weight gain, are established. These material models are used to predict temperature dependent moisture diffusion coefficient and temperature/relative humidity dependent moisture saturation level. Using these information, fast moisture diffusion prediction can then be performed. Filler effects on moisture saturation level are studied here. This will enable a quick initial selection for EMC of specific applications.

2.2 Moisture diffusion theory

Moisture diffuse differently in different packaging materials and their behaviour need to be understood before their diffusion parameters can be characterized.

The governing equation for one dimensional diffusion in a polymer sheet of thickness *h* is given by

$$\frac{dC}{dt} = D\frac{d^2C}{dx^2} \tag{2.1}$$

where C is the moisture concentration, D is the moisture diffusion, x is spatial coordinate and t is time. A solution to Eq. 2.1 is given by Crank [Crank, 1975]

$$C = C_0\left[1 - \frac{4}{\pi}\sum_{n=0}^{\infty}\frac{(-1)^n}{2n+1}\cos\frac{(2n+1)\pi x}{h}\exp\{-(2n+1)^2\pi^2 D/h^2\}\right] \tag{2.2}$$

where C_0 is the boundary condition to the polymer sheet. The measurable weight gain can then be computed by integration over the entire thickness.

$$M_t = M_\infty\left[1 - \frac{8}{\pi^2}\sum_{n=0}^{\infty}\frac{1}{(2n+1)^2}\exp\{-(2n+1)^2\pi^2 Dt/h^2\}\right] \tag{2.3}$$

where M_t and M_∞ denote the moisture weight gain after time t and infinite time.

Fig. 2.1 gives an illustration of a moisture diffusion experiment. The weight gain initially increases linearly with respect to time as predicted by Fick's law of diffusion. After the initial fast diffusion rate, the uptake continues to increase but this rate gradually reduces. The moisture diffusion is assumed to be controlled by the concentration gradient in this research.

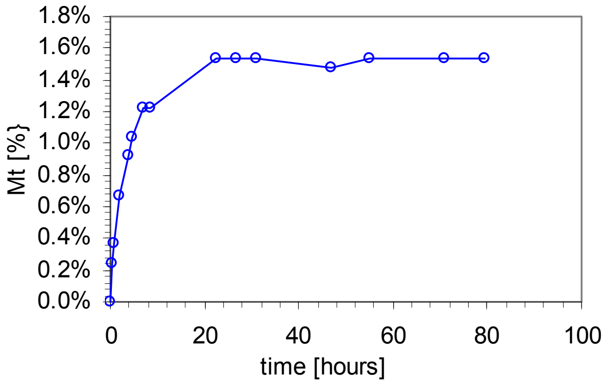

Fig. 2.1 Moisture weight change vs time

The moisture weight gain (increase or change), M_t, is defined as:

$$M_t(wt\%) = \frac{M_t - M_0}{M_0} \times 100\% \tag{2.4}$$

where M_t and M_0 are the weights of the wet sample at exposure time, t, and the dried sample respectively.

In order to get a better fit of moisture absorption process, a Matlab code is written to model the multi steps humidity experiments. For each steps in relative humidity, the well-known solution of the Ficks diffusion equation Eq. (2.3) is used.

M_t can also be computed by superposition of the response of each humidity.

$$M_t(t) = M_1(t - t_1) + M_2(t - t_2) + \cdots \tag{2.5}$$

where t_i is the start of absorption/desorption step i, see Fig. 2.2

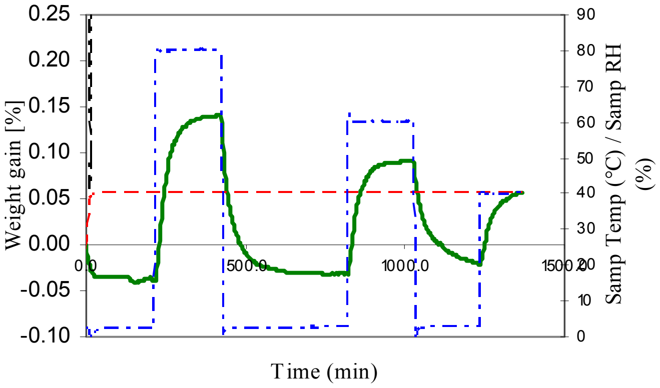

Fig. 2.2 Step-RH moisture weight gain vs time

Eq. 2.5 is based on the assumption that the rates of diffusion are the same in all directions. However, the sample used to determine *D* is of certain dimensions and a correction factor for the effect of diffusion through the edges can be made according to [Crank, 1975]

$$D_c = D\left(1+\frac{h}{L}+\frac{h}{w}\right)^{-2} \tag{2.6}$$

where *L* and *w* are the sample length and width, respectively.

Another important parameter is the M_{sat}, which is the saturated moisture weight gain in the sample, and it is dependent on the temperature and relative humidity. It can be written as [Merdas, et al., 2002]:

$$M_{sat} = M_{sat}^{100} \cdot X_{RH}\ , \tag{2.7}$$

$$M_{sat}^{100} = k_0 \cdot e^{(-H/RT)} \tag{2.8}$$

where M_{sat}^{100} is moisture saturation level for 100% humidity, k_0 is the proportional constant, X_{RH} is the relative humidity factor which varies from 0 to 1, i.e. (representing RH from 0% RH to 100 %RH respectively); *H* is the activation energy constant; *R* is the universal gas constant which is equal to 8.314 $JK^{-1}mol^{-1}$ and *T* is the absolute temperature. M_{sat} can be obtained by performing moisture absorption tests at different temperatures and different relative humidity levels. A linear regression of $\ln(M_{sat})$ against the reciprocal of the absolute temperature (i.e. $1/T$) is used to determine the activation energy. Furthermore, k_0 can also be determined from the interception of the $\ln(M_{sat})$-axis.

Another material property needed for our simulation is the diffusion coefficient (*D*), which is dependent on the temperature as follows [Nogueira, et al., 2001]:

$$D = D_0 \cdot e^{\left(-E_D / RT\right)} \tag{2.9}$$

where D_0 is a constant.

In order to make eq. 2.9 more easier for characterizing D, there is a need to taking natural logarithm of Eq. 2.9 and rewritten it in the following form:

$$\ln D = \ln D_0 - E_D / RT \tag{2.10}$$

The diffusion activation energy E_D can be determined from the slope of the data plot of ln$D$ against $1/T$. lnD_0 can be found at from the interception of the ln$D$-axis (i.e at $1/T = 0$).

2.3 Moisture diffusion experimental

2.3.1 Moisture diffusion in epoxy

Materials and sample preparation

Novolac epoxy EPN1180 samples cured with bisphenol A, is used in this search. Please refer to [Yang, D.G., 2007] for more details.

Experiments

Moisture diffusion tests

The diffusion of moisture into the epoxy is tested using an environmental chamber (Espec corp. SH-661 bench-top type temperature and humidity chamber, see Fig. 2.3) with temperature constancy is ±0.3˚C (-40 to +100˚C) and humidity constancy is ±3%RH. Furthermore, a fan is used to maintained uniform RH and temperature in the chamber.

The samples are first baked in a standard oven (see Fig. 2.4) at 110˚C for 24h to drive all the moisture out of the sample. It is then placed into the humidity chamber which is maintained at constant temperature and humidity for moisture diffusion tests. The moisture absorption, as a function of time, is measured by weighing (balance SBC33 WEDA resolution is 0.0001g) the sample periodically until equilibrium is reached. Then the samples are dry baked again and weighed to be compared with the initial dry weight to ensure the accuracy of the experiments.

Fig. 2.3 Humidity chamber (Espec SH-661)

Fig. 2.4 Oven for drying

2.3.2 Test results of pure EPN1180 and EPN1180 with silica filler

In order to investigate the filler content effects on the moisture diffusion, four samples with silica filler at different weight percent (0 wt%, 40 wt%, 50 wt% and 65 wt%) are tested. After dry baking, the samples are placed into the humidity chamber that is maintained at certain temperature and humidity (85˚C/85%RH, 75˚C/75%RH and 65˚C/65%RH). The moisture absorption, as a function of time, is then measured for each condition and the tests results are shown in Fig. 2.5, Fig. 2.6 and Fig. 2.7.

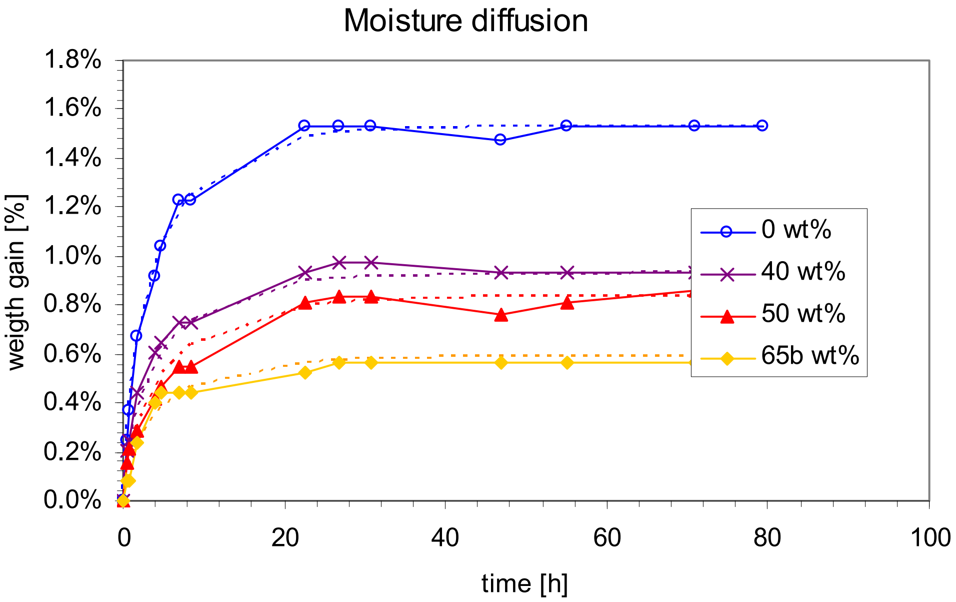

Fig. 2.5 Weight gain vs time at 85˚C/85%RH

(Full lines with symbols are experiment data; dashed lines are model fits)

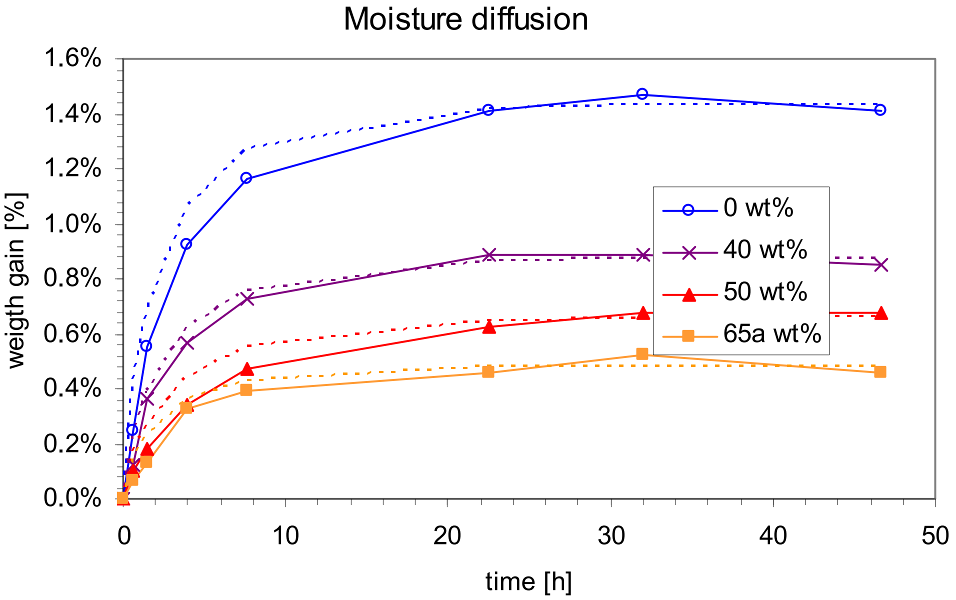

Fig. 2.6 Weight gain vs time at 75˚C/75%RH

(Full lines with symbols are experiment data; dashed lines are model fits)

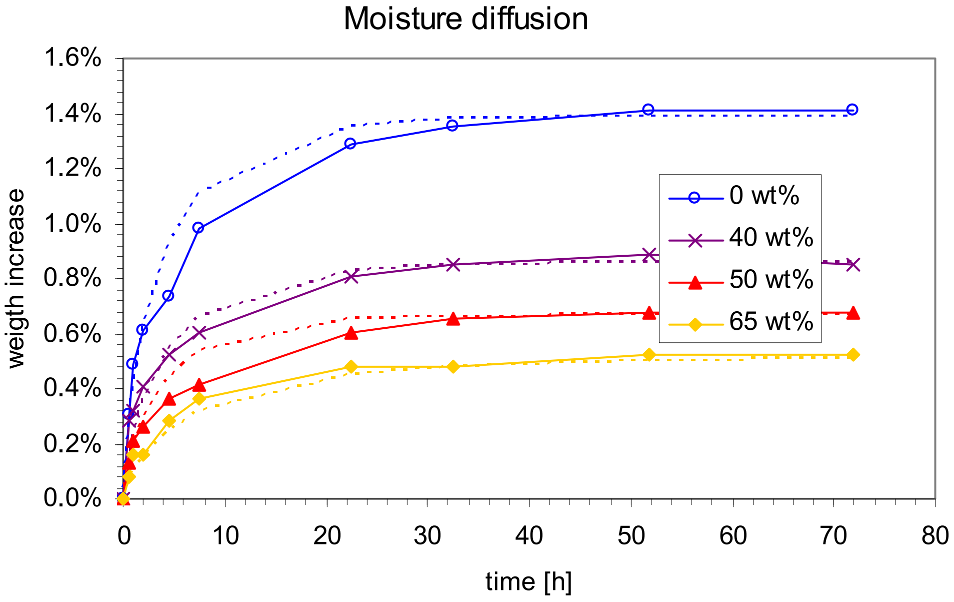

Fig. 2.7 Weight gain vs time at 65˚C/65%RH.

(Full lines with symbols are experiment data; dashed lines are model fits)

In Fig. 2.5, Fig. 2.6 and Fig. 2.7, the full curves represent the test results and the dashed curves represent the fitted results using Eq. 2.3. Fig. 2.5 shows the moisture absorption of different samples at 85˚C/85%RH, it is representative of a typical moisture diffusion curve. The sample is considered to reach moisture saturation level if no more weight gain is detected. The saturated moisture weight gains are 1.53, 0.94, 0.83 and 0.56 wt% respectively with accuracy of ±0.03% for EPN1180 with 0, 40, 50 and 65 wt% filler. The resolution of the measurement is about ±0.1mg. It is intuitive to understand that the moisture saturation levels decrease with increasing filler content because no moisture can diffuse into the silica filler. Fig. 2.6 and Fig. 2.7 show the moisture diffusion results at 75˚C/75%RH and 65˚C/65%RH respectively. Similar to Fig. 2.5, very fast weight gain is observed at the initial stage and the rate gradually slows down. Similar diffusion behaviour at the 75˚C/75%RH and 65˚C/65%RH experiments is observed. Table 2.1 and Table 2.2 summarise all test results of moisture saturation levels and moisture diffusion coefficients at different conditions fitted to Eq. 2.3.

Table 2.1 Summary of moisture saturation weight gains (model fits) [wt%]

	0 wt% filler	40 wt% filler	50 wt% filler	65% filler
85˚C/85%RH	1.53	0.94	0.83	0.56
75˚C/75%RH	1.44	0.88	0.68	0.54
65˚C/65%RH	1.38	0.85	0.67	0.51

Table 2.2 Summary of moisture diffusion coefficients (model fits) [$10^{-12}m^2/s$]

	0 wt% filler	40 wt% filler	50 wt% filler	65% filler
85˚C/85%RH	4.67	3.86	4.01	4.51
75˚C/75%RH	4.69	3.91	3.67	2.67
65˚C/65%RH	3.76	3.75	3.92	2.91

It can be seen from table 2.1 that $M_{sat,}$ systematically decrease with increasing filler content and with decreasing temperature. Fig. 2.8 summarized the moisture saturation levels of different filler contents. Furthermore, it also shows that their relationship can be predicted using the rule of mixtures and hence they can be represented by the following equation, y = Ax + B, y represents M_{sat} and x represents filler contents. Parameter B is found to be 0.0153, 0.0144 and 0.0138 at 85˚C/85%RH, 75˚C/75%RH and 65˚C/65%RH respectively. The moisture weight gain M_{sat} will theoretically fall to zero when the filler content is at 100 wt%, as predicted by the regressed relationship.

In Table 2.2, the listed moisture diffusion coefficients are obtained by regressing with Eq. 2.3. Generally speaking, the moisture diffusion coefficient should increases with increasing temperature. However, uncertainties may be introduced during some of the measurements. These uncertainties may have been introduced due to temperature or relative humidity uniformity problem and frequent removal of the sample from the chamber. In order to overcome the above measuring problems, a new gravimetric balance is used for characterizing the materials for system in package (SiP) materials as discussed in the next section.

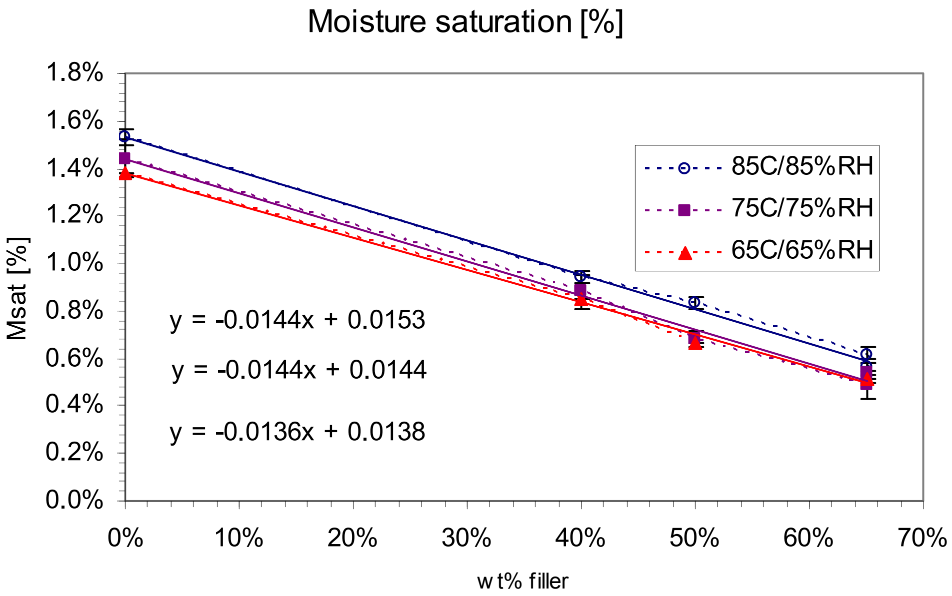

Fig. 2.8 Moisture saturation weight gain M_{sat} vs wt% filler

2.3.3 Generalized model for moisture saturation level

Since the epoxy binders in EMC have similar absorption characteristics, Table 2.1and Fig. 2.8 can be used to develop a generalised model for predicting the dependency of M_{sat} at the filler content and pre-conditioning condition. This equation will allow a quick estimation of the moisture absorption properties by just measuring the filler content alone. Hence, significant time and effort will be saved as it is relatively easier and to measure the filler content than conducting moisture absorption experiments.

As stated in the above discussion, M_{sat} decreases linearly with filler content. Hence, the following model is proposed by forcing $M_{sat} \to 0$ as $x_f \to 0$ in the regression.

$$M_{sat}\left(x_f, T, X_{RH}\right) = M_{sat}^{100,e}\left(T\right) \bullet X_{RH}\left(1 - x_f\right) \tag{2.11}$$

$$M_{sat}^{100,e}\left(T\right) = k_0 \bullet e^{-H/RT} \tag{2.12}$$

where $M_{sat}\left(x_f, T, X_{RH}\right)$ is moisture saturation level and $M_{sat}^{100,e}\left(T\right)$ is pure epoxy moisture saturation levels at temperature T and 100% relative humidity condition, X_{RH} is relative humidity and x_f is filler content, R is the universal gas constant, 8.314 $\mathrm{JK^{-1}mol^{-1}}$. H is the activation energy constant and k_0 is the proportional constant, see Table 2.7.

Using Eq. 2.11, M_{sat} of the EMC at 85ºC/85%RH is predicted to be around 0.228 wt% while the characterized M_{sat} at the same condition is about 0.194 wt%. Similar approach has been adopted for predicting underfill's M_{sat} at 85ºC/85%RH and the predicted and characterized M_{sat} values are found to be 0.762 wt% and 0.892 wt% respectively. Although this difference in predicted and characterized values may be due to the different binder, filler size and processing methods used in these samples, this equation can be used to sufficiently predict M_{sat} of different materials.

The filler content can be estimated from the filler volume fraction using following equation:

$$\varphi_f = \frac{\rho_e x_f}{\rho_e x_f + \rho_f \left(1 - x_f\right)} \tag{2.12}$$

where φ_f is filler volume fraction, ρ_e and ρ_f denote the density of the filler particles and pure epoxy, Typically ρ_e=1.2, ρ_f=2.2 (fused quartz), Hence, 40, 50 and 65 wt% will correspond to 26.0, 34.5 and 49.5 vol% [Yang, 2007]. Lastly, Eq. 2.13 can be inverted to describe x_f as a function of φ_f:

$$x_f = \frac{\varphi_f \rho_f}{\rho_e - \varphi_f \left(\rho_e - \rho_f\right)} \tag{2.13}$$

2.3.4 Moisture diffusion in commercial die attach, EMC and underfill

In this section, the moisture diffusion properties of three different packaging materials used in our SiP carrier (see Chapter 1) are characterized. They are die attach, EMC and underfill. The moisture diffusion method used in section 2.3.1 [IPC/JEDEC J-STD-022-A120A] is not only laborious, high inaccuracy may be resulted from the need for constant removal of the sample from the humidity chamber. In order to overcome this problem, an in-situ moisture sorption method is used for characterizing the die attach, EMC and underfill materials. This will allow the characterization of the material moisture properties to be performed in a shorter duration and yet with a high accuracy as discussed in the next session. At least four days can be shortened using this method to characterize the moisture properties needed for fast moisture diffusion.

Experimental materials

Die attach

The die attach material used in this research is produced from Loctite. It contains about 90% silver particles with an average size of the silver particle about 5μm in diameter. The sample is prepared by curing at 180^{o}C for 15 minutes and then grinded and polished to a thickness of about 0.37mm.

Moulding compound

The moulding compound contains about 85 wt% silica filler with an average size of the particles of about 15µm in diameter. The material is prepared by post-curing at 180^{o}C for 3 hours. The samples are then grinded and polished to a thickness of about 0.35mm in order to reduce the time needed for moisture equilibrium.

Underfill

The underfill used is a commercially available underfill from Namics. Filler average size is about 10µm and the filler content is less than 50 wt%. The sample is prepared by first sandwiched between two Teflon foil using two glass plates to allow quick removal of the sample after curing. They are then cured at 150°C for 20 min in the oven before they are grinded and polished to a thickness of about 0.3mm.

Equipment of moisture absorption test

A programmable SGA-100 gravimetric moisture absorption balance, which can perform in-situ isothermal moisture absorption test; and thermal and humidity cycling test, is used for the moisture absorption test, see Fig. 2.9. The working temperature range of this equipment is from 5ºC to 90ºC and relative humidity range is from 5 to 95%RH. The listed weight sensitivity of the equipment is 1µg. Furthermore, an extra heater is needed to be mounted for high temperature and high humidity measurement. Lastly, the diffusion coefficient can be automatically calculated from the analysis software.

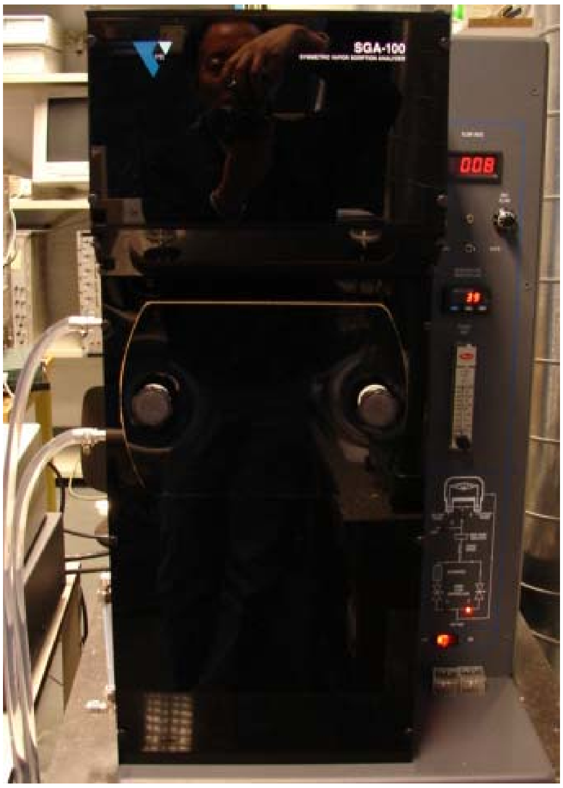

Fig. 2.9 Gravimetric moisture absorption balance

Test procedures

The samples are first dry baked at 125ºC for 24 hours in the oven to ensure complete dryness. As discussed in the previous section, the standard test outlined in section 2.3 will require at least one test to be performed at each specified condition for every material's moisture properties that need to be characterized. Since the development of material moisture property prediction model required material moisture properties from a wide range of temperature and humidity, this method is lacking due to their huge amount of effort and time need. In order to overcome this shortcoming, a more efficient temperature and relative humidity cycling/stepping method is developed and adopted in this research to perform moisture absorption.

For the moisture absorption test, temperature, at 30ºC, 60ºC and 85ºC, and relative humidity, at 0%RH, 30%RH, 60%RH, and 85%RH respectively, will be preferred as these correspond to the standard test conditions in MSL test, which has been widely adopted in the industry and academia. However, due to the inability for SGA-100 to achieve high stability at high temperature and humidity, the testing scheme is instead performed at 20, 40 and 60ºC and relative humidity at 40, 60 and 80%RH respectively. High temperature and high relative humidity moisture parameters will be extrapolated from these temperature and relative humidity material moisture model. These extrapolated parameters are validated in Chapter 4 by comparing the experiment and simulation.

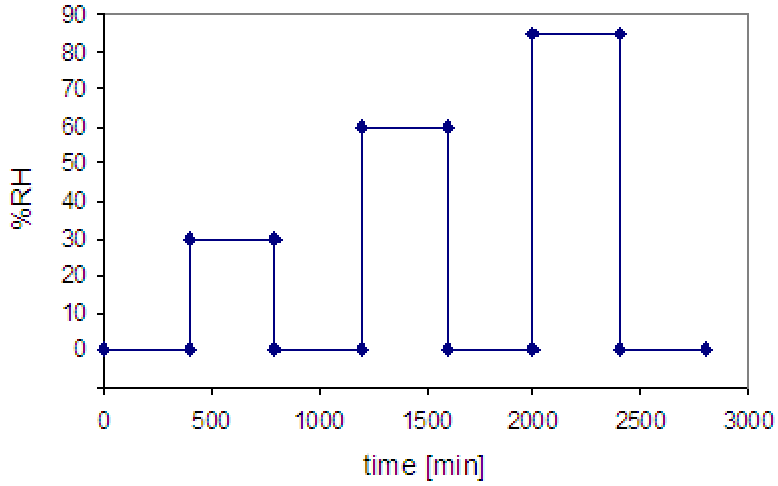

Fig. 2.10 Typical RH% profile

From Fig. 2.10, it can be seen that relative humidity value varies in a stepwise manner in the following sequences: 0-30-0-60-0-85-0% RH. Furthermore, the time span required for each relative humidity change has a range from 300 to 600 min depending on the sample thickness and packaging materials. This sequence is also reversed and relative humidity are then stepped from high to low relative humidity to compare the sensitivities of the material properties characterized on the sequence order. Both methods are found to produce similar characterized material moisture absorption properties.

Test results

Although only results from the die attach moisture absorption test are shown here, this is representative of the results from other test. Due to the similarity of these results, only some of the die-attach moisture absorption results and the calculated results for moulding compound and underfill will be presented here.

Die attach moisture test results

The size of die attach sample used in this research is about 14.5x5.5x0.37mm^3 with a mass of 94.4mg. These samples are first dry bake in the oven for 24 minutes at 125ºC to drive out all the moisture content that may be present in the sample before they are transferred to SGA-100 for moisture absorption test. Three different temperatures are performed in these tests, they are 20ºC, 40ºC, 60ºC respectively with a relative humidity sequence programmed for (0-80-0-60-0-40-0%RH). Furthermore, the dwelling time for every relative humidity is set to about 200 to 600 minutes depending on the thickness of the sample and the temperature. Generally, moisture absorption time is shorter for thin sample at high temperature. Fig.2.11 shows the die attach moisture absorption test result at 40ºC.

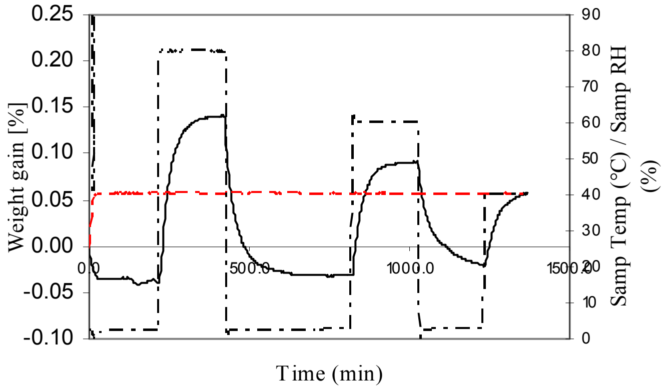

Fig. 2.11 Die attach moisture absorption at 40 ºC for dry baked for 24hours at125ºC

The solid curve in Fig 2.11 represents the moisture weight gain (wt%) whereas dash line and dot-dash line is the temperature and the relative humidity respectively. It is noted from Fig.2.11 that the sample weight changes as humidity changes. Another observation from Fig 2.11 is that moisture equilibrium values are strongly dependent on the relative humidity. This is consistent with the diffusion theory.

Fig. 2.12 shows die attach moisture absorption at 40ºC with 30 min of dry baking at150ºC. Final saturation levels are not reached at this condition. Hence, a Matlab code has been developed to extrapolate these data to predict the saturation levels. This estimated value is found to have a derivation of less than ± 0.05%, see Fig 2.13.

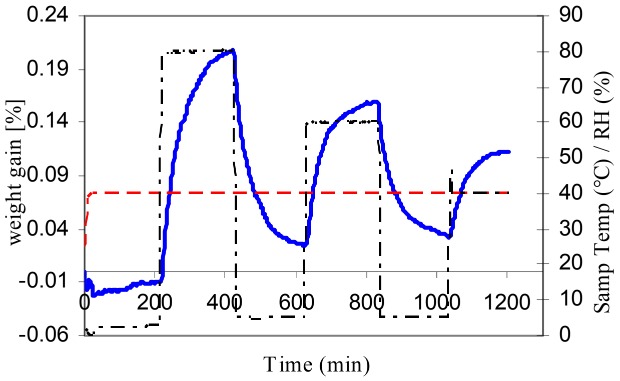

Fig. 2.12 Die attach moisture absorption at 40ºC for pre-drying 30 min at150ºC

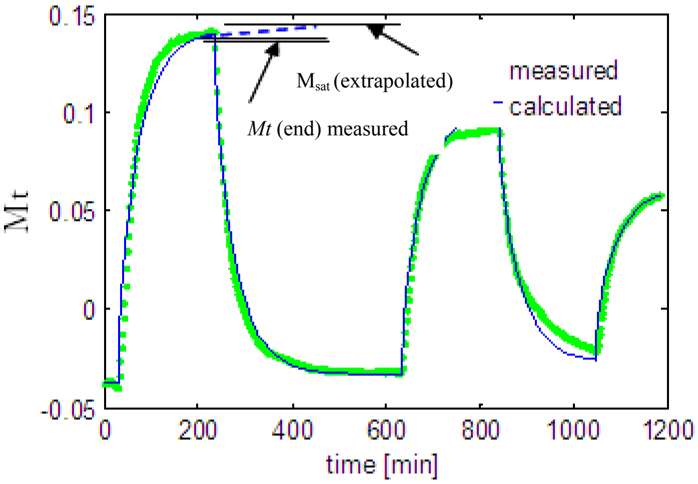

Fig. 2.13 Estimated saturation level extrapolated using Matlab

Comparisons are made between the standard dry baking procedure (125ºC for 24 hours) and the proposed faster dry baking procedure (30 min at 150ºC) developed in this research. In Fig. 2.14 and Fig. 2.15, the thin curve is the moisture absorption line for 24 hours dry baking at 125ºC and thick solid line is the moisture absorption line for 30 minutes at 150ºC. It is noted that the initial stages of both procedures are different due to the initial moisture difference in the samples. This means samples are not completely dry.

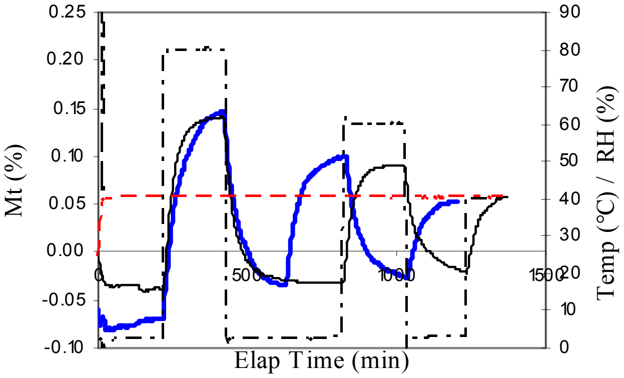

Fig. 2.14 Comparison of different pre-dry moisture absorption stages

Fig 2.14 shows that the moisture absorption and desorption processes for the first step (80RH% step) are similar for both pre-conditioning conditions, (see Fig. 2.14) whereas Fig. 2.15 shows that moisture absorption and desorption profile is also for the 2nd and 3rd RH steps (last part of the curves). Hence, it can be assumed that moisture absorption and desorption process is independent of the initial moisture level in the pre-dried sample and the shorter prebake condition will be sufficient. This observation is important as it is also difficult to define "dry" state due to the environmental influences.

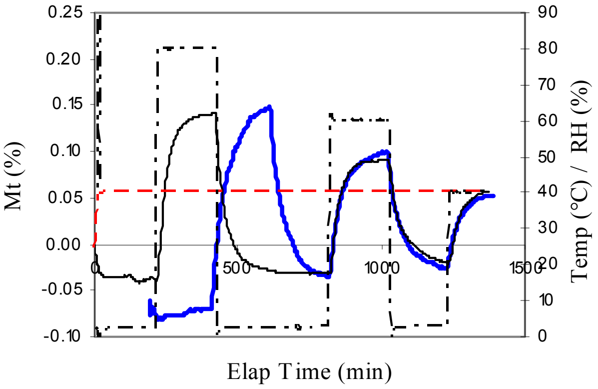

Fig. 2.15 comparison of different pre-dry moisture absorption stages
(data of Fig. 2.14 shifted in time)

Reproducibility of the result for die attach sample is also compared for 60ºC and 20ºC (relative humidity steps are 0-80-0-60-0-40-0RH%) testing condition.(not shown here again) and great reproducibility has been observed for this method except at the initial stage due to the small differences in the initial dryness of the samples.

Moulding compound moisture absorption tests

The moulding compound's sample size used in this research is 16.08x5.05x0.335mm^3 and has a mass of 52.8mg. They are first dried baked in the oven for 30 minutes at 150ºC before they are transferred to SGA-100 for moisture related test. The temperature is set at 20ºC, 40ºC, 60ºC respectively and a sequence of relative humidity is programmed (0-80-0-60-0-40-0RH%). At every relative humidity, the dwell time is from 200 to 600 minutes depending on the thickness of the sample and the temperature. Test results are similar to the die attach results although their moisture absorption equilibrium is different from die attach. Therefore, moisture absorption graphs are not shown again but summarised in Table 2.3 to 2.6.

Underfill moisture absorption tests

The test procedure is the same as for die attach and moulding compound. The sample size is 12.5x4.89x0.385mm^3 and has a mass of 36.0mg. As in the case of EMC, their test results are similar to that of the die attach although their moisture absorption equilibrium is different from die attach. Therefore, moisture absorption graphs are not shown again here.

Summary of data material properties

Table 2.3 Moisture saturation weight gain of die attach

Temperature [ºC]	M_{sat} [wt%]		
	40RH%	60RH%	80RH%
20ºC	0.106	0.157	0.210
40ºC	0.113	0.174	0.231
60ºC	0.125	0.188	0.249

Table 2.4 Moisture saturation weight gain of moulding compound

Temperature [ºC]	M_{sat} [wt%]		
	40RH%	60RH%	80RH%
20	0.042	0.061	0.080
40	0.053	0.081	0.109
60	0.068	0.104	0.138

Table 2.5 Moisture saturation weight gain of underfill

Temperature [°C]	M_{sat} [wt%]		
	40RH%	60RH%	80RH%
20	0.188	0.282	0.380
40	0.251	0.376	0.495
60	0.320	0.482	0.645

Table 2.6 Moisture diffusion coefficients of different packaging materials

Temperature [°C]	Moisture diffusion coefficients [m^2/s]		
	Die attach	Moulding compound	Underfill
20	1.66×10^{-12}	1.68×10^{-12}	1.40×10^{-12}
40	4.40×10^{-11}	2.82×10^{-12}	2.14×10^{-12}
60	1.04×10^{-10}	4.06×10^{-12}	3.11×10^{-12}

According to above experimental data, the constants of Eq. 2.7 and Eq. 2.9 can be calculated combined with Fig. 2.16, Fig. 2.17 and Fig. 2.18.

Following graphs are relations between lnM_{sat} and 1/T and between ln$D$ and 1/T.

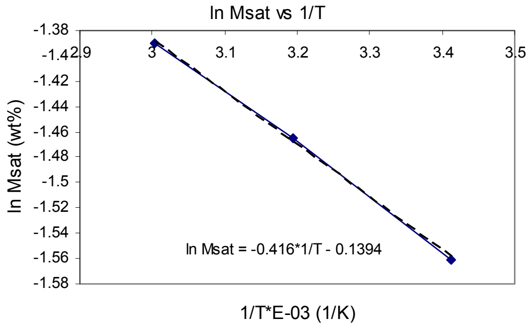

Fig. 2.16(a) Slope of lnM_{sat} vs $1/T$ for die attach

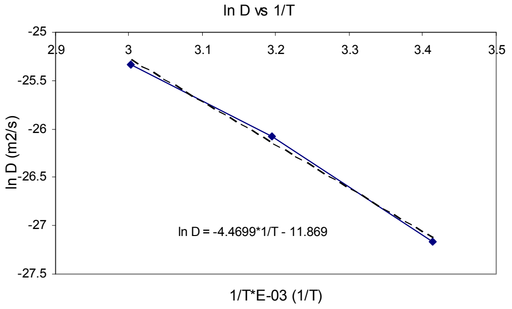

Fig. 2.16(b) slope of ln$D$ vs $1/T$ for die attach

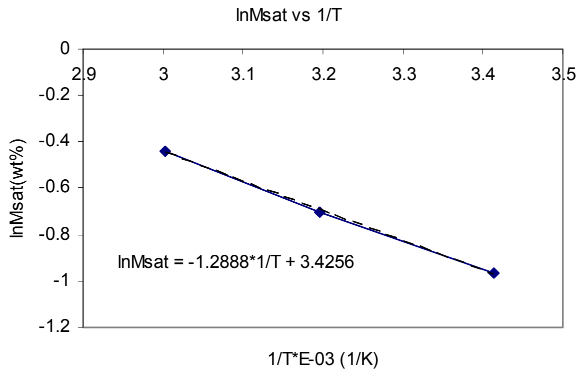

Fig. 2.17(a) Slope of lnM_{sat} vs $1/T$ for underfill

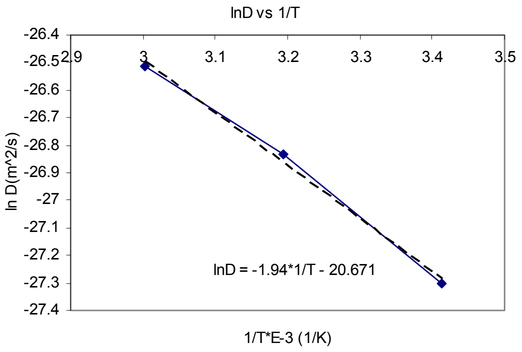

Fig.2.17(b) slope of ln$D$ vs $1/T$ for underfill

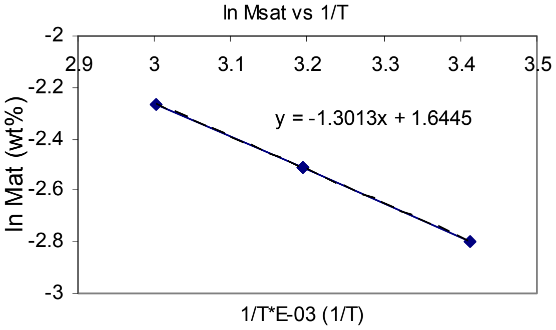

Fig. 2.18(a) Slope of lnM_{sat} vs *1/T* for EMC

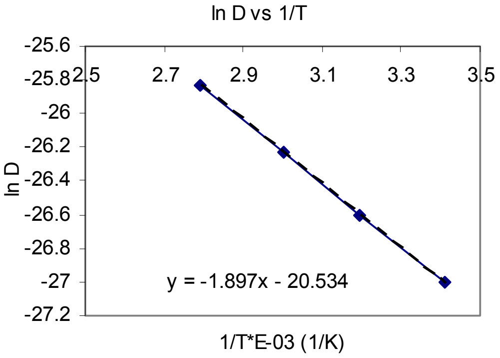

Fig. 2.18(b) slope of ln*D* vs *1/T* for EMC

Table 2.7 presents prediction model parameters for three packaging materials used in the carrier. Diffusion coefficients and M_{sat} can be obtained from Eq. 2.7 and Eq. 2.9 at different conditions using parameters in Table 2.7.

Table 2.7 Parameters of packaging material models

parameters	EMC	Underfill	Die attach	EPN1180(0wt%)
k_0 [-]	8.63	38.43	1.09	10.22
H [kJ/mol]	10.82	10.72	3.46	5.18
D_0 [m^2/s]	1.2x10^{-9}	1.054x10^{-9}	7.0x10^{-9}	19.58x10^{-9}
E_D [kJ/mol]	15.76	16.13	37.16	11.10

These material models agree well with our measurement as shown in Table 2.3 to Table 2.6. Hence, these materials prediction data can be used in the validation experiment that is discussed in Chapter 4.

In Table 2.6, the diffusion coefficients at 20ºC of all three materials are about the same order. However the temperature dependency of the die attach is much larger, see Table 2.6. This is caused by the rubbery state of the die attach which causes more expansion when heated. This will results in more free volume and more free space for moisture at higher temperature

2.4 Moisture induced expansion measurements

Fundamentals of moisture induced expansion and its measurements

Moisture induced failure in plastic encapsulated packages is an important failure mechanisms in microelectronics. Therefore, it is important to investigate moisture effects on mechanical properties of plastic packaging materials.

The coefficient of moisture expansion (CME) is a measure of the induced strain in the materials with moisture absorption. Furthermore, hygro-mechanical or hygro-swelling stress is induced due to the CME mismatch among various materials. This concept is analogous to the coefficient of thermal expansion (CTE) mismatch and thermal-mechanical stress and hence, the thermal moisture analogy can be used to simulated hygro-mechanical stress. The moisture loading is applied from 0% to 100% relative humidity at different temperature conditions.

Hence, moisture induced expansion can be calculated using Eq. 2.14

$$\varepsilon^{RH} = \beta \bullet C \tag{2.14}$$

where ε^{RH} is the moisture induced strain, β is the CME [mm^3/mg] and C is the moisture concentration [mg/mm^3].

TGA (Thermal Gravimetric Analyzer)/TMA (Thermal Mechanical Analyzer) method [Tee, et al., 2004, Wong, et al., 2002] is the most commonly adopted CME characterization methods for plastic packaging materials in industry. The nominal sizes of the samples are usually 2x2x2mm^3 or larger. For TGA/TMA methods, two identical material samples are preconditioned with moisture under same temperature and humidity, e.g. 85ºC/85%RH for about 2 weeks until moisture saturation is reached. Then the samples are monitored for moisture desorption in the thermal gravimetric analyzer and thermal mechanical analyzer respectively at a temperature of 85ºC until the moisture is fully dried out. The change in thickness direction from the TMA readings can then be used to deduce the average strain in the thickness direction whereas the change in weight or moisture loss of the sample during desorption is obtained from the readings of the TGA. Since the average moisture concentration is calculated from just the moisture loss divided by the sample volume, the measured CME value is an average value. This method is often used in industry because of its relative simplicity but these CME values are often largely over estimated [Zhang, et al., 2006, Zhou, et al., 2005a, Zhou, et al., 2005b]. A better method for characterizing moisture induced expansion of polymer materials is the optical Moire interferometer method [Stellrecht, et al., 2004] but that is very difficult to implement.

In this research, an alternative method that is simple to implement and yet is able to produce precise CME values has been developed. A high precision DMA (Dynamic Mechanical Analyzer) is used to measure the change in length of a sample while a humidity generator is used to regulate the relative humidity in the DMA chamber. Temperature and relative humidity are controlled in the DMA chamber so as to enable measurement of the length change under different relative humidity conditions. Furthermore, the comparison of the CME values measured by the DMA plus humidity generator method and TGA/TMA method has been preformed and these results will be presented in Chapter 4.

2.4.1 TGA / TMA method

Fig. 2.19 shows the principle of using TGA/TMA method to characterise the CME of plastic packaging materials. TGA, see Fig. 2.20, is used to measure the weight change whereas TMA, see Fig. 2.21, is used to measure the length change. By combining both the TMA and TGA measurements, the CME can be determined.

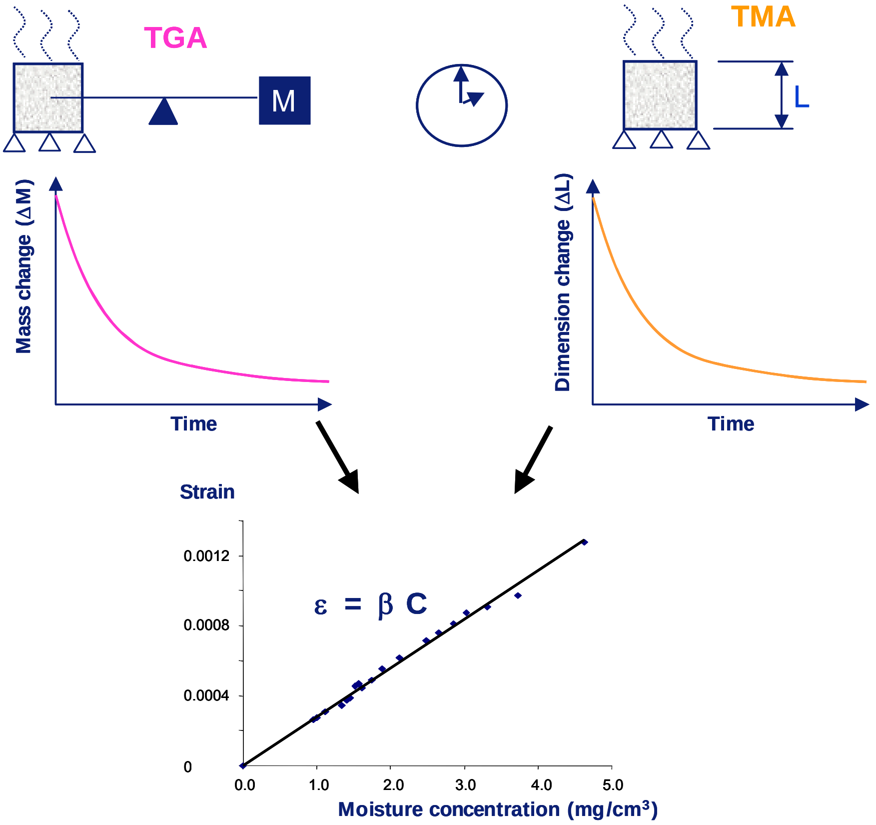

Fig. 2.19 Combined TGA/TMA technique to determine CME

Fig. 2.20 Thermal Gravimetric Analyzer (TA-Instrument TGA-2050)

Fig. 2.21 Thermal Mechanical Analyzer (TA-Instrument TMA-2940)

Sample making and pre conditioning

Three types of materials are cured according to the specification provided by the supplier. Then the samples made from these materials are cut and polished to a nominal size of 2x2x2mm^3. The dimension should be identical for TGA and TMA samples to minimize error of the measurements. These samples are kept in the moisture diffusion oven for 168 hours at the condition of 85°C/85%RH before they are placed in the TGA and TMA for weight change and length change measurement respectively. The following temperature profiles are applied for measurements at 85°C:

TMA: temperature ramp at 100°C/min to 85°C

TGA: temperature ramp at 100°C/min to 65°C first and then 10°C/min to 85°C

Test results of moulding compound

Fig. 2.22(a), (b) shows the relationship between measured strain and time (tma1 and tma2) and the relationship between measured moisture concentration and. time of the measurement (tga1 and tga2) respectively. Both the measured strain and the measured moisture concentration decrease with time due to moisture desorption as expected. Fig. 2.22(c) and Fig. 2.22(d) are two typical correlated CME values using measured strain vs time and measured moisture concentration vs time. The CME values of TGA1/TMA1 and TGA2/TMA2 are 0.46 and 0.65 [mm^3/mg] respectively. However, different CME values are obtained depending on the range of data used. Therefore, consistency in the measurement is difficult to be ensured.

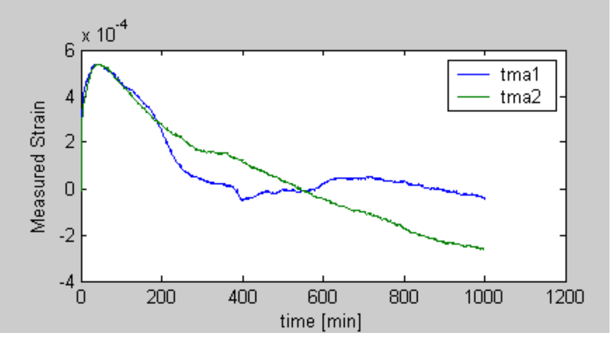

Fig. 2.22(a) Strain vs time of EMC

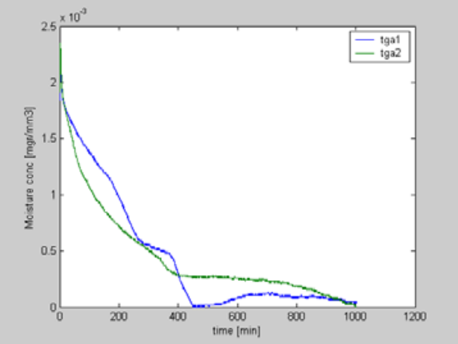

Fig. 2.22(b) C vs time of EMC

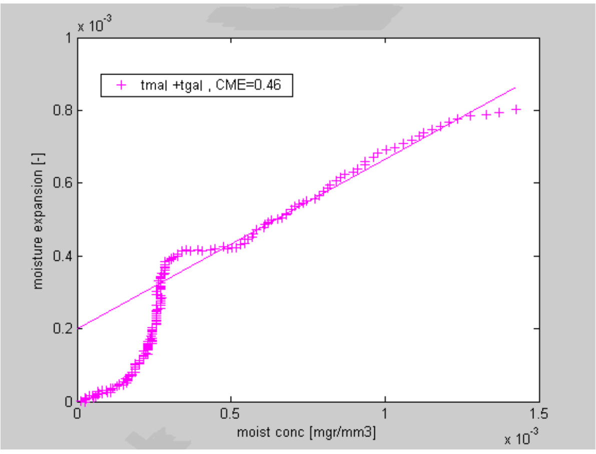

Fig. 2.22(c) Correlated CME of EMC

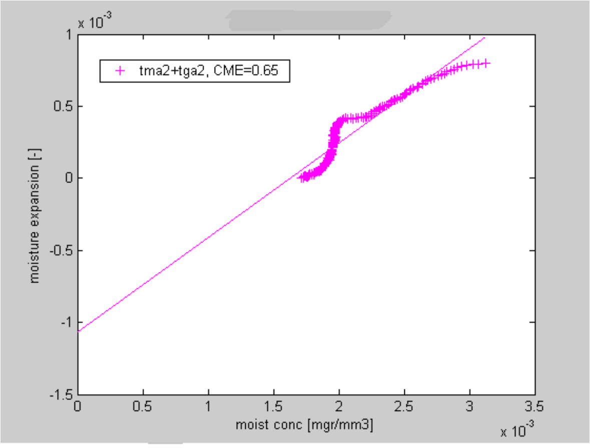

Fig. 2.22(d) Correlated CME of EMC

Test results of underfill

Fig. 2.23(a), (b) are the measured strain vs time and the measured moisture concentration vs time respectively of underfill. Again, it can be seen that the measured strain and the measured moisture concentration decreases with time due to moisture desorption at high temperature. Fig. 2.23(c) shows one typical correlated CME values using measured strain vs time and measured moisture concentration with time.

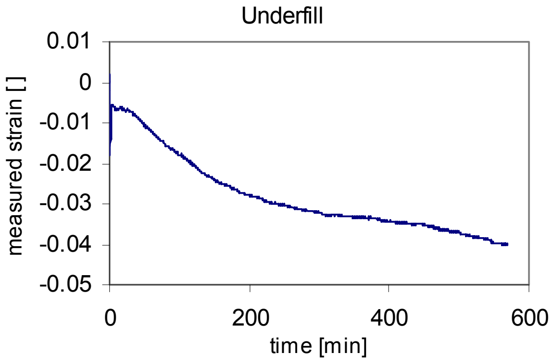

Fig. 2.23(a) Strain vs time of underfill

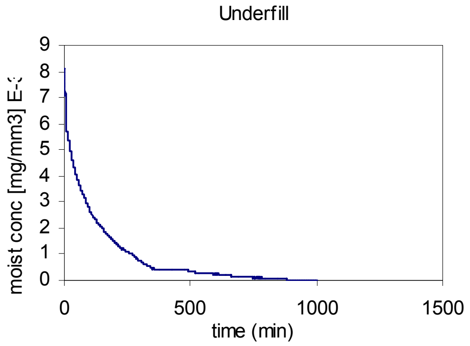

Fig. 2.23(b) C vs time of underfill

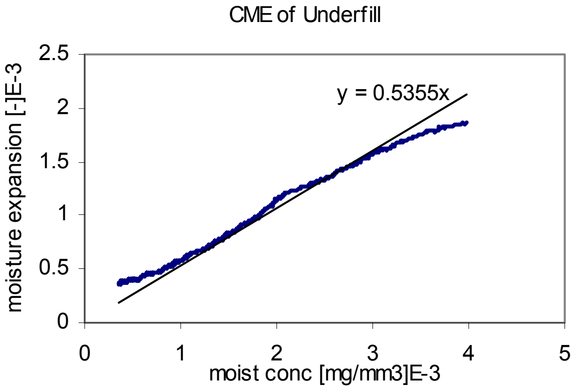

Fig. 2.23(c) Correlated CME of underfill

Test results of die attach

Fig. 2.4(a), (b) are measured strain vs time and measured moisture concentration vs time respectively for the die attach. Again, it can be seen that the measured strain and the measured moisture concentration decreases with time due to moisture desorption at high temperature. Fig. 2.24(c) shows a typical correlated CME values using measured strain vs time and measured moisture concentration vs time.

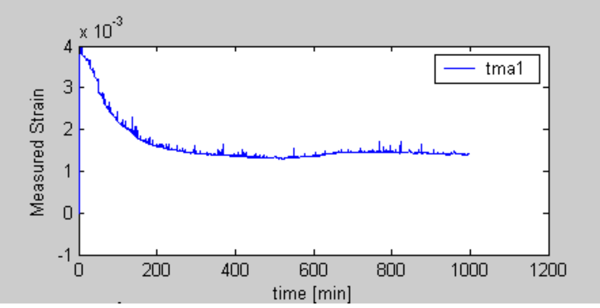

Fig. 2.24(a) Measured strain vs time of die attach

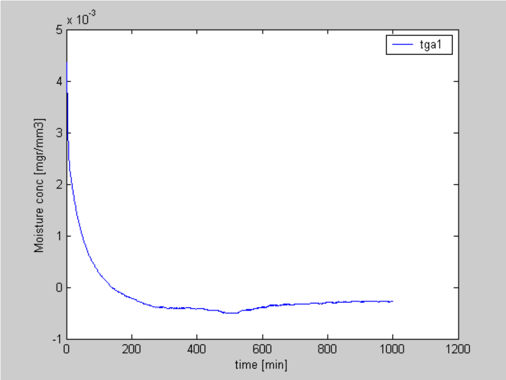

Fig. 2.24(b) Measured C vs time of die attach

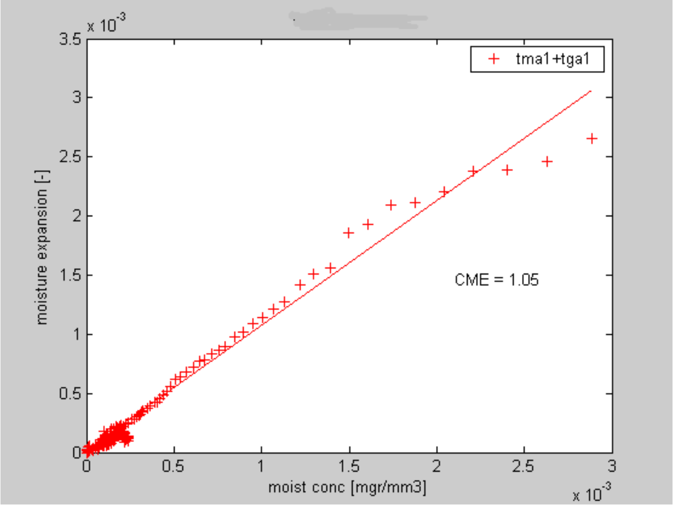

Fig. 2.24(c) Correlated CME of die attach

Table 2-10 lists the CME values measured using the TGA/TMA method. Comparison with the results of the DMA method will be covered in next section.

2.4.2 DMA method

Sample preparation

In order to reduce the duration needed for the moisture induced expansion tests, samples should be as thin as possible but they should be thicker than the size of their filler. Therefore the samples are grinded and polished to a thickness of about 0.3mm for most optimal result.

Fig. 2.25 Initial samples

Fig.2.25 shows the initial samples of EMC with a nominal dimension of 80x6x2mm^3. The final dimension of the test sample is polished to around 40x6x0.3 mm^3. Again, the same die attach, EMC and underfill are used in this experiment.

Experimental equipments

The main test equipments used in this research are DMA (TA Instruments Q800) and humidity generator (VTI VX-G 100). The DMA is for the temperature control and the induced sample elongation or strain measurement whereas the humidity generator maintains constant relative humidity airflow into the DMA chamber. The setup is shown in Fig. 2.26. The moisture air flows from the top of the chamber and into the DMA are monitored using moisture sensor placed in the DMA chamber, see the top arrow. Moisture induced expansion can then be measured at desired temperature and relative humidity values. This programmable moisture generator can produce a range of relative humidity from 5% to 90%RH at temperature from room temperature to 85ºC.

Fig. 2.26 DMA combined with humidity generator setup

Test procedures and setup check

Samples are dry baked in an oven at 125ºC for 24 hours to ensure that the sample is completely dried. The sample is then placed between the clamps in the DMA once the DMA and moisture generator are programmed to function synchronously. Moisture absorption time should be long enough to ensure that moisture equilibrium is reached in the test samples after each RH-step. Using the experiment developed in this research [Ma, et al., 2007a, Ma, et al., 2007b] and section 2.3, the moisture absorption equilibrium time can be estimated. For a thin strip sample with thickness between 0.3 to 0.4mm, 300 to 600 minutes is found to be sufficient for moisture absorption equilibrium.

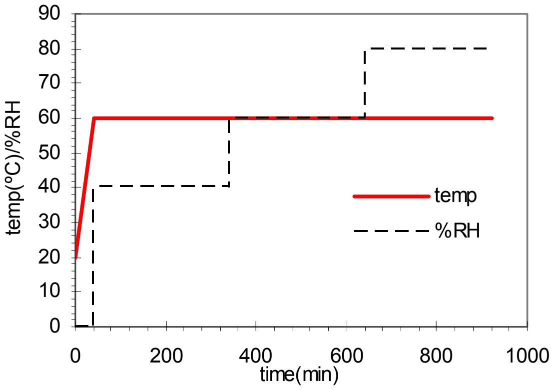

Fig. 2.27 Programmed DMA and moisture generator temperature and %RH profiles

Fig. 2.27 shows the temperature and relative humidity profile for the moisture induced expansion tests. DMA's temperature is ramped up at a rate of 2ºC/min in order to avoid any temperature overshoot. Additional 20 minutes is required to ensure that the temperature reaches equilibrium after humidity air flow is supplied into the chamber.

Fig. 2.28 shows the temperature and relative humidity behaviour during the test. The relative humidity is measured with a humidity sensor mounted in the DMA as shown in Fig. 2.26. Fig. 2.28 plots the sensor output and it shows that although the temperature is relatively stable, stable relative humidity is not achieved in the chamber. Therefore, it is important to estimate the effect of the unstable relative humidity on the test results.

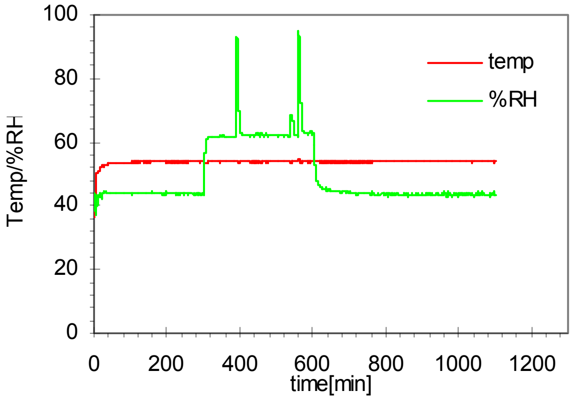

Fig. 2.28 Temperature and relative humidity check

Fig. 2.28 also shows that the actual relative humidity in the chamber is 43%RH, 63%RH and 43%RH respectively at different time periods although the programmed relative humidity is set to be 40%RH, 60%RH, and 40%RH. Furthermore, the measured temperature is found to be a few degrees lower than the set temperature. This could be attributed to the location of the thermocouple in the DMA chamber.

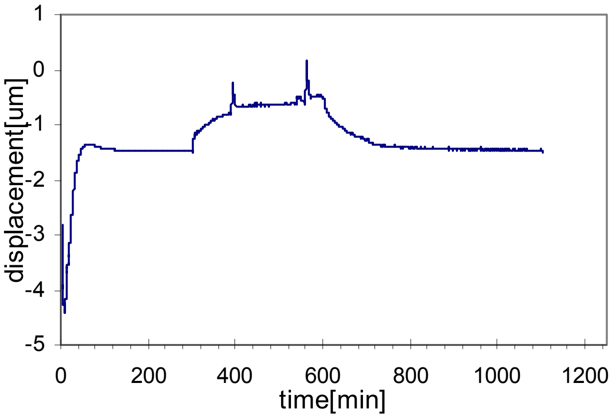

Fig. 2.29 Relative humidity effects on the sample length change (EMC)

Fig. 2.29 shows the elongation response of the sample placed under the loading described in Fig. 2.28. It can be observed that Fig 2.28 and Fig 2.29 follow similar trends and shape. For example, a corresponding peak length change can be observed in the DMA measurement (Fig. 2.29) at peak of the relative humidity (Fig. 2.28). After the peak, the sample length returns to the same values before the instability is induced. Therefore, these sudden relative humidity changes will not affect the average CME values which are obtained from the equilibrium data.

CME test results

Fig. 2.30 shows a typical CME test results for the die attach. The test condition is as follows: the sample is dry baked at 125ºC for 24 hours and this sample is then placed in the DMA chamber at is maintained at 60ºC and a sequences of RH steps of 40%RH, 60%RH, and 80%RH. The time span at each relative humidity is around 600min but the time span for 0%RH is 20min.

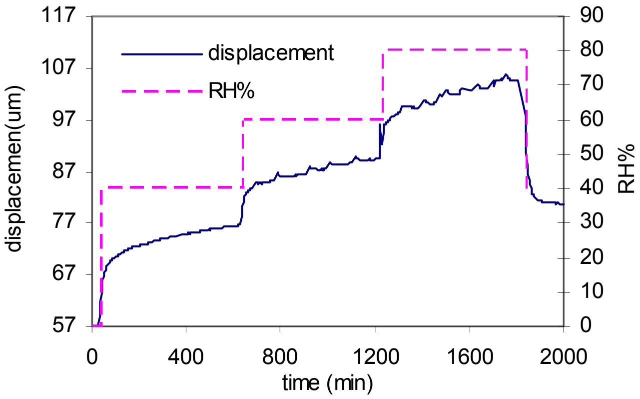

Fig. 2.30 Displacement vs %RH change at 60ºC for die attach for RH= 40, 60, 80%

From Fig. 2.30, it can be seen that the displacement changes with relative humidity at 60ºC. Furthermore, large increases in the change in displacement are observed, at the start of every relative humidity change but the rate reduces considerably after that. The large increases in the initial displacement are due to the ability for moisture to penetrate the die attach quickly at the cavities, cracks and gaps in the polymer. Similar behaviour can be observed in the result for moisture weight change, see Fig. 2.1.

Strain ε^{RH} is calculated from Eq. 2.14. The moisture properties of die attach, underfill, and moulding compound are characterized in our previous papers [Ma, et al., 2007a, Ma, et al., 2007b]. Furthermore, C_{sat}, which is the saturation moisture content at certain conditions, is the product of M_{sat} (Eq. 2.8) and the density of the dry material. A summary of C_{sat} for different materials are listed in Table 2.8.

Table 2.8 C_{sat} of packaging materials

Materials/Density [mg/mm^3]	60C/80%RH	60C/60%RH	60C/40%RH
	[10^{-3}mg/mm^3]	[10^{-3}mg/mm^3]	[10^{-3}mg/mm^3]
Die attach/ 3.95	9.84	7.43	4.90
Underfill/ 1.53	9.87	7.36	4.92
EMC/ 1.94	2.68	2.02	1.35

$$\varepsilon^{RH} = \Delta l / l_{T,0} \tag{2.14}$$

$$\Delta l = l_{T,C} - l_{T,0} \tag{2.15}$$

where Δl is the length change of the tested sample. $l_{T,C}$ is the sample length at the temperature T and the moisture concentration C in the sample. $l_{T,0}$ is the initial dry sample length at temperature T. Using Fig. 2.31(a), which is the calculated strain at 40, 60 and 80RH% at 60ºC, and the equation Eq. 2.14 and Eq. 2.15, the CME value of the die attach is determined to be 0.20[mm^3/mg].

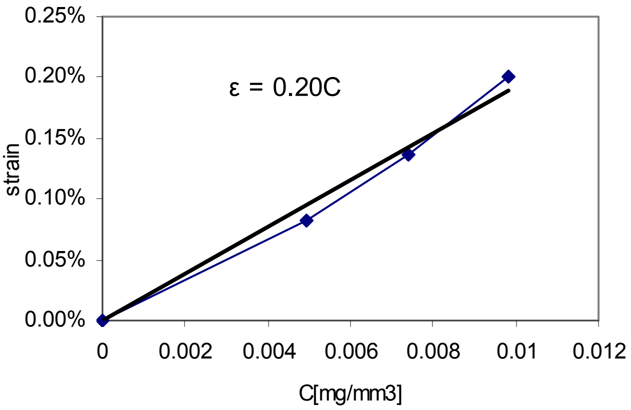

Fig.2.31(a) Relation between strain and moisture concentration for die attach

Similar measurements are performed for EMC and underfill and the CME values of EMC and underfill are shown in Fig. 2.31(b) and (c). Table 2.10 summarized the CME values for these packaging materials.

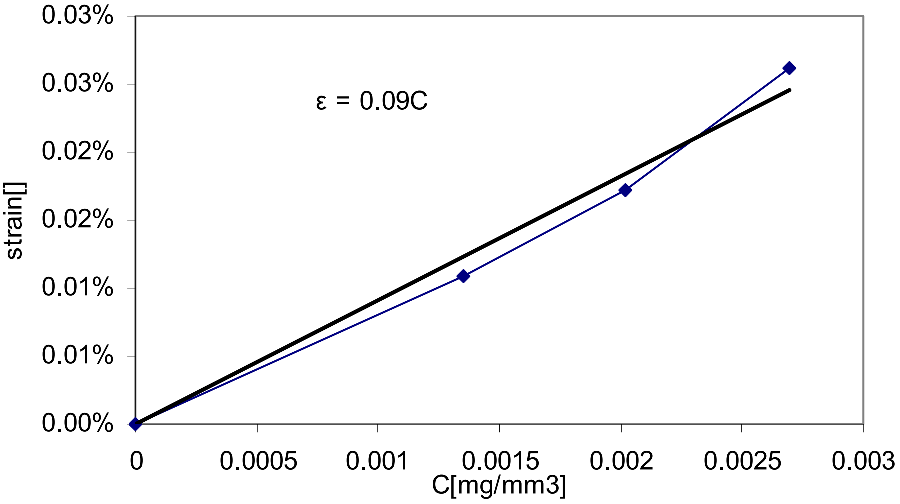

Fig.2.31(b) Relation between strain and moisture concentration for EMC

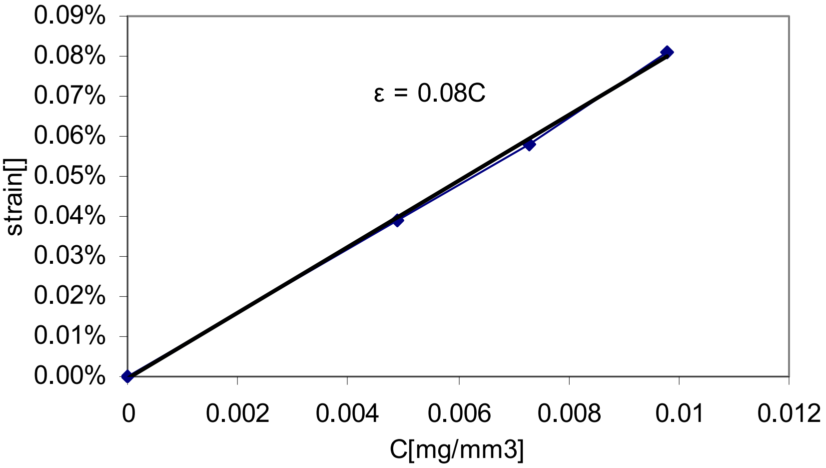

Fig. 2.31(c) Relation between strain and moisture concentration for underfill

Table 2.10 Test results of CME

Materials	DMA	TGA/TMA
	CME [mm^3/mg]	CME [mm^3/mg]
Die attach	0.20	1.06
Underfill	0.08	0.53
Moulding compound	0.09	0.46 to 0.65

The CME of underfill and moulding compound are similar because they are similar in compositions, epoxy type and silica filler. However, the higher CME value of die attach is due to the different filler particles (silver) and occurrence of the rubbery phase at the time of the measurement.

From Table 2.10, it is seen that the CME value measured by TGA/TMA method is about 3.5 to 6.6 times higher than that measured by DMA method. The TGA/TMA method test results are consistent with the results reported by other researchers [Tee, et al., 2004, Wong, et al., 2002] although large over-predictions of the TGA/TMA method have been reported in the literature. [Zhou, J., et al., 2005, Zhang, G. Q., van Driel, W.D., and Fan, X.J., 2006]

Another advantage of this method is the significant reduction in measurement duration needed. The regular TGA/TMA method will spend around 210 hours: 24 hours for dry baking of the sample, 168 hours for moisture absorption and 17 hours for the TGA and TMA tests during moisture desorption. However, the new method will need only around 42 hours, 24 hours for dry baking, 18 hours for the DMA measurement. In conclusion, this method is able to achieve 5 factor reduction of measurement time

In order to verify which CME values are more accurate, a bi-material warpage validation is performed using the aids of both experiments and simulations. However, for continuity of the structure of this thesis, these results will only be discussed in Chapter 4.

2.5 Thermal cycling effects on mechanical property of packaging materials

2.5.1 Introduction

In general, some of the packaging materials' properties used in simulations, such as T_g and Young's modulus, are assumed to remain constant but this assumption may not be valid. To the best of the author's knowledge, there are only a few papers [Simmons, et al., 2003, Butkus, et al., 1998, Kaush, et al., 2005, Kim, et al., 2002, Shimokawa, et al., 2002] addressing thermal cycling aging problems. These papers mainly focus on pure epoxy or fiber filled epoxy [Butkus, et al., 1998, Shimokawa, et al., 2002]. No aging problems for particle filled materials are reported in the literature. Hence, in this research project, thermal cycling effects on the mechanical properties of particle filled packaging materials are investigated. Two types of packaging materials are tested, namely the epoxy moulding compound and underfill.

2.5.2 Materials and sample preparation

Moulding compound

The same moulding compound as in section 2.3.4 is used in this research. The material is post-cured at 180ºC for 4 hours after being moulded. The final size of the samples is about 30x5x0.3mm^3.

Underfill

The same underfill material as in section 2.3.4 is used in this research. The sample is cured at 150ºC for 20 minutes in the oven. The final size of the samples is about 30x5x0.5mm^3.

Sample Pre-conditioning

Samples are dry baked for 24 hours at 125ºC in the oven in order to drive out the moisture in the sample. Then the samples are placed in a humidity chamber at 60ºC/60%RH for 40 hours. These samples are then subject to 1 cycle of reflow with the peak temperature of 260ºC.

Thermal Cycling

A dual chamber oven is used for thermal cycling test. In the dual chamber cycling, the loaded samples are placed on a moving platform that shuttles between stationary chambers that are maintained at two fixed temperatures.

Although 10 temperature cycling test conditions and 4 mode conditions are outlined in JESD22-A104 [JESD22-A104 2005], thermal cycles with a temperature range of 215ºC (-65 to +150ºC) and a ramp rate of less that 7 minutes is used in this research. The total duration of a single cycle is about 30 minutes. Samples are collected after 0, 30, 100, 300 and 400 cycles respectively.

DMA experiment

TA Instrument DMA Q800 (Dynamic Mechanical Analyzer) is used to carry out the DMA test with a test condition is 1ºC/min for temperature scanning.

2.5.3 Results and Discussion

The relationship for various cycles between the characterized storage modulus and tan δ response with respect to different temperature are shown in Fig. 2.32 and Fig. 2.33. Similar tests were done for underfill but not included here due to the limited thermal cycling effects on these two properties.

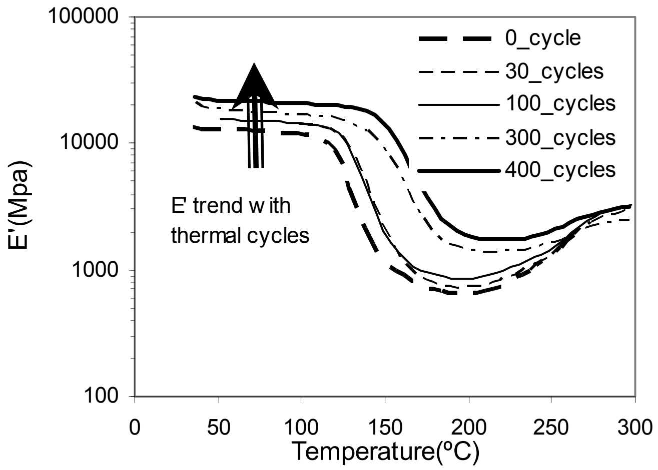

Fig. 2.32 Storage modulus (E') response vs temperature at 1Hz of EMC

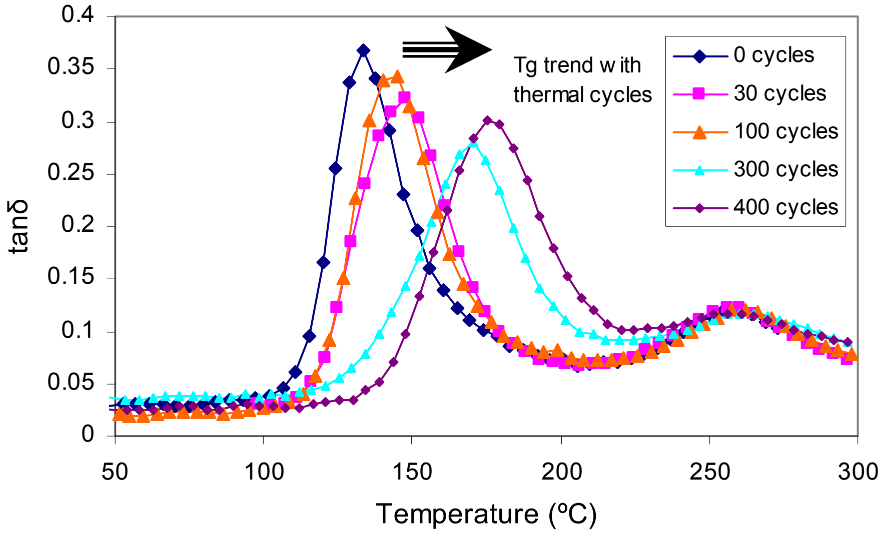

Fig. 2.33 Tan δ response vs temperature at 1 Hz of EMC

It can be seen from Fig. 2.32, the storage modulus increases with thermal cycles. Moreover, for all curves the rubber modulus increase above 200°C. This is most probably caused by extra cross linking reaction at high temperatures. T_g can be determined by the peak of the tan δ curves as shown in Fig. 2.33. It can be seen that T_g increases with thermal cycles. These two properties are discussed in detail below.

Thermal cycling effects on glass transition temperature

The results in Table 2.11 show that thermal cycling increases the glass transition temperature of the EMC. This increase is probably due to the increase in cross linking (as discussed above) as the sample is exposed to a temperature of 150ºC for a short duration during thermal cycling during a DMA scan, For the underfill, it can be seen that the glass transition temperature begins to decrease after a number of cycles, see Table 2-11. This result is consistent with Simmons et al., [Simmons, et al., 2003] observation. In Simmons' results, it is shown that different materials have different sensitivity to different treatments, such as thermal cycling, hot/dry, hot/wet and RT/wet conditions. A summary of thermal cycling effects on the glass transition of underfill and moulding compound is given in Table 2.11.

Table 2.11 Thermal cycling effect on T_g of underfill and EMC [DMA]

Cycle Numbers	T_g of underfill [ºC]	T_g of EMC [ºC]
0	149.3	122.1
30	153.5	131.9
100	156.8	128.9
300	160.7	150.0
400	153.6	154.0

Fig. 2.34 shows that the glass transition of moulding compound increases from 120ºC to 150ºC whereas the glass transition of the underfill increases from 149.3ºC to 160.7ºC after 300 thermal cycles. Hence, thermal cycling has more effects on EMC than on that of underfill for this thermal cycling range mainly due the thermal cycling range and the T_g of EMC and underfill.

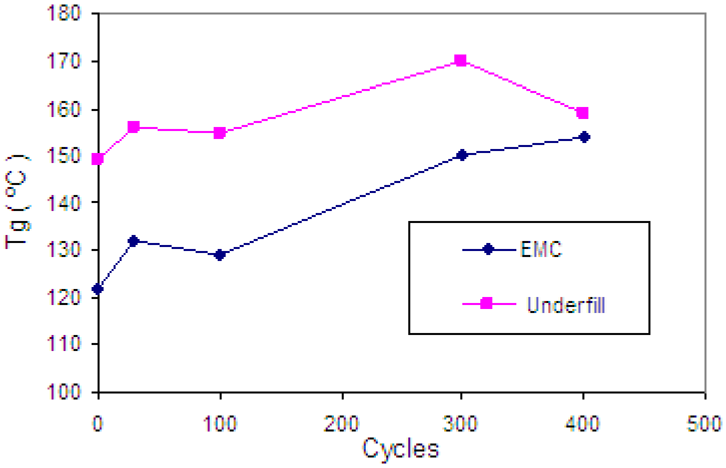

Fig. 2.34 Relation between T_g and thermal cycles

Thermal cycling effects on mechanical properties

Fig. 2.35 and Fig. 2.36 show the thermal cycling effects on the mechanical properties. It can be seen from Fig. 2.35 that the storage modulus of EMC gradually increases with the thermal cycling due to the extra cross linking reaction but for underfill it remains more or less constant.

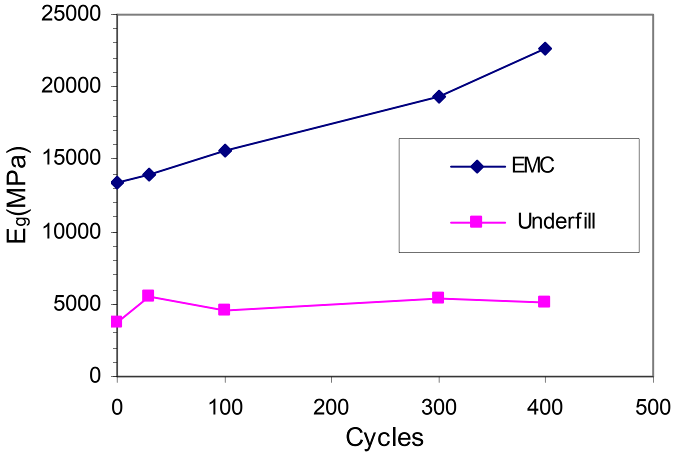

Fig. 2.35 Glass plateau vs thermal cycles of underfill

The thermal cycling effects on the rubber plateau are show in Fig. 2.36. It can be seen from Fig. 2.36 that the rubber plateau of moulding compound increases with the thermal cycles. This is probably caused by an extra cross-linking reaction at high temperature as discussed earlier. While for the underfill the rubber plateau is nearly constant within the thermal cycling range.

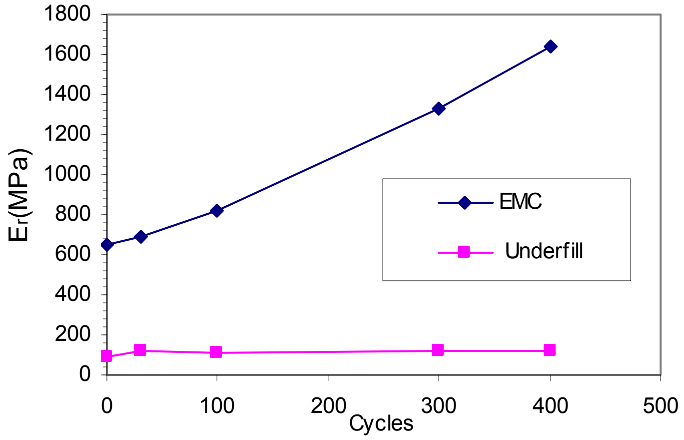

Fig.2.36 Rubber plateau vs thermal cycles of underfill

2.6 Conclusion

In this chapter, in depth study of moisture diffusion and moisture induced expansion are conducted.

Conclusions for moisture diffusion:

Moisture diffusion properties of EPN1180 with different filler contents are characterized. It can be seen from the characterized properties that the moisture saturation level decreases linearly with the filler content. Hence, a generalised moisture saturation equation is developed using this information which can be used for preliminary EMC selection. Result from the verification test showed that good agreement between the predicted value and the experimental result (the predicted M_{sat} and the characterized is 0.228 wt% and 0.194 wt% respectively for the condition of 85ºC/85%RH). Similar model has been developed for underfill in this research. Again, good agreements between the predicted and characterized M_{sat} values are observed. (0.762 wt% as compared to 0.892 wt%) for underfill at the condition of 85ºC/85%RH. This demonstrated the versatility of this model

Moisture diffusion coefficients are found to be temperature dependent. Our result show that higher temperature will result in a higher moisture diffusion coefficient for EMC, underfill and die attach. The moisture diffusion coefficients of EMC and underfill are similar whereas moisture diffusion coefficients of die attach is higher than that of EMC and underfill. This is because both EMC and underfills are silica particle filled packaging materials whereas the die attach’s fillers are mainly silvers base. Furthermore, die attach is in the rubbery phase for this temperature range. Moisture weight gain is also found to be highly temperature and relative humidity dependent since the moisture saturation level increase with higher temperature and relative humidity. These moisture coefficient and saturation models can then be used to predict moisture properties.

This research has also developed superior materials characterization techniques as part of the research. This is critical as it will not only speed up the characterization processes which is normally very time consuming, it is able to increases their accuracy too. For example, RH% steps at constant temperature methodology developed in this research could not only reduce the time duration needed for moisture diffusion characterization by 5 fold, it is also able to produce a more accurate results. Furthermore, the DMA plus moisture generator method is found to be more efficient than that of traditional TGA/TMA method used to determine moisture induced expansion. Compared to the regular TGA/TMA method, the CME characterization time is shortened from 210 hours to 42 hours.

Conclusions for thermal cycling effects on mechanical properties of EMC and underfill

Thermal cycling is also found to be able to increase the glass transition temperature, T_g for EMC, but has minimal effect on underfill. This may be due to the enhanced cross linking reaction at higher temperatures for EMC. However, T_g for underfill decreases after a certain number of cycling due to the materials degradation. Furthermore, the storage modulus of EMC gradually increases with the thermal cycling but it remains practically constant for the underfill. Rubber plateau of EMC increases with the thermal cycles while for underfill the rubber plateau is nearly constant within the thermal cycling range. This is critical since industries consider it to be constant in their FE models. This may induce significant error in their calculation.

References

Simmons, K.A., et al., Aging Characterization of Advanced polymer System, The Journal of Adhesion, Vol. 79, pp:1183-1205, 2003.

Butkus, L.M., et al., Tensile properties and Plane-Stress Fracture Toughness of Thin Film Aerospace Adhesives, J. of Adhesion, Vol. 66, pp:251-273, 1998.

Crank, J., The mathematics of diffusion, 2nd ed. Oxford: Clarendon Press; 1975.

Gils, M.A.J.van, Haberts, P.J.J.H.A, Zhang, G.Q., van Driel W.D. and Schreurs, P.J.G. Characterization and modelling of moisture driven interface failures, Microelectronics reliability, Vol. 44, pp:1317-1322, 2004.

Kausch, H.H. et al., The Effects of Degradation and Stabilization on the Mechanical Properties of Polymers Using Polypropylene Blends as the Main Expample, Macromol Science. Vol. 225, pp: 165-178, 2005.

Kim, Jungin, Woo, Il Lee, Tsai, Stephen W., Modeling of mechanical property degradation by short-term aging at high temperatures, Composites: Part B, Vol. 33, pp: 531-543, 2002.

Lee, K.C., Vythilingam, A., and Alpern, P., A simple moisture diffusion model for the prediction of optimal baking schedules for plastic SMD packages Microelectronics reliability, Vol. 45, pp:1688-1671, 2005.

Ma, Xiaosong, Jansen, K.M.B.,L.J. Ernst, van Drie, W.D., van der Sluis, O., and Zhang, G.Q., Charactrization and modeling of moisture absorption of underfill for IC pacakging, ICEPT Proceedings, pp:380-384, 2007.

Ma, Xiaosong, Jansen, K.M.B., Ernst, L.J., van Driel, W.D., van der Sluis O., and Zhang, G.Q., Charactrization of moisture properties of polymers for IC pacakging, Microelectronics Reliability, Vol. 9, pp:1685-1689, 2007.

Stellrecht, E., Han, B., Petch, M.G., Characterization of hygroswelling behaviour of molding compounds and plastic packages, IEEE Transactions on Component and Packaging Technologies, pp:499-506, 2004.

Shimokawa, Toshiyuki, et al., Effects of the thermal cycling on Micro-cracking and Strength Degradation of High-Temperature Polymer Composite Materials for Use in Next-Generation SST Structure, Journal. of Composite.Materials, Vol. 36(07), pp:885-895, 2002.

Tee, T.Y., Zhong, Zhaowei, Integrated vapour pressure, Hygroswelling, and thermo-mechanical stress modelling of QFN package during reflow with interface fracture mechanics analysis, Microelectronics reliability, Vol. 44, pp:105-114, 2004.

JESD22-A113F JEDEC, Pre-conditioning of Nonhermetic solid State Surface Mount Devices Prior to Reliability Test, 2006.

J-STD-020D IPC/JEDEC, Moisture/Reflow Sensitivity Classification for Nonhermetic solid State Surface Mount Devices, 2007

JESD22-A104C JEDEC, Temperature Cycling, May 2005.

JESD22-A120A, Test Method for the Measurement of Moisture Diffusivity and Water Solution in Oragnic Materials Used in Electronic Devices, 2001

Wong, E.H., Rajoo, R., Kon, S.W., and Lim, T.B., The mechanics and impact of hygroscopic swelling of polymer materials in electronic packaging, Transactions of ASME, Vol. 124, pp:122-126, 2002.

Yang, D.G, Cure-Dependent Viscoelastic Behaviour of Electronic Packaging Polymers, INBS 90-9022180-9, 2007.

Zhang, G. Q., van Driel, W.D., and Fan, X.J., Mechanics of Microelectronics, Springer, pp:311-320, 2006.

Zhou, J., Lahoti, S., and Sitlani, M., Investigation of non-uniform moisture distribution on determination of the hygroscopic swelling coefficient and finite element modeling for a flip chip pacakge, IEEE EuroSime, pp:112-119, 2005.

Zhou, J., Lahoti, S., and Sitlani, M., Investigation of inner-layer dielectric (ILD) failure by hygroscopic swelling, IEEE 55th ECTE, 2005.

Chapter 3

Characterization of Die Attach-Copper Interface Properties

3.1 Introduction

Interfacial delamination is one of the most common failure modes in the microelectronic packaging industry [Zhang, 2006, Ortiz, 1999 and Ferguson, et al., 2002]. Therefore, the ability to predict/simulate delamination is essential to the understanding of the reliability of these packages. As with any simulation, accurate interface properties at those critical locations are needed. Silver filled die attach is a typical adhesive used between the die and copper die pad for its improved heat dissipation capacity. However, delamination between die attach and copper die pad will severely impact the heat conduction and this will result in failure of the product. As mentioned above, the die attach-copper interface properties should be characterized in order to accurately predict this delamination. Hence, tri-material, copper-die attach-EMC, samples are made with the same packaging process as the one in the factory to characterize these material properties. A four point bending testing [Charalambides, 1989] system is established in this research in order to perform delamination tests at different temperatures. In addition, an optical system is used to capture a series of snapshot of the delamination processes. This will provide the delamination geometry information needed for determining the interface properties. Furthermore, the four point bending tests will be performed at room temperature, 40, 60, 85, and 150ºC respectively in order to investigate the effect of temperature on the interface toughness. In addition moisturized samples are also tested at room temperature and 85ºC to determine the effect of moisture on the interfacial properties. However, experiments alone is not able to quantify the interface properties, numerical simulations of the four point bending test have to be performed by using a finite element model comprising cohesive zone elements is needed. Cohesive zone method is used since it is known to be able to describe the transient delamination process [Sluis, 2011]. By means of an extensive model parameter sensitivity study, a method has been developed to determine the critical opening value. This critical opening value can be obtained by fitting the relation between measured delamination lengths in the horizontal direction along the interface to the delamination length (maximum opening) in the vertical direction.

Fracture mechanics has been studied extensively for predicting cracks behaviour [Friedrich, K., 1989, Nestor Perez, 2004, Crews, et al., 1998, Reeder, et al., 1991]. There are three modes of crack extension in fracture mechanics: the opening mode, sliding mode and tearing mode (see Fig. 3.1). The opening mode (see Fig. 3.1(a)), Mode I, is characterized by the symmetric separation of the crack surfaces with respect to the plane. The sliding mode (see Fig. 3.1(b)), Mode II, is characterized by the displacement in which the crack surfaces slide over one another perpendicular to the leading edge of the crack. The tearing mode (see Fig. 3.1(c)), Mode III, is characterized by the surfaces sliding over each other in the direction that is parallel to the leading edge. Mode I and II are common failure modes.

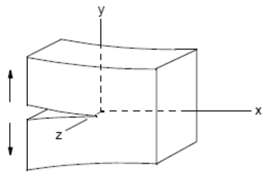

Fig. 3.1(a) Opening mode

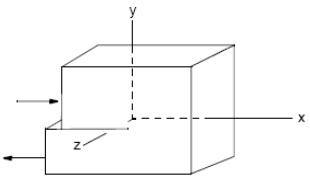

Fig. 3.1(b) Sliding mode

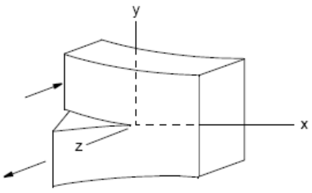

Fig. 3.1(c) Tearing mode

Since different failures are caused by different loadings, different test methods are needed for investigating different failure modes. Fig. 3.2 summarized the different set up in the literature that has been employed to investigate using different loadings. The mode II test, see Fig. 3.2(a), (b), (c) remains controversial for practical reasons, such as unstable propagation in the end notched flexure (ENF) sample, friction effects and difficulty in defining a starter defect. Furthermore, Figure 3.2(d) shows the double cantilever beam (DCB) sample for investigating

Mode I failure using the Irwin-Kies equation [Davies, et al., 1998]. The sample for mixed mode bending (MMB), Fig. 2(e) as introduced by Reeder, Crews and Reeder [Crews, et al., 1998, Reeder, et al., 1991] has become the most widely used sample for the determination of mixed mode envelopes. Furthermore, MMB are suitable for bi-material samples.

For the tri-materials samples and fast interface properties characterization, some modifications are needed to ensure that the delamination occurs at the required interface. Based on Charalambides work [Charalambides, et al., 1989], a four point bending Mode I/II tool (see Fig. 3.2(f)) is designed and constructed in this research. This test method is able to produce not only stable delamination, it is able to produce reproducible results [Ma, et al., 2010] (see section 3.3).

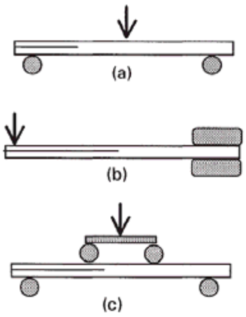

Fig. 3.2 Mode II, (a) ENF (end notched flexure); (b) ELS (end-loaded split); (c) 4-point ENF.

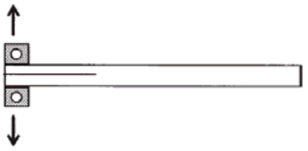

Fig. 3.2(d) Mode I, DCB

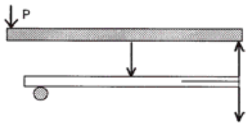

Fig. 3.2(e) Mode I/II mixed

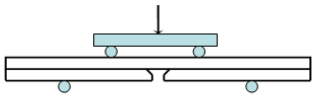

Fig. 3.2(f) Mode I/II mixed

3.2 Sample Preparation

Tri-material sample

In order to obtain the similar interface toughness as in the actual package, samples are made with the exact same packaging processes as in their factory. The test samples are tri-material strips consisting of copper layer (0.2mm in thickness), epoxy moulding compound layer [EMC] (0.6mm in thickness) and a die attach adhesive (60μm) layer in between. The sample nominal dimension is 60x9x0.85mm^3.

Due to the difficulty with the application of the die attach, the die attach glue is not always uniformly distributed between copper and EMC layers, (see Fig. 3.3). These samples cannot provide accurate critical load values for delamination. Therefore, a method to control the uniformity of die attach layer is needed. A thin layer of adhesive glue is dispensed on the surface of the copper lead frame by using a flexible foil stencil that is fixed in a frame as shown in Fig. 3.4(a). Fig. 3.4(b) shows the glass blade which is used to dispense the die attach glue. Fig. 3.4(c) and Fig. 3.4(d) shows the lead frame before processing and after moulding.

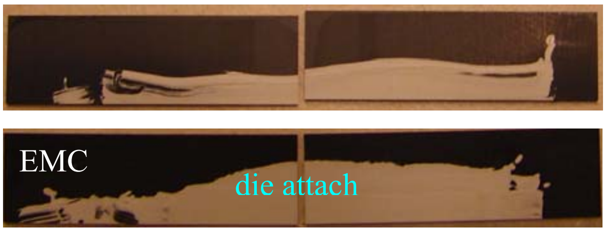

Fig. 3.3(a) Insufficient die attach on samples

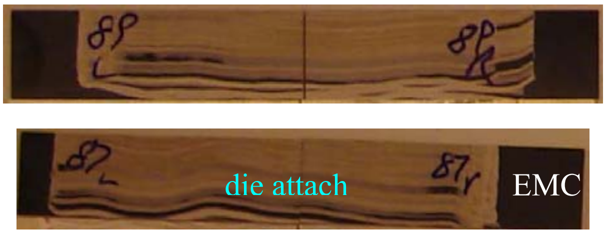

Fig. 3.3(b) Non-uniform die attach application

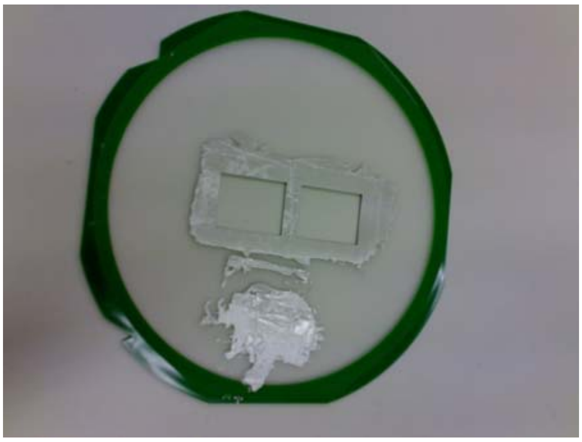

Fig. 3.4(a) Stencil for die attach dispensing

Fig. 3.4(b) Blade for die attach dispensing

Fig. 3.4(c) Lead frame before processing

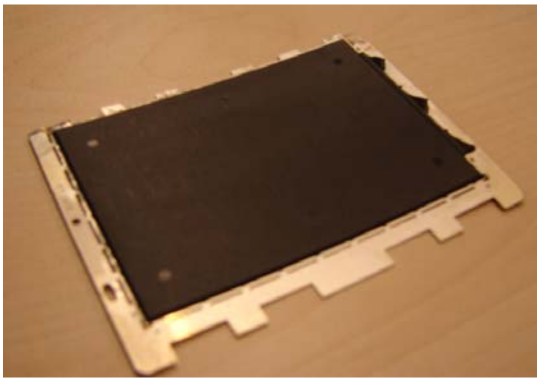

Fig. 3.4(d) Leadframe + die attach + EMC after moulding

The thickness of the adhesive glue on the surface of the lead frame is controlled by the thickness of the stencil foil in order to ensure that the die attach glue is uniformly distributed, see Fig. 3.5(a). The die attach thickness is around 60μm as shown in Fig. 3.5(b).

Fig. 3.5(a) Uniformly distributed die attach

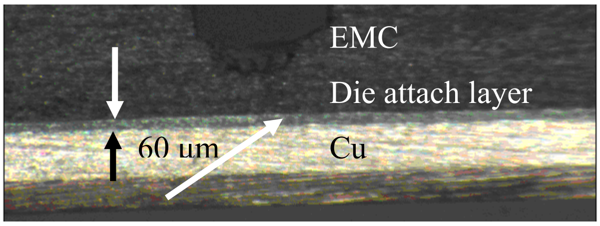

Fig. 3.5(b) Uniform die attach thickness layer

After dispensing the die attach glue, samples are cured in a pre-heated oven at 180°C for 15 minutes. Then the leadframe is placed in the mould and the EMC is moulded in a pre-heated mould at 180°C within 60 seconds. The final map mould is as shown in Fig. 3.6(a). Before cutting the sample, the map mould is post cured at 175°C for 4 hours to ensure that the epoxy moulding compound is fully cured. Then the map moulds are cut into 60x9x0.85mm^3 strips as shown in Fig. 3.6(b).

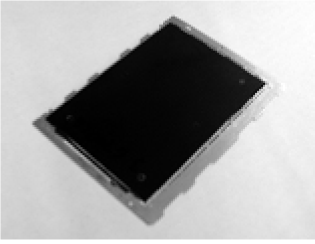

Fig. 3.6(a) Map mould

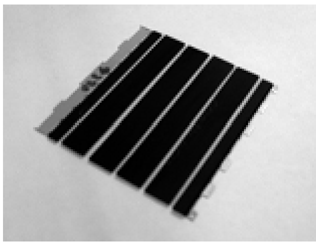

Fig. 3.6(b) Cut samples

To trigger the interface delamination, a pre-defined notch (0.5mm wide and 80% depth of EMC) is created in the epoxy moulding compound materials by dicing saw. This notch is to ensure that crack occur in EMC first before it penetrate into die attach layer. The geometry and dimensions of the sample are shown in Fig. 3.7.

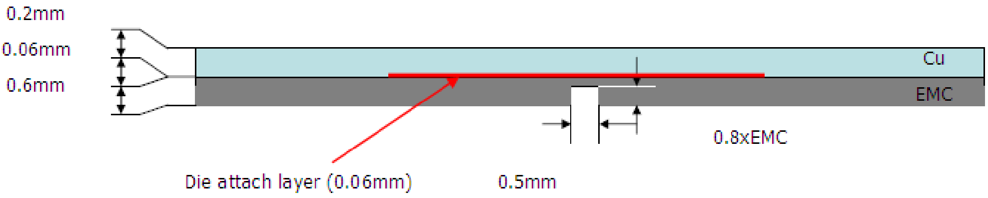

Fig. 3.7 Geometry and dimensions of the sample

3.3 Four point bending test setup

3.3.1 Four point bending tool

A four point bending tool is designed and manufactured to investigate the interface properties. Fig. 3.8 schematically shows the test setup whereas Fig. 3.9 shows the actual four point bending tool, which consists of three main parts. They are the four point bending frame which is used to support the two rollers, the two rollers, which are used to support the test sample and the loading head for applying displacement or loading to the test sample as shown in Fig. 3.10. In order to decrease the friction between the rollers and the moulding compound layer of the test sample, two rollers are designed in such a way that they are allowed to rotate freely. The two rollers are supported by ball bearings. Silicon lubricant grease is also used in the bearings to ensure the proper functioning of the setup at the high elevated temperatures. The loading head is also allowed to rotate to ensure that the loading force and supporting force are parallel to each other.

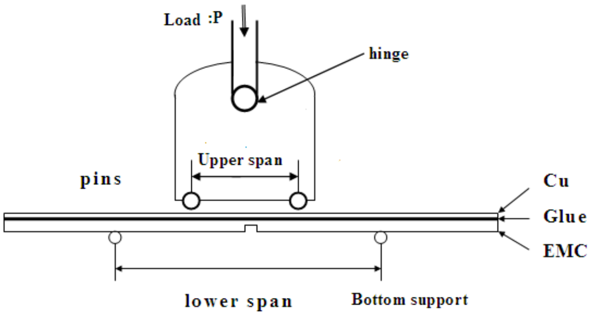

Fig. 3.8 Schematic overview of four point bending test setup

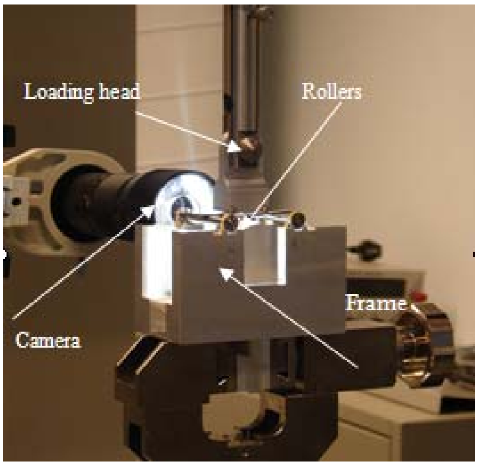

Fig. 3.9 Four point bending tool setup

3.3.2 Loading system and optical system

Fig. 3.10 shows the universal tester Zwick/Roell Z005 used in this research. Displacement control with a loading rate of 0.1mm/min in the downward direction is used in this set-up.

Furthermore, the reaction force of the loading head is measured by the force sensor. In order to monitor the deformation and delamination between die attach and copper, a Keyence optical camera system is mounted at the back of the bending tool, as shown in Fig. 3.9.

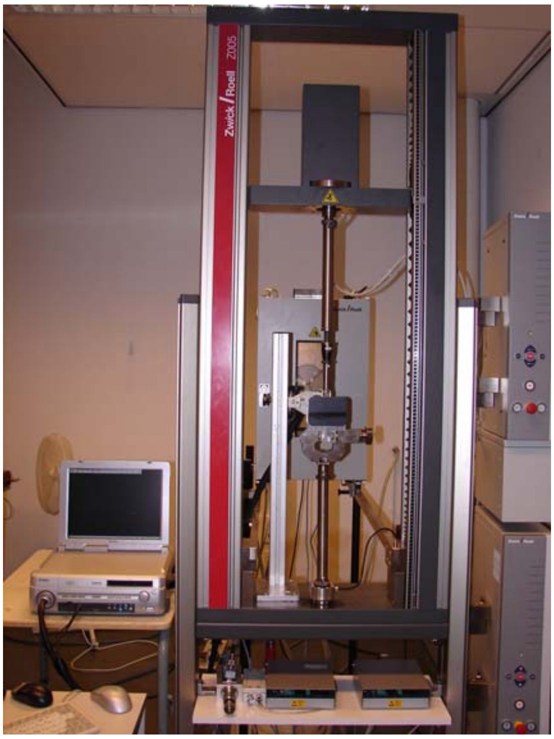

Fig. 3.10 Zwick Roell test bench with four point bending delamination setup

3.4 Four point bending experiments

3.4.1 Four point bending test crack and delamination processes

In order to investigate the temperature influence on interface toughness, four point bending tests are performed at different temperatures. Fig. 3.11 to Fig. 3.14 depicts the typical steps of four point bending tests, from the onset of the delamination to delamination propagation. Their corresponding relationship between displacement and loading in this experiment is shown in Fig. 3.15. Using different loading rates of 0.05, 0.1 and 0.2 mm/min, experiments are found that the loading speeds have no effects on the “allowable load”.

The initial state of the three layers before loading is shown in Fig. 3.11. The thickness of glue layer is approximately 60μm and is uniformly distributed between the copper and the moulding compound layer.

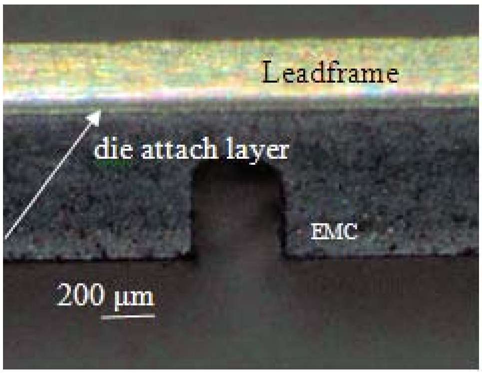

Fig. 3.11 Initial state of the notch

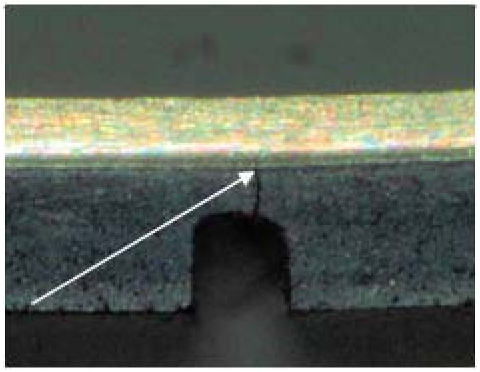

Fig. 3.12 Initial moulding compound crack

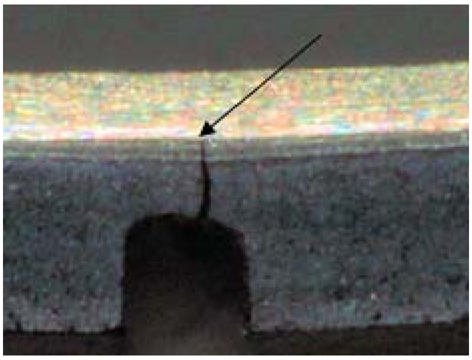

Fig. 3.13 Initial delamination

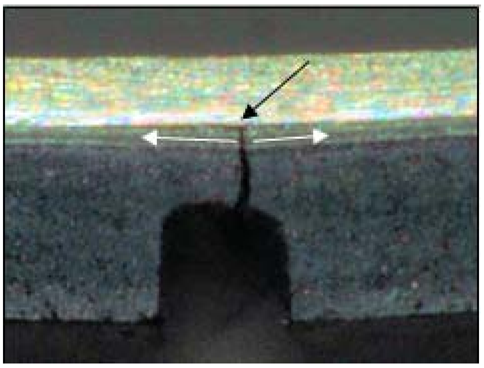

Fig. 3.14 Delamination propagation

Initially when the load head first engage with the test sample, it deforms elastically as shown in Fig. 3.15. At some critical displacement, a sudden load drop is detected and this corresponds to the cracking of the EMC notch. The EMC notch then propagates through the moulding compound towards the interface as shown in Fig. 3.12.

The crack then penetrates through the die attach layer very quickly and reaches the interface between the glue and copper, (see Fig. 3.13). This load continues to increase until the interface delamination starts and propagates along both sides between copper and die attach glue as shown in Fig. 3.14. In Fig 3.14, the top arrow marks the delamination location between the copper and die attach while the two bottom arrows marks the propagation direction along both sides.

When this load starts to decrease as shown in Fig. 3.15, this signals the start of the delamination. After the delaminations at both sides have started, the crack propagation load “stabilizes” around a constant value. With this stabilize value, the interface fracture toughness value can then derived with the aid of the results of numerical simulations (see section 3.5). The analytical expression for G_c (Eq. 3.2) is used to calculate the initial interface toughness value.

By adjusting this G_c until the simulated constant delamination load is equal to the measured constant delamination load, the interface toughness at this temperature is corresponded to the G_c value in the simulation. Lastly, in order for the correct G_c to be characterized, care has been taken to ensure that all the delamination is between copper and die attach glue.

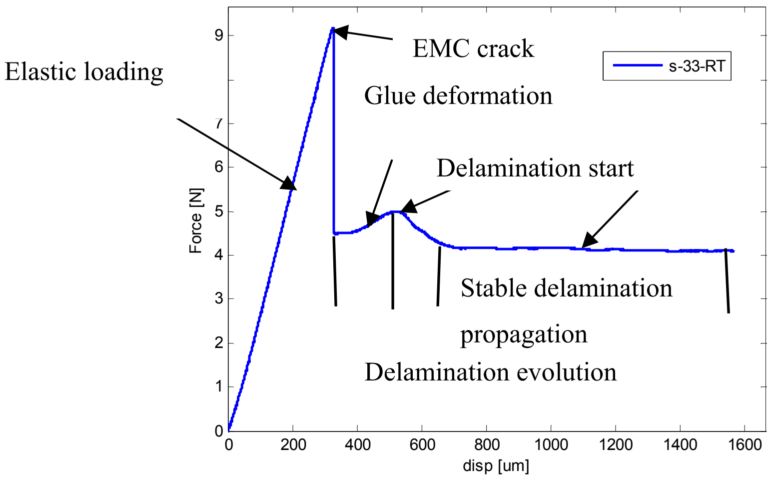

Fig. 3.15 Relation between displacement and load

3.4.2 Test results at different conditions

Test results at different temperatures of dry samples

Fig. 3.16 shows the responses of four repetitive tests at room temperature. The stable crack propagation force is reproducible within error of 0.1N. Detailed test results at 150ºC are shown in Fig. 3.17.

Fig. 3.18 shows the response of the four point bending tests at 40, 60, 85 and 150ºC respectively and these results show that the temperature has a great influence on the critical crack propagation load. This implies that the interface toughness decreases with increasing temperature. Furthermore, Fig 3.18 also shows that the shapes of the response curves are a bit different due to the temperature effect. The initial stiffnesses of the samples at different temperatures are different due to the temperature dependent mechanical properties of the samples' materials. Furthermore, the response curve of 150ºC is different from the results at other temperatures during elastic loading as since the test is conducted at a temperature higher to than the T_g of EMC which is about 110°C. Their slope (stiffness, as shown in Fig. 3.18) is smaller due the higher temperature effects on EMC.

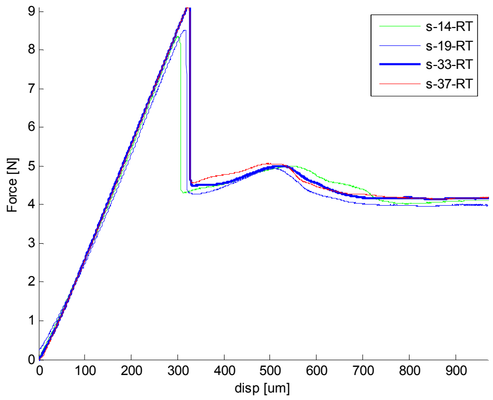

Fig 3.16 Response of four point bending at room temperature

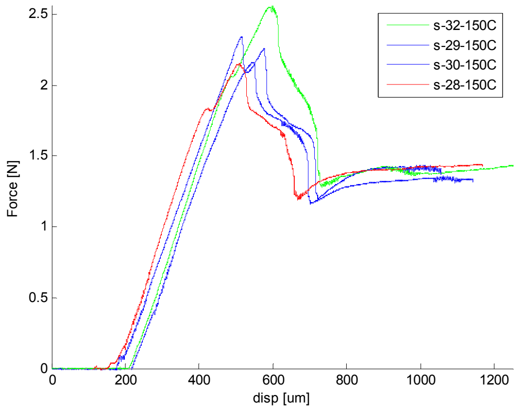

Fig. 3.17 Response of four point bending at 150ºC

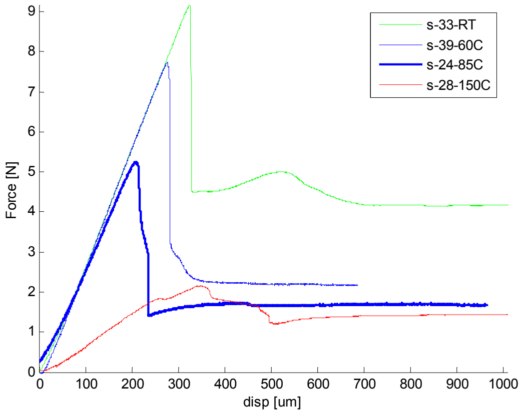

Fig. 3.18 Response of four point bending at different temperatures

Test results at different temperatures of wet samples

In order to investigate the moisture effects on the interface toughness, test samples are placed in a humidity oven at 85ºC/85%RH for at least 48 hours in order for it to reach moisture saturation. Four point bending tests are then performed at room temperature and 85ºC respectively after moisture pre-conditioning. Since moisture absorption and desorption is a much slower processes as compared to the delamination test (see the moisture diffusion coefficient in Table 2.5), only the moisture at the surface of the EMC layer desorps a little while 99% moisture still remains in the interface between the die attach and the copper leadframe (see Chapter 2) in the short 5 minutes needed to perform the delamination test. Therefore, under these conditions, minimal changes on the moisture concentration at the interface are expected.

Table 3.2 shows the average crack propagation load for both dry and pre-conditioned samples. Test results show that the average crack propagation load of the pre-conditioned sample at room temperature and 85ºC are almost identical to that of the dry sample tested both at room temperature and 85ºC respectively. This means that moisture has apparently no effect on the interface toughness between the die attach and copper leadframe for this carrier. This is unexpected, since it is generally assumed that moisture at the interface weakens the adhesion [Ferguson, et al, 2002]. This “unexpected” result may be due to the type of resin used in this research. Die attach uses BIM (bismaleimide) as resin, for their low induced stress on the metal substrate while EMC uses epoxy as resin. This type of die attach is known to be “hydrophobic” and relatively stable at high temperature from supplier.

3.5 Characterization of cohesive zone interface properties

3.5.1 Material properties of the test sample

The main material properties used in the test sample and simulations are summarized in Table 3.1.

Table 3.1 Material properties [NXP]

Materials	E (GPa)	v [-]	CTE (ppm/ºC)
Copper Lead frame	120	0.33	17.5
Die attach	Visco-elastic	0.3	69, T < -64, 152, T > -64
EMC	Visco-elastic	0.25	6, T < 110, 30, T > 110

3.5.2 Interface toughness analytical equation

The critical interface fracture toughness, G_c can be deduced analytically by taking the difference in the strain energy of a uncracked and cracked beam. Since there is negligible strain energy in the beam above the crack, G_c can hence be deduced from just the consideration of energies in the uncracked section, and the lower section below the crack. Using the Euler-Bernoulli theory and plane strain conditions, these energies can be expressed in terms of the applied moment M [Charalambides, et al., 1989], see Fig. 3.19.

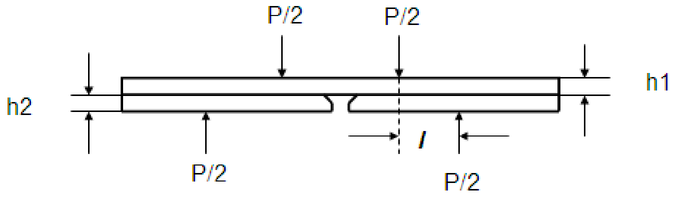

Fig. 3.19 Schematic sample for four point bending

$$U=\left(1-\upsilon^2\right)M^2/2EI \tag{3.1}$$

where U is the strain energy per unit cross-section and I is the second moment of area per unit width, G_c can then derived into Eq. 3.2

$$G_C=\frac{M^2\left(1-\upsilon_2^2\right)}{2E_2}\left(\frac{1}{I_2}-\frac{\lambda}{I_C}\right) \tag{3.2}$$

where I_2 and I_c are second moment of inertia per unit cross-sectional area for the bottom layer and the composite beam, respectively, and

$$\lambda=E_2\left(1-\upsilon_1^2\right)/E_1\left(1-\upsilon_2^2\right) \tag{3.3}$$

$$I_2=\frac{1}{12}h_2^3 \tag{3.4}$$

$$I_C=\frac{1}{12}h_1^3+\frac{\lambda}{12}h_2^3+\frac{\lambda h_1 h_2\left(h_1+h_2\right)^2}{4\left(h_1+\lambda h_2\right)} \tag{3.5}$$

The subscript 1 indicates quantities relevant to the top layer, whereas the subscript 2 denotes the corresponding quantities for the bottom layer. Subscript c refers to the composite beam. Note that the moment per unit width can be computed using $M= PI/2B$, with P is the constant load and I is the spacing between inner and outer span. Hence, by using Eq. 3.2, an analytical expression for G_c can be obtained. This G_c value can be used initially to estimate the crack propagation load in the simulation model (see Table 3.2). The corresponding G_c values are then derived as outlined in section 3.5.3. Temperature effects on Young's modulus are considered in Eq. 3.2. However, moisture effects are not considered the Eq. 3.2 since moisture effects on EMC mechanical properties are very limited.

Table 3.2 G_c value of equation and simulation

Temp (ºC)	Load (N)		G_c (J/m^2)	
	Dry	PRECON85ºC/85%RH	Dry, Eq. (3.2)	Dry Simulation

25	4.1	4.0	27.2	26.5
40	2.75	x	12.2	13
60	2.1	x	7.1	8
85	1.7	1.76	4.7	5.6
150	0.71	x	3.0	1.9

3.5.3 Interface toughness numerical model

In addition to the analytical model, the interface toughness G_c can be obtained by matching the simulated G_c value for the crack propagation load with the experimental propagation load.

A four point bending model (see Fig. 3.20), is constructed in the finite element package MSC.Marc and Mentat. Due to the symmetry of the model, only half of the sample is modelled. The top layer is copper and the bottom layer is EMC. The vertical displacement is assumed to be fixed at the bottom support (see arrow bottom supports). The top load is directed downwards. Symmetry_dx fixes displacement of all symmetric nodes in the horizontal direction. Symmetry_4PB boundary conditions fix the displacement of only symmetric nodes of the copper layer in horizontal direction. In order to mimic the actual initial stress state, residual stress due to the moulding process is modeled in the analysis.

Four stages are prescribed in the simulation model. The first stage is the modeling of the cooling down from the initial condition of 175ºC to room temperature. The second stage is the heating up from room temperature to the test temperature whereas the third stage is the stress relaxation at the test temperature. Finally, the last one is the four point bending stage. The temperature is kept at the test temperature and other boundary conditions of bottom support, top load and symmetry_4PB is prescribed in this stage. Top loading with displacement control is also enforced.

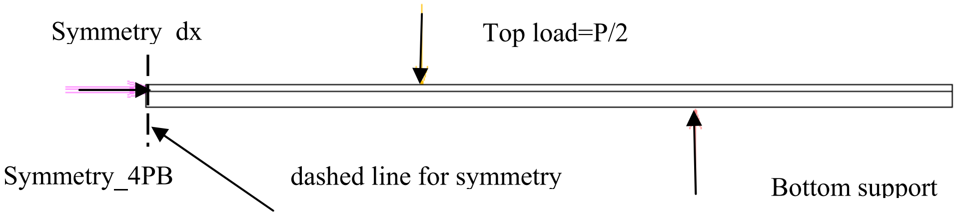

Fig. 3.20 2D four point bending FE model

3.5 4 Cohesive zone element

The simulation package MSC Marc/Menta has a library of interface elements, which can be used to simulate the onset and propagation of delamination. Although J-integral calculation could also be supported by the simulation package, cohesive zone is more suitable for simulating the transient delamination [Sluis, 2011]. Since this research focus on predicting the transient delamination in the 3D package model, cohesive zone method is employed in this research. The constitutive behaviour of these elements is expressed in the terms of tractions versus relative displacements between the top and bottom edge/surface of the elements, as schematically shown in the Fig. 3.21(a). The initial thickness of the element between top and bottom edges is zero when no traction force is applied.

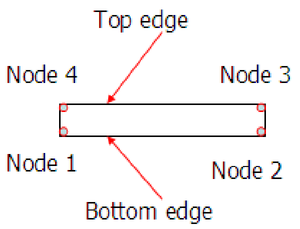

Fig. 3.21(a) 2D Interface element

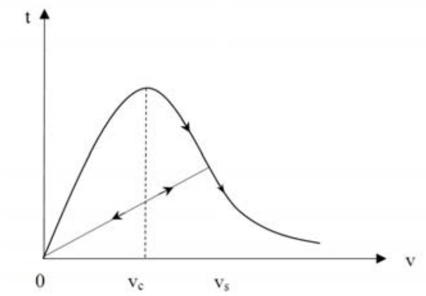

Fig. 3.21(b) Exponential model

In Fig. 3.21(b), the traction *t* is introduced as a function of effective opening displacement *v*. It is characterized by an initial reversible response and the irreversible damage once the critical effective opening displacement v_c has been reached. An exponential function is used in the simulation to describe the traction *t*.

$$t = G_c \frac{v}{v_c^2} e^{\frac{-v}{v_c}} \tag{3.6}$$

in which G_c is the interface toughness.

It can easily verify that the maximum effective traction t_c, corresponding to the critical effective opening displacement v_c and it is given by [MSC, 2008, Ortiz, and Pandolfi, 1999]:

$$t_c = \frac{G_c}{e v_c} \tag{3.7}$$

If the maximum effective traction is known, the critical or effective opening displacement can then be determined by:

$$v_c = \frac{G_c}{et_c} \tag{3.8}$$

Damage (i.e., irreversible behaviour) is considered to start when the opening displacement reaches the critical opening value. Hence, G_c can be extracted using four point bending tests and FE simulation of the fitted crack propagation load using the following procedure: G_c values is first predicted from analytical equation and this is served as an initial input for our FE simulation. A optimization algorithm using FE simulation is performed until simulation load matches the measured load, the actual G_c can that optimizes G_c (see simulation results in Fig. 3.22).

Fig. 3.22 shows typical four point bending delamination simulation results where the relationship between applied displacement and load for different temperatures. Note that the loading peak that is typical observed in the experimental curves (Fig. 3.15) is absent in the simulation. This is because our simulation cannot capture the physic when EMC crack starts suddenly. The mesh size is chosen such that convergence of the results is obtained.

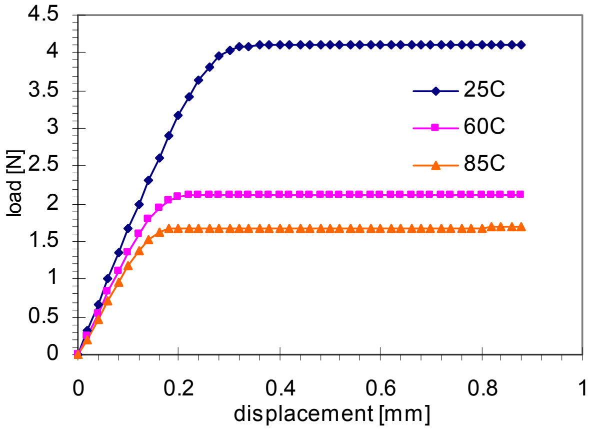

Fig. 3.22 Fitted load by changing G_c

Table 3.2 summaries the theoretical propagation load, G_c values from Eq. 3.2 and simulation (dry). The x in the table indicates that experiments are not conducted at these conditions. The wet G_c simulation value is not calculated due to the very limited moisture effects on polymer materials. From Fig. 3.23, it can be seen that these two curves are in good agreement with each other and that G_c value decreases rapidly with increasing temperature. As discussed, tests results show that moisture has no effects on the G_c value for our material system.

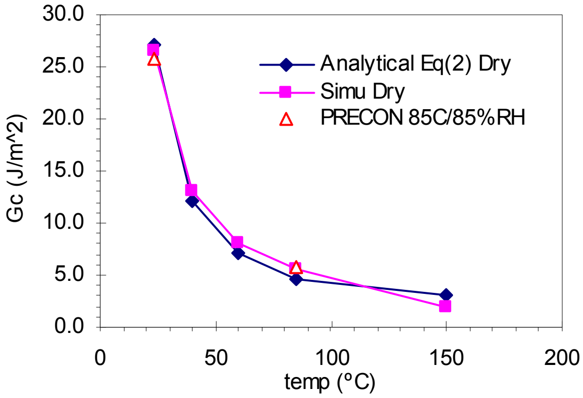

Fig. 3.23 Temperature and moisture effects on G_c value

3.5.5 Determination of the interface critical opening

Interface toughness and critical opening are two important cohesive zone material properties needed for conducting delamination's simulations. The determination of the interface toughness is relatively standard, as discussed in the previous section but there is a lack of standard tests for critical opening measurement. In order to extract the critical opening parameter from the sample's delamination test, a special optical camera experimental set-up is installed (see Fig. 3.24, A, B, C and D indicate all the set screws for focusing camera).

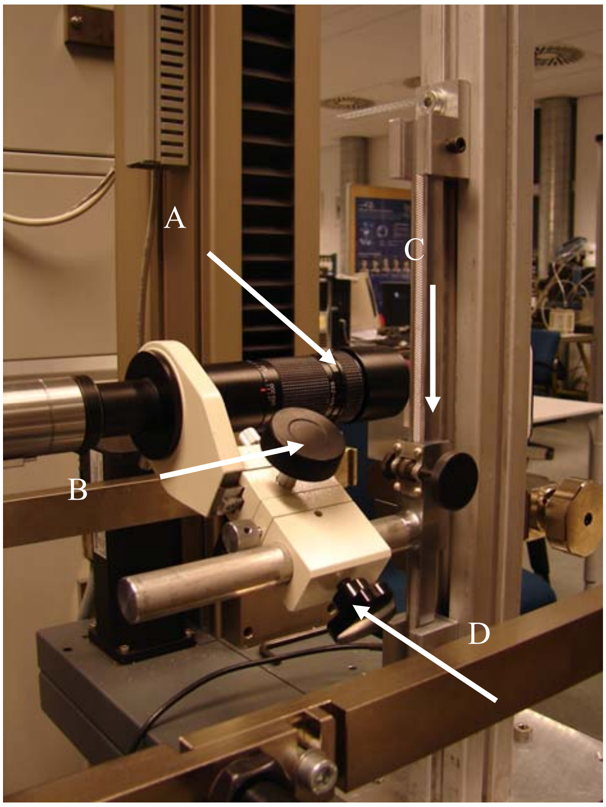

Fig. 3.24 Delamination test with camera setup.

A: Fine camera set screw, B: Rough camera set screw

C: Vertical set screw, D Rotation angle set screw

The Keyence optical camera system is placed at the back of the four point bending tool frame to monitor interface delamination during our experiment. The camera can be manually adjusted to track of the movement of the sample as the loading is applied to the sample. A series of pictures were taken at the start and during propagation of delamination.

In the work by Sluis [Sluis, et al., 2010], the critical opening parameter is determined by analyzing the local deformation around the crack tip in the samples. Using this method, the critical opening value can be deduced using results from the experimental measurements and simulations.

Fig. 3.25(a) shows a snapshot of our simulation result at certain delamination length (schematically indicated by length E). Although not shown in Fig 3.25(a), the delamination length is found to be dependent on the values of the critical opening. When the damage value reaches 1 at the interface nodes, the cohesive zone element will be fully damaged. Fig. 3.25(b) shows four point bending results with the same G_c value but with different critical opening values. When the load reaches a stable value, a steady-state delamination is reached. Therefore, different critical openings result in different energy consumption before steady-state delamination is reached. Due to these energy differences, the energy for delamination is different and hence, different delamination lengths can then be obtained from using different critical opening values.

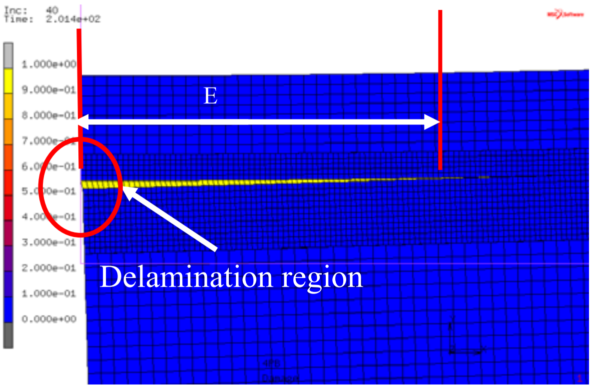

Fig. 3.25(a) Simulation result of delamination; contour bands denote the damage values D

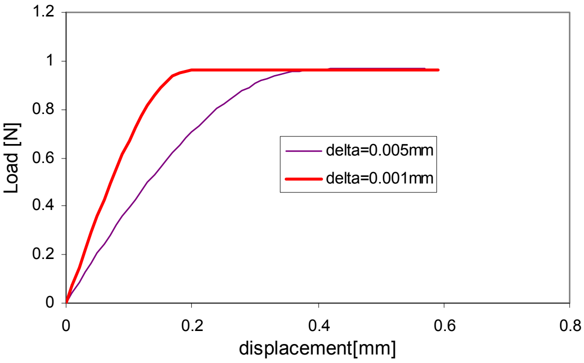

Fig. 3.25(b) Four point bending results with different critical opening values

Fig. 3.26(a) is an enlargement of Fig. 3.25(a), which shows another delamination parameter, the interface opening at the symmetry line. Our simulation suggests that this vertical distance between point M and point N in vertical direction (maximum opening) is independent of critical opening values. This is because delamination depends only on the G_c and not on the critical opening value after steady-state delamination is reached. Combining Fig. 3.25(a) and Fig. 3.26(a), the relationship between maximum opening length and delamination length can be deduced. Hence, the curves with different critical value ranges can then be determined (see Fig. 3.28).

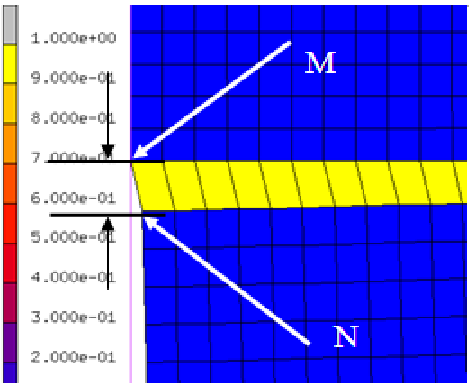

Fig. 3.26(a) The interface opening at symmetry line

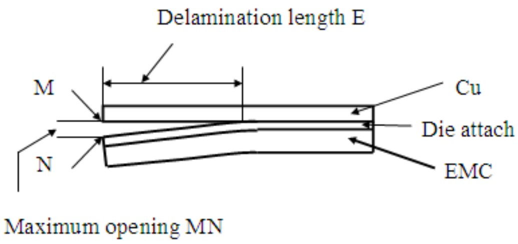

Fig. 3.26(b) Schematic figure of Fig.2.26(a)

The test procedure is similar as in section 3.4.2 with the exception of the displacement speed of the clamp head of the four point bending tool. The loading speed is decreased from 0.1 to 0.05 mm/min in order to allow more snapshot of the delamination. The displacement speed has found to have minimal effect on the measured critical delamination force applied to the sample. Fig. 3.27 shows one of the typical delamination snapshot with the measured dimensions. Horizontal delamination lengths are 166 (left side) and 169µm (right side) respectively. The measuring error of the delamination length and maximum opening are also found to be around 5%. A few of delamination snapshots can be taken in each test for critical opening calculations.

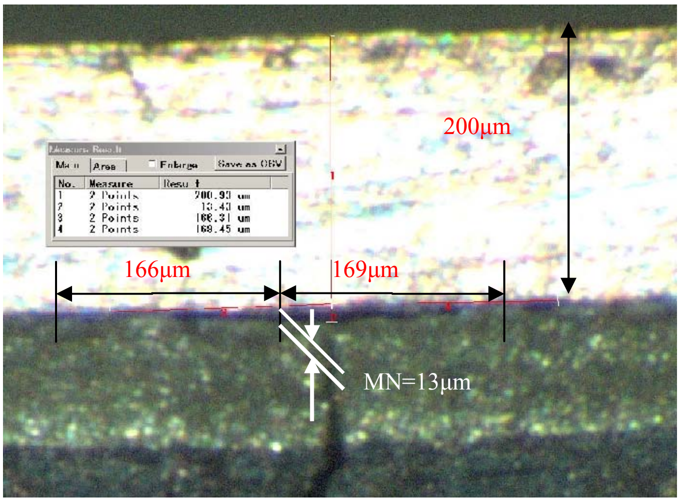

No.	Measure	Result
1	2 Points	200.93 um
2	2 Points	13.43 um
3	2 Points	166.31 um
4	2 Points	169.45 um

Fig. 3.27 Delamination measurements

The symbols with different shapes in Fig. 3.28 represent results from different sample whereas symbols with the same shaped represent the results from the same sample but with different delamination lengths at different stages of the delamination.

The two curves depict the simulation results using different critical opening values. It is evident that the delamination length increases with increasing vertical delamination MN. Furthermore, the results from all the tests fall between the two simulation curves with critical opening values of 0.5 to 1.0µm. Hence, it can be concluded that the critical opening at room temperature is between 0.5 and 1.0µm. The variation of the critical opening is largely due to the movement of the test sample and the vibration during the test.

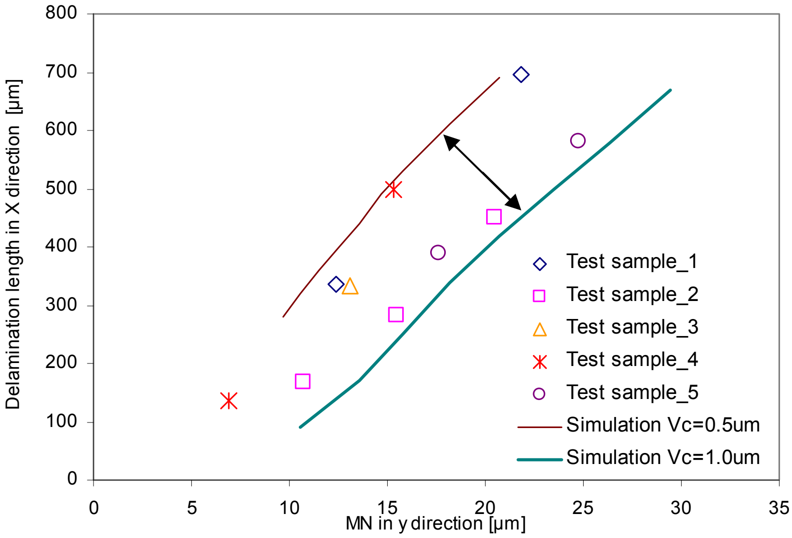

Fig.3.28 Comparison of results between tests and simulations

Since this optical camera system can not be used in the oven, the critical opening value at higher temperatures and below room temperature is not determined. However, it can be seen from Table 3.2 that the critical delamination force decreases with increasing temperature. This is because the ability for their resistance force to withstand deformation becomes smaller as the interface properties decrease. Maybe, the critical opening value would be temperature dependent. At high temperatures the critical opening value would be expected to be larger than that at lower temperatures due to the tougher interface behaviour.

3.6 Conclusions

The cohesive zone method has been employed successfully in this research to model the delamination since the predicted interface toughness from numerical simulations has good agreement with the analytical equation.

From a series of four point bending tests and cohesive zone simulation, it is shown that temperature has a large effect on the interface toughness with the G_c value decreases significantly with increasing temperature. In addition, moisture has been found to have no effect on the interface toughness of copper and die attach interfaces in our samples. This result is different from other interface, such as EMC and copper [Ferguson, et al, 2002]. The main reason is the binder used in EMC and die attach. The binder used in EMC and underfill is epoxy resin whereas the binder used in die attach is BIM (bismaleimide) resin.

.

Using results from both experimental tests and cohesive zone simulations, the critical opening is found to be between 0.5 to 1.0μm at room temperature.

These two interface properties will be used in Chapter 5 to predict the possibility of delamination in microelectronic packages model.

References

Charalambides, P.G., A Test Specimen for Determining the Fracture Resistance of Bimaterial Interface, Journal of Appllied Mechanics, Vol. 56, pp:7-82, 1989.

Crews, J. H. and Reeder, J. R., A Mixed-Mode Bending Apparatus for DelaminationTesting, NASA TM 100662, 1988.

Davies, P., Blackman, B.R.K., and Brunner, A.J., Standard Test Methods for Delamination Resistance of Composite Materials: Current Status, Applied Composite Materials, Vol. 5(6), pp. 345-364, 1998.

Ferguson, T., and Qu, J.M., Effect of Moisture on the Interface adhesion of the Underfill/Soder Mask Interface, Journal of Electronic Packaging. Vol. 124(2), pp:106-110, 2002.

Friedrich, F., Application of Fracture mechanics to composite materials, Elsevier, 1989.

Hashemi, S., Kinloch, A. J., and Williams, J. G., Corrections needed in double-cantilever beam tests for assessing the interlaminar failure of fibre-composites, Journal of Material Science Letter 8, pp: 125-129, 1989.

Hashemi, S., Kinloch, A. J., and Williams, J. G., The Analysis of Interlaminar Fracture in Uniaxial Fibre-Polymer, Proc. Royal Soc. A 427, pp:173-199, 1990.

Hojo, M., Kageyama, K. and Tanaka, K., Pre-Standardization Study on Mode I Interlaminar Fracture Toughness Test for CFRP, Japan Composites, Vol. 26(4), pp:243-255, 1995.

Ma, X.S., Jansen, K.M.B., Ernst, L.J., van Driel, W.D., van der Sluis. O., Zhang, G.Q., Regards, C., Guitier, C., and Frémont, H., "Die attach Interface Property Characterization as Function of Temperature Using Cohesive Zone Modelling Method," International Conf. on Thermal, mechanical and multiphysics simulation and experiments in Micro-Electronics and Micro-Systems, EuroSime2010, 2010, pp: 647-654.

MSC.Marc/Mentat, volue A, 2008 r1, 2008.

Nestor Perez, Fracture Mechanics, Kluwer Acadamic Publishers, ISBN:1-4020-7745-9, 2004.

Ortiz, M. and Pandolfi, A. I, Finite-Deformation irreversible cohesive elements for three dimensional crack-propagation analysis, International Journal for numerical methods in engineering, Vol. 44, pp:1267-1282, 1999.

Reeder, J. R. and Crew, J. H., Nonlinear Analysis and Redesign of the Mixed-Mode Bending Delamination Test, NASA TM 102777, 1991.

Sluis, O. van der, Hsu, Y.Y., Timmermans P.H.M., Gonzalez, M. and Hoefnagels, J.P.M., Stratching induced interconnect delamination in stretchable electronic circuits, Journal of Physiscs D: Applied Physics, Vol. 44, pp:1-10, 2011

Chapter 4

Validation of Hygro-mechanical Model

4.1 Introduction

The coefficient of moisture expansion is a measure of the material’s ability to expand after moisture uptake. However, differential swelling occurs between the different materials that made up of the electronic packages may induce hygroscopic stress in the package. This stress will increase the likelihood for the package to fail and thus a good understanding of this failure mechanism will be important for predicting the reliability of these packages.

Despite its importance, the commercial available FE software does not have the inherent capability to perform moisture analysis. Luckily since the moisture analysis is analogous to thermal analysis, a thermal-structure analogy has been developed in the packaging industry for hygro-mechanical modelling using the thermal mechanical function [Wong, 1998]. Hence, this will be implemented in this research for our moisture analysis.

Nevertheless, a good material database for moisture analysis is still lacking in the literature due to the effort needed to perform these characterization. Hence, a novel and superior method for characterizing the moisture rate properties has been developed in this project and it is outlined in Chapter 2.

As with any new developed methods, validation needs to be performed on their accuracy. Hence, in this chapter, the validation of our material models and the hygro-mechanical model are presented. In order to validate our characterized moisture diffusion and CME properties, bi-material samples similar to the four point bending samples, (see Chapter 3.2) but without die attach glue and without a notch in the EMC are designed and fabricated. These validation tests include moisture diffusion validation and bi-material warpage validation study for CME. In Chapter 2, it is shown that the CME value of the classical TGA/TMA measuring method was about 5 times larger than that of DMA plus moisture generator measuring method. The objective of this chapter is to compare and validate these CME characterization techniques so the moisture effects can be modelled accurately for our research carrier.

4.2 Bi-material sample warpage measurement

In order to validate the CME test results, bi-material samples, consisting of a layer of copper and EMC, are prepared. The same EMC materials are used for both CME and diffusion for these validation experiments. Furthermore, the nominal dimension of the bi-material sample used in this research is 60x9x0.85 mm^3 (as shown in Fig. 4.1). The thickness of the copper is 0.2 mm whereas the thickness of EMC is 0.65mm.

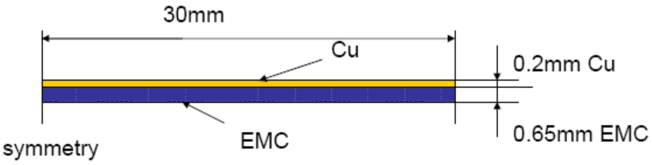

Fig. 4.1 Sample dimensions

The sample warpage at room temperature is measured using an optical camera system and a TDM warpage tester see Fig. 4.2(a). Fig. 4.2(b) shows a typical measurement result of a sample with a sample's length (vertical) of about 30mm and width (horizontal) of about 10mm.

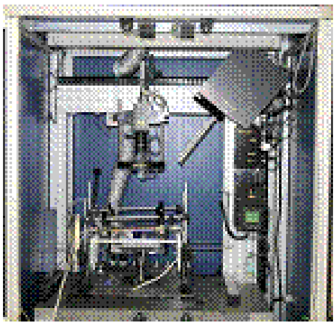

Fig. 4.2(a) TDM warpage tester

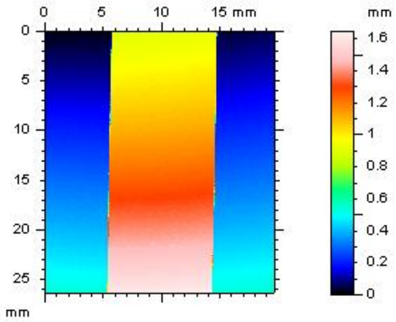

Fig. 4.2(b) TDM test result

Two experiments, using the above TDM tester, are performed to verify the accuracy of the characterized moisture properties. The first test is performed with the dry baked samples where the test samples are first pre-conditioned in an oven at 125ºC for 24 hours to remove all moisture before warpage measurement at room temperature (see Fig. 4.3). Fig 4.3 shows that a residual warpage with a maximum of about 250µm due to the residual stresses induced during moulding and subsequent cooling is observed.

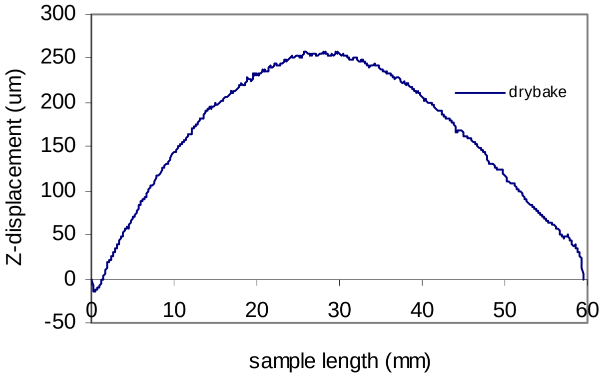

Fig. 4.3 Warpage at room temperature after dry bake

The second test is the warpage measurement at room temperature on a sample that is pre-conditioned at MSL1. This means that the sample is preconditioned in the moisture oven at 85ºC/ 85%RH for 168 hours or until moisture saturation is reached. It can be seen from Fig. 4.4 that the displacement in z direction decreases to around 140 µm at room temperature after MSL1 pre-conditioning. This is because the EMC layer of the bi-material sample expands after moisture uptake while no moisture is diffused in the top copper layer. In order to have a better understanding of this phenomenon, moisture diffusion and moisture induced expansion will be simulated using FE model and validated with the warpage measurement.

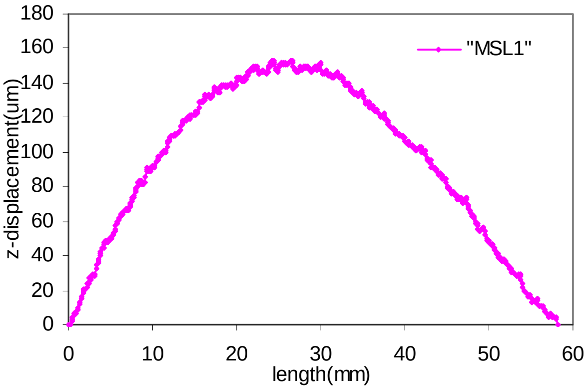

Fig. 4.4 Warpage at room temperature after MSL1

4.3 Modelling and validation of moisture diffusion and warpage

4.3.1 Modelling and validation of moisture diffusion

As mentioned, there is no moisture diffusion module in MSC.Marc/Mentat software and hence, moisture diffusion simulation is performed using the inherent transient heat conduction analysis. Due to the similarity between the transient moisture diffusion equation and the transient heat conduction equation (as shown in Eq. 4.1), a thermal-moisture analogy outlines in Table 4.1 is used to perform moisture diffusion modelling using the thermal diffusion function heat conduction:

$$\frac{\partial C}{\partial t} = D\left(\frac{\partial^2 C}{\partial x^2} + \frac{\partial^2 C}{\partial y^2} + \frac{\partial^2 C}{\partial z^2}\right) \tag{4.1}$$

where C [mg/mm^3] is the moisture concentration, x, y, z are spatial coordinates, D [mm^2/s] is the diffusion coefficient which measures the rate of diffusion and t is time. However, this simple analogy is only restricted to homogeneous system because of the concentration discontinuity, across a material interface. To solve this, a ‘wetness ratio’ variable, as defined in Eq. 4.2, developed by Wong et al, [Wong et al., .1998] has been adopted in this project.

$$w = C / C_{sat} \tag{4.2}$$

Table 4.1 FE thermal and moisture analogy

Properties	Thermal	Moisture
Field variable	Temperature, T	Wetness, $w = C/C_{sat}$

Density	ρ [kg/m^3]	1
Conductivity	k [W/mºC]	$D*C_{sat}$ [mg/s mm]
Specific capacity	c_p	C_{sat} [mg/mm^3]

For validating the moisture related properties, a 3D FE model is developed for this project, see Fig. 4.5. The dimensions are the same as in Fig. 4.1 but only half of this sample is modelled due to the symmetry of the model. In this bi-material model, the top layer is the copper and the bottom layer is the EMC. Two different FE models as shown in Fig 4.5 are built simultaneously. The model at the lower half of Fig. 4.5 is for moisture diffusion simulation and it simulates the moisture concentration or wetness changes with time. While the model at the top half of Fig 4.5 is for the hygro-mechanical combination model, it is used to calculate strain induced by the thermal and moisture induced expansion. The moisture diffusion coefficient and moisture saturation level used in this model are $6.04\text{x}10^{-6}$ [mm^2/s] and $3.76\text{x}10^{-3}$ [mg/mm^3] as stated in Table 2.7. Eq. 2.7 and Eq. 2.9 is also used to describe the material properties (see Chapter 2).

The simulation condition is as follows:

The model is first cooled down from 175ºC (sample moulding temperature) to 25ºC before heating it up again to 85ºC. This is followed by exposure to pre-conditioning of 85ºC/85%RH for 168 hours. To simulate this condition, a boundary condition using C_{sat} at 85ºC/85%RH is applied to the exterior of EMC outer nodes except at the symmetry face.

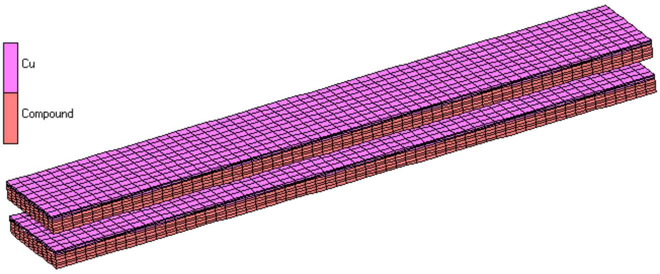

Fig. 4.5 3D bi-material FE model

The simulated change in moisture concentration with time at the interface between copper and EMC is shown in Fig. 4.6. It can be seen that the moisture concentration changes linearly with time initially but after the rate of changes decreases gradually. Moisture saturation is already reached by 48 hours as shown in Fig 4.6 and Fig. 4.7. Using this moisture diffusion result, it can be seen that it is not necessary to keep the sample at 85ºC/85%RH condition for 168 hours.

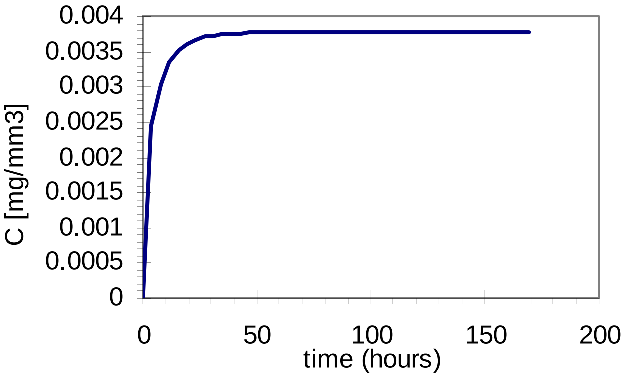

Fig. 4.6 Moisture concentration at bi-material interface versus time

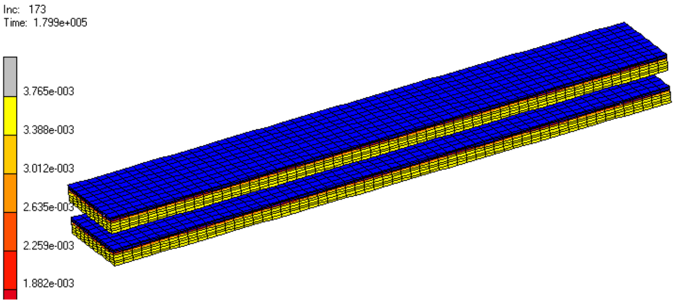

Fig. 4.7 Moisture saturation is reached in about 48 hours

In order to validate the moisture diffusion, the moisture absorption weight gain is measured at various times. Experiments have also validated our simulated result since weight gain remained constant after 48 hours. Fig. 4.8 shows the weight gain comparison between the simulation result and experimental result. The curves have similar shape and only differ slightly in the saturation value, 0.153% and 0.166% respectively. This shows the validity of the model and it can now be used for the simulations of real package.

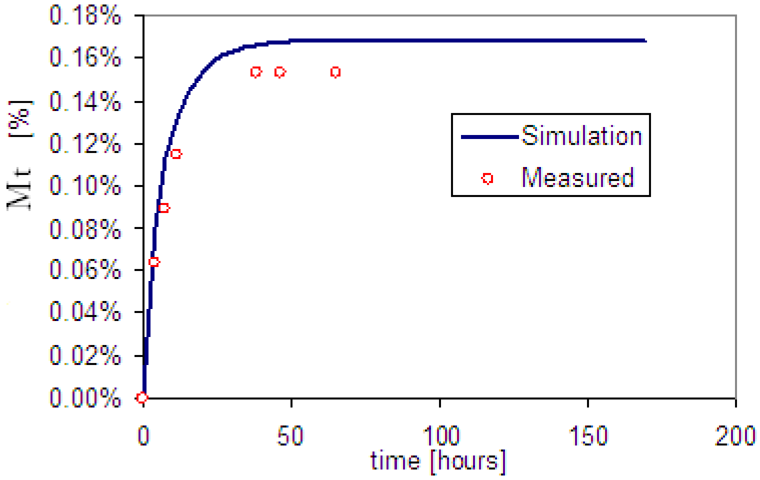

Fig. 4.8 Weight gain comparison between simulation and experiment

Package moisture absorption simulation and measurements can now be performed to validate material model. To avoid repetition, these results are not shown as they will be presented in Chapter 5.

4.2.2 Bi-material sample modelling and validation of warpage

The warpage after moulding is first simulated using the following temperature history:

The bi-material is first cooled down from 175ºC (stress free) to 25ºC before heating up to 125ºC. It is then maintained at 125ºC for 24 hours to simulate dry baking of the sample. After that, it is cooled down again to 25ºC before the initial warpage profile is simulated. The boundaries condition for summary is enforced as shown in Fig. 4.1. Fig. 4.9 shows the comparison between simulation (thick line) and test result (thin line) and these results show good agreement between the simulation and experiment data for dry sample.

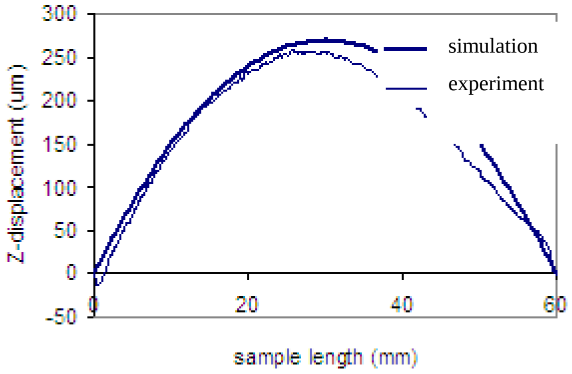

Fig. 4.9 Warpage after dry bake at 25ºC comparison between test and simulation

Same simulation history for MSL1 as described in section 4.3.1 is used in this verification test. Using the CME characterized by DMA method and the traditional TGA/TMA methods, the simulation produces total different outcome. Figure 4.10 shows that the bi-materials warp upward using the materials property characterized using DMA whereas the bi-material warps downward using CME characterized using the traditional methods. Since the experimental result show that the bi-materials warp upward after pre-conditioning, DMA method is able to produce much accurate result as compared to TGA/TMA method which tends to over estimated the CME characterized.

There are still some differences between the simulation and test results and these results show that either the actual CME value should be smaller or that not all absorbed moisture contributes to the expansion. Best fit can be achieved if the CME value is between 0.06 to 0.07mm^3/mg.

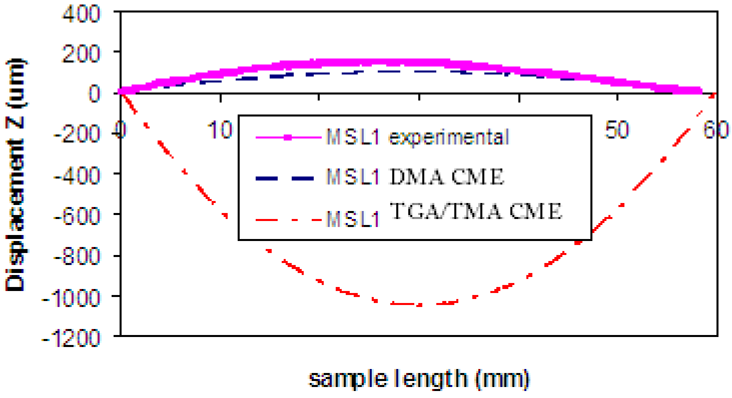

Fig. 4.10 Warpage comparison at 25ºC between test and simulation after MSL1 conditioning

4.4 Conclusions

In this chapter, bi-material samples are modelled to validate the moisture diffusion and swelling simulation in the FE model. Since the FE prediction and experimental results of the moisture diffusion model agree well, the corresponding diffusion parameters can be used in the package model.

Validation of the CME measured by DMA method is also performed by making comparison with the experimental results and the simulation result using CME from TGA/TMA method. The simulation confirms that the CME value measured by DMA is much more accurate than that measured by the TGA/TMA method.

References

Tee, TongYan and Zhong, Zhaowei, Integrated vapor pressure, hygroswelling, and thermo-mechanical stress modelling of QFN packaging during reflow with interfacial fracture mechanics analysis, Microelectronics Reliability, Vol. 44, pp:105-114, 2004.

Wong, E.H., Rajoo, R.., Kon, S.W. and Lim, T.B., The mechanics and impact of hygroscopic swelling of polymer materials in electronic packaging, Transactions of ASME, Vol. 124, pp:122-126, 2002.

Wong E.H., Teo Y.C., and Lim T.B., Moisture diffusion and vapour pressure modelling of IC packaging, 48th ECTC, pp:1372-1378, 1998.

Stellrecht, E., Han, B. and Petch, M.G., Characterization of hygroswelling behaviour of molding compounds and plastic packages, IEEE Transactions on Component and Packaging Technologies, pp:499-506, 2004.

Zhang, G. Q., van Driel, W.D. van and Fan, X.J., Mechanics of Microelectronics, Springer, pp:311-320, 2006.

Zhou J., Lahoti, S. and Sitlani, M., Investigation of inner-layer dielectric (ILD) failure by hygroscopic swelling, IEEE 55th ECTE, 2005.

Zhou, J., Lahoti, S. and Sitlani, M., Investigation of non-uniform moisture distribution on determination of the hygroscopic swelling coefficient and finite element modeling for a flip chip pacakge, IEEE EuroSime, pp:112-119, 2005.

Ma, Xiaosong, Jansen, K.M.B., Ernst, L.J., van Driel, W.D, van der Sluis, O. and Zhang, G.Q., Characterization and modeling of moisture absorption of underfill for IC pacakging, ICEPT Proceedings, pp:380-384, 2007.

Ma, Xiaosong, Jansen, K.M.B., Ernst, L.J., van Driel, W.D, van der Sluis, O. and Zhang, G.Q., Characterization of moisture properties of polymers for IC pacakging, Microelectronics Reliability, Vol. pp:1685-1689, 2007.

Chapter 5

Fast Qualification Methods, Simulation and Tests

5.1 Introduction

As stated in Chapter 1, qualification methods are tests which accelerate failure and they are used in the packaging industry to qualify new packages design. Examples of these qualification methods are moisture sensitivity level analysis, thermal cycling and stress driven qualification analysis. In this chapter, two types of fast qualifications are discussed. One is the moisture sensitivity level analysis and the other is thermal cycling. Using information from Chapter 2 and Chapter 3, knowledge based fast qualifications are developed and performed in this research.

The traditional design rule is based on design first concept, they will first design a new product and then conduct reliability tests, such as MSL tests, thermal cycling test in the later stage of the development. If the new designed products failed the reliability qualification tests, redesign must be performed until the new products are able to pass the reliability qualification tests. Hence, the whole design cycle will usually take long time. For example, if these new products need to pass either MSL level 1, level 2 or level 2a reliability qualification tests, these packages should be put in the oven of 85ºC/85%RH for 168 hours, 85ºC/60%RH for 168 hours or 30ºC/60%RH 696 hours respectively according to IPC/JEDEC J-STD-020D and that is before the pre-conditioned samples is subjected to three reflows. These moisture absorption durations, which could be as long as 29 days, are too long. In the IPC/JEDEC J-STD-020D standard, 60ºC/60%RH can be used instead of 30ºC/60%RH for accelerated test. It assumes that moisture content to be equal between different pre-conditioning conditions but it offers no explanation on the validity of this assumption. In this research, a knowledge-based acceleration model that could address the relationship between design and reliability qualification is developed. Significant acceleration factor can be achieved with the developed qualification test. For example, moisture diffusion time for MSL reliability qualification is decreased to a factor of 16 to 112 if equal weight gain is assumed and to a factor of 2 to 17 and if a more stringent condition of local moisture concentration is considered. Furthermore, by having only one precondition of 85ºC/85%RH instead of 4 pre-conditioning requirements outlined in the standard, significant number of humidity chamber could be reduced. Furthermore, significant time can also be reduced since all MSL can be conducted concurrently.

Moisture sensitivity level analysis

The degradation effect of moisture increases enormously when the package is exposed to the high temperature during solder reflow, such as 260ºC for Pb-free solder reflow. Under certain conditions, this effect can cause internal delamination of the packaging materials between the die and EMC or EMC and lead frame/substrate [Tee, et al., 2004, Wong, et al., 2002, Stellrecht, et al., 2004, Zhang, et al., 2006, Nogueira, et al., 2000, and Zhou, et al., 2005]. In the most severe case, this stress can also result in cracks. This is commonly referred to as the “popcorn” phenomenon in the industry because the internal stress will cause the package to bulge and crack with an audible “pop” sound. The failure of the “popcorning” is normally due to delamination, which is the interfacial fracture between different materials. Surface mount devices (SMDs) are more susceptible to this problem because they are exposed to high temperature during reflow.

In IPC/JEDEC J-STD-020D [J-STD-020D, 2007], there are 8 moisture sensitivity levels (MSL) with different pre-conditioning duration, temperature and humidity settings. According to this standard, the duration for moisture absorption ranges from 48 to 696 hours. Using 60ºC/60%RH acceleration, the moisture absorption time can be shortened to 168 hours. However, 168 hours is still a very long duration. Furthermore, IPC/JEDEC J-STD-020D just explains that moisture weight gain should be equal between the standard and acceleration pre-conditioning. But to the best of our knowledge, no verification has been performed on the accuracy of using this predicted time. In this chapter, the increase in moisture absorption weight at 85ºC/85%RH is calculated and it has been found that actual acceleration time needed is much shorter than the acceleration time required by the 60ºC/60%RH standard.

5.2 Fast moisture sensitivity level qualification

5.2.1 Moisture sensitivity level analysis standard

Table 5.1 shows the eight moisture sensitivity levels in IPC/JEDEC J-STD-020D [J-STD-020D, 2007] that is used to identify the classification levels of non-hermetic surface mount devices (SMDS). This will ensure that they can be properly packed, stored and handled to avoid damage induces during assembly solder reflow attachment or repair operations. For example, the rate floor life for level 3 is 168 hours at the condition of 30ºC/60%RH. It means that the maximum allowable time period that it can be exposed to the environment before the solder reflow process after removal from a moisture barrier bag. If 60ºC/60%RH accelerated condition is applied, moisture diffusion time can be shorten to 40 or 52 hours.

Table: 5.1 Moisture sensitivity levels [J-STD-020D]

level	Floor life		Soak requirements				
			Standard		Accelerated equivalent		
					0.4-0.48eV	0.30-0.39 eV	Conditions [ºC/%RH]
	Time [hours]	Conditions [ºC/%RH]	Time [hours]	Condition [ºC/%RH]	Time [hours]	Time [hours]	
1	unlimited	30/85	168	85/85	NA	NA	NA
2	1 year	30/60	168	85/60	NA	NA	NA
2a	4 weeks	30/60	696	30/60	120	168	60/60
3	168	30/60	192	30/60	40	52	60/60
4	72	30/60	96	30/60	20	24	60/60
5	48	30/60	72	30/60	15	20	60/60
5a	24	30/60	48	30/60	10	13	60/60
6	Time on label	30/60	Time on label	30/60	NA	NA	NA

Note: all temperatures refer to the centre of the packages.

5.2.2 Package moisture diffusion modelling and validation

Since moisture diffusion can be increased through higher temperature and humidity, higher acceleration can be achieved with 85ºC/85%RH. In order to ensure the validity of this assumption, FE analysis is performed to compute the weight gain and the equivalent moisture content in the package at several critical locations for the standard test. Using this computed result, the duration for 85ºC/85%RH conditions to achieve the same moisture content as different conditions is then predicted. This will be the new duration for our 85ºC/85%RH pre-conditioning.

The research carrier used in this research is the QFN package, see Fig. 1.1. Being a package with copper pad on bottom of the package, the QFN packages provide many advantages over other lead frame package configurations, such as small size ("nearly chip size" footprint), low weight, high electrical performance. Furthermore, the exposed copper die pad offers effective removal of heat.

In order to perform the coupled moisture diffusion and hygro-thermal mechanical simulations, two symmetric 3D finite element models are used: namely the moisture diffusion and the hygro-thermal mechanical model, see Fig. 5.1(b).

Fig. 5.1(a) shows the QFN package (6x6x0.85mm^3) modeled in this research and for visualisation purposes, the EMC is removed in Fig. 5.1(b). Top and middle green blocks are the passive (5.1x5.1x0.26mm^3) and the active die(2.1x2.1x0.2mm^{3}and they are connected by micro bumps (solder ball with 0.03mm in thickness and 0.05mm in diameter) after the first reflow. Furthermore, to increase the package's reliability, underfill is used to strengthen the interconnection. Furthermore, as shown in Fig 5.1 (b), the active die is glued on top of the copper pad (3.5x3.5x0.07mm^3) and this will allow heat to be dissipated through the copper pad. Last but no least, the passive die and bottom lead frame are aslo connected by the solder balls (0.16mm in thickness and 0.152mm in diameter) after the second reflow.

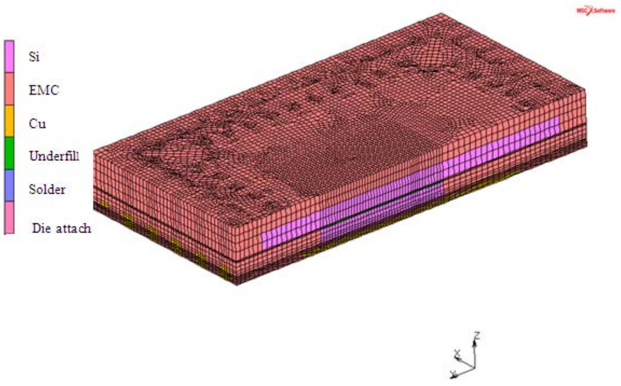

Fig. 5.1(a) 3D model for moisture diffusion

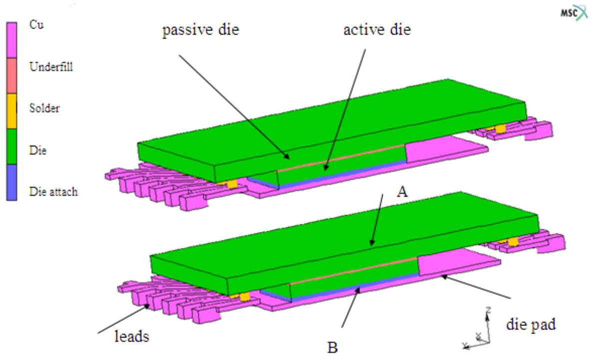

Fig. 5.1(b) 3D model (EMC is removed)

In order to validate the moisture absorption material model, moisture absorption tests is preformed at 60ºC/60%RH and 85ºC/85%RH, (see Fig. 5.2 and Fig. 5.3). For increasing the accuracy, the measurement is an average of a series of packages instead of just one package.

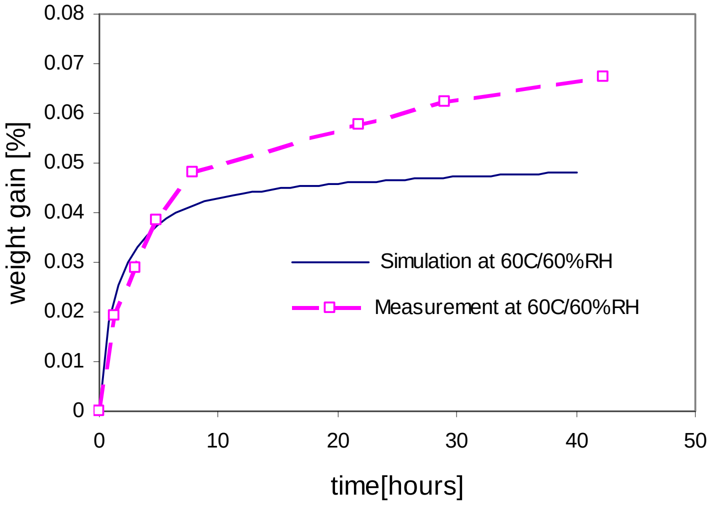

Fig. 5.2 Weight gain comparison between simulation and measurement at 60ºC/60%RH (Charles, 2010)

Moisture weight gain is simulated in this research using the thermal moisture analogy presented in the earlier section. It can be seen from Fig. 5.2 that the simulation and measurement result agree very well for the first 5 hours of moisture diffusion for 60ºC/60%RH condition. However, their deviation increases gradually as time progresses.

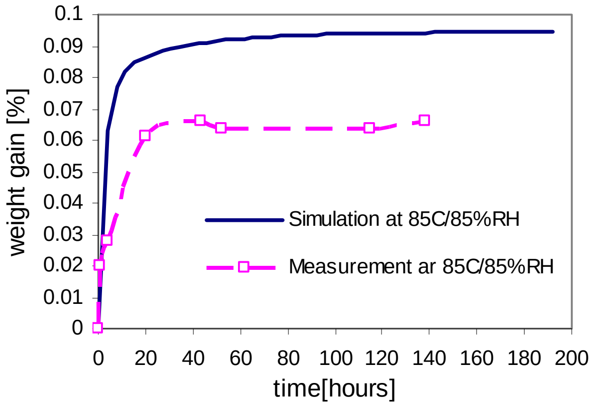

Fig. 5.3 Weight gain comparison between simulation and measurement 85°C/85%RH

The moisture uptake at the 85°C/85%RH condition is shown in Fig. 5.3 and it can be that the simulation tends to over predict the saturation level. A possible explanation is the differences between the accuracy of the respective measuring methods. Material properties are characterized in situ using automatic measuring in the moisture oven with resolution of 1µg, ±0.1°C and ±1%RH. However, the packages are measured using an electronic balance with resolution of 100µg whereas the measurement of test packages requires constant removal of the packages from a moisture oven that has only a resolution of ±0.3°C and ±3%RH. Another reason is that not only single package is weighted at a time but many packages are weighed at the same time.

5.2.3 Fast moisture sensitivity level qualification prediction

In order to accurately simulate moisture diffusion, the diffusion coefficients and saturation levels at each condition are needed. This can be predicted using the parameters in Table 2.7, in conjunction with Eq. 2.7 and Eq. 2.9 in Chapter 2.

In Table 5.2 and Table 5.3, the diffusion coefficients and saturation concentrations for different temperatures and humilities are also listed.

Table 5.2 Diffusion coefficients of packaging materials

	Diffusion coefficients[$10^{-6}mm^2/s$]		
	85°C	60°C	30°C
EMC	6.04	4.06	2.31
Underfill	4.67	3.11	1.75
Die Attach	26.47	10.37	2.75

Table 5.3 Moisture saturation concentration at different conditions

	C_{sat}, Moisture saturation concentration[$10^{-3}mg/mm^3$]			
	85°C/85%RH	85°/60%RH	60°C/60%RH	30°C/60%RH
EMC	3.77	2.66	2.02	1.37
Underfill	13.65	9.64	7.36	5.01
Die attach	11.40	8.05	7.38	6.52
	85°C/31%RH	30°C/85%RH		

EMC	1.37	1.95
Underfill	4.16	7.01
Die attach	5.00	9.24

From Table 5.3, it can be seen that the moisture saturation levels are temperature and relative humidity dependent with higher temperature and relative humidity resulting in faster moisture diffusion and higher moisture contents.

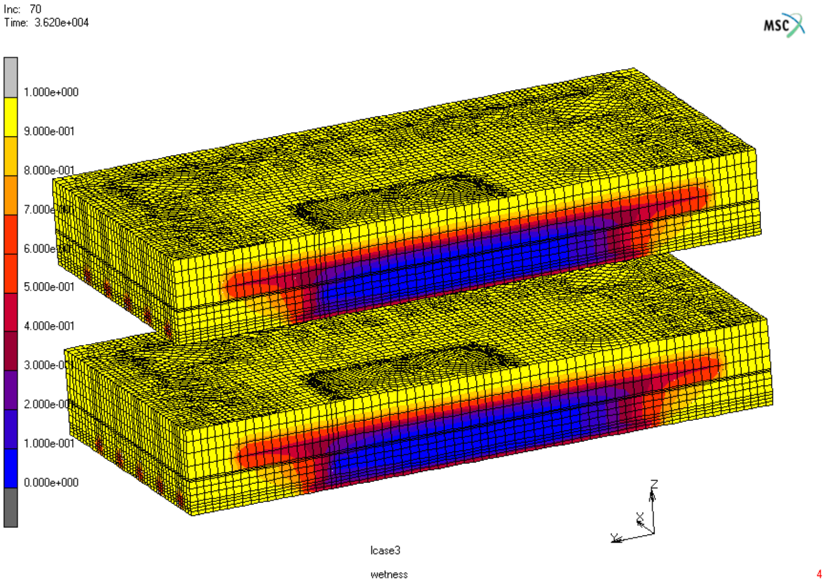

Fig. 5.4 Wetness diffusion for 10 hours at 85ºC/85%RH

Fig. 5.4 shows the wetness distribution after 10 hours of moisture diffusion at 85ºC/85%RH whereas Fig. 5.5(a) and Fig. 5.5(b) show moisture absorption weight gain for different conditions and different time duration. From Fig. 5.5(a), it can be seen that the amount of absorbed moisture increases with temperature, relative humidity and time. Furthermore, Fig. 5.5(a) shows that only 130 hours of moisture absorption at 85ºC/85%RH is needed for moisture saturation. Hence, the actual moisture absorption time can be shorten from 168 hours to 130 hours for 85ºC/85%RH pre-conditioning. Similarly only 110 hours and 530 hours are needed to achieve moisure satuaration at 85ºC/60%RH and 30ºC/60%RH as shown in Fig. 5.5(a) and Fig. 5.5(b) respectively. Furthermore, Fig. 5.6 shows the weight gain will reach 0.08% in only 10 hours at the condition of 85ºC/85%RH. Table 5.4(a) shows the standard moisture absorption time, acceleration time and the acceleration factors. Significant acceleration fators has been achieved since only three hours of moisture absorption is needed at 85ºC/85% as compared to 168 hours at standard 85ºC/60%RH condition.

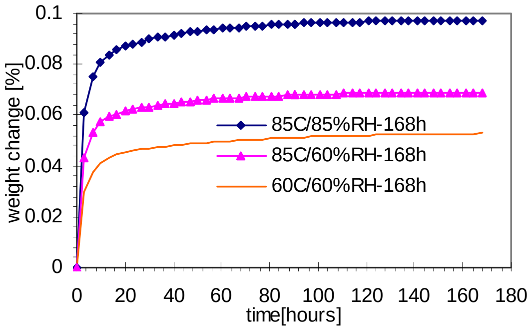

Fig. 5.5(a) Prediction of moisture weight gains at different conditions for 168 hours

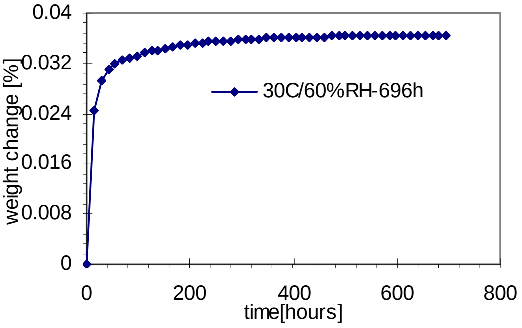

Fig. 5.5(b) Prediction of moisture weight gains at 30ºC/60%RH for 696 hours

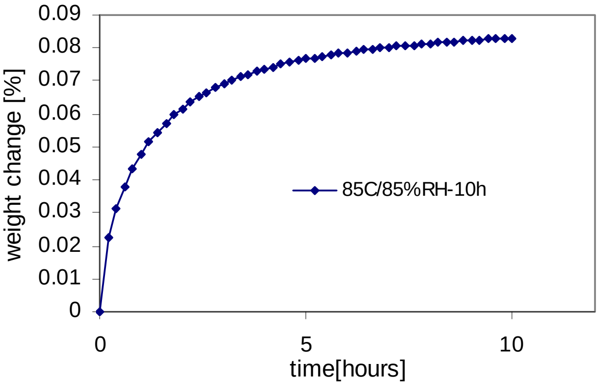

Fig. 5.6 Prediction of moisture weight gain at 85ºC/85%RH for 10 hours

As discussed earlier, the time needed for saturation depends strongly on the sample thickness (diffusion distance) and that it can be estimated from the saturation equation (Eq. 2.2 or Eq. 2.3) but solving this equation is not straight forward. Luckily the term becomes larger than unity after the initial duration, and Eq. 2.2 or Eq. 2.3 further reduces to the following more managable equation:

$$\frac{C}{C_{sat}} \approx 1 - \frac{8}{\pi^2} e^{-Dt/h^2} \tag{5.1}$$

For example, the following procedure can be used to computed time duration for 95% saturation, C/C_{sat} need to be solved for 0.95.

thus $\frac{8}{\pi^2} e^{-Dt/h^2} = 1 - 0.95$

and finally Eq. 5.1 reduces to

$$t_{precon} = \frac{-h^2}{D}\ln\left(\frac{\pi^2}{8}\left(1-0.95\right)\right) = 2.8\frac{h^2}{D} \tag{5.2}$$

From this equation, it can be seen that a package with half the EMC thickness will reach saturation 4 times faster.

The first two rows of Table 5.4(a) show the weight gain at the condition of 85ºC/60%RH for 168 hours is 0.069 wt%. However, simulation shows that only 3 hours of moisture absorption at 85ºC/85%RH is required to reach similar weight gain, see the third and fourth rows of Table 5.4(a). Hence, significant acceleration can be achieved with 85ºC/85%RH.

Table 5.4(b) shows the diffusion times and their corresponding weight gains at the condition of 30ºC/60%RH; and the accelerated pre-conditioning times and the corresponding weight gains at 60ºC/60%RH and 85ºC/85%RH respectively. The last row of Table 5.4(b) listed is the acceleration factor.

Table 5.4(a) Weight gain predictions after different pre-conditioning tests for SiP package

85ºC/60%RH [hours]	168 hours
Weight gain [wt%]	0.069%
85/85%RH [hours]	3
Weight gain [wt%] 85ºC/85%RH	0.069%
Acceleration factor	56

Table 5.4(b) Weight gain predictions after different pre-conditioning tests for SiP package

30ºC/60%RH [hours]	696	192	96	72	48
Weight gain [wt%] 30ºC/60%RH	0.036	0.035	0.034	0.033	0.032
60ºC/60%RH Acceleration [hours]	168	52	24	20	13
Weight gain[wt%] 60ºC/60%RH	0.053	0.049	0.047	0.046	0.044
85ºC/85%RH acceleration [hours]	1.5	1.4	1.0	0.9	0.8
Weight gain[wt%] 85ºC/85%RH	0.053	0.049	0.047	0.046	0.044
Acceleration factor	112	37	24	22	16

It can be seen from Table 5.4 that the moisture absorption time can be significantly decreased using 85ºC/85%RH acceleration instead of 60ºC/60%RH acceleration. Depending on the moisture sensitivity level, moisture absorption time is decreased by a factor of around 16 to

112 if only weight gain is considered as the qualifying criterion. However, care is needed to ensure that the failure modes do not change after reflows. In order to check this, test samples are removed from the chamber after 0.8, 0.9, 1.0, 1.4, 1.5 and 3 hours' moisture diffusion to perform reflow tests.

Local moisture concentration calculation

The JEDEC standard does not provide any explanation for their moisture diffusion duration. This research attempts to provide some validations. It has been known that average moisture concentrations may not be sufficient for failure predictions since local moisture condition is critical. This is because moisture is known to weaken the materials or the material interface. Hence, simulations are needed to evaluate these local moisture concentrations since experiments only capture the average moisture uptake.

Two critical locations, A and B, are investigated in this research, see Fig. 5.1(b). Location A, which is at the centre of the package between the EMC and passive die interface, is chosen since most delamination occurs at that location is observed during reflow. The second location B, which is at the interface between copper die pad and die attach glue, is chosen since it has the longest moisture transport route and therefore it is the most difficult location for moisture to penetrate into.

Table 5.5(a) Moisture concentration at location A in SiP package

85ºC/60%RH [hours]	168 hours
C[10^{-3}mg/mm^3] at 85ºC/60%RH	2.66
85ºC /85%RH [hours]	16.9
C[10^{-3}mg/mm^3] at 85ºC/85%RH	3.77

Table 5.5(b) Moisture concentration at location A in SiP package

30ºC/60%RH [hours]	696	192	96	72	48
30ºC/60%RH [10^{-3}mg/mm^3]	1.37	1.37	1.37	1.37	1.37
60ºC/60%RH [hours]	168	52	24	20	13
60ºC/60%RH [10^{-3}mg/mm^3]	2.02	2.02	2.02	2.02	2.02

From Table 5.5(a) and (b), it can be seen that at location A, moisture saturation levels are reached within the standard specified duration under the condition of 30ºC/60%RH and

60ºC/60%RH. Simulations also show that at the condition of 30ºC/60%RH and 60ºC/60%RH, moisture saturations are 1.37 and 2.02 [10^{-3}mg/mm^3] respectively. At the condition of 85ºC/85%RH, the same moisture content can be reached in only 16.9 hours.

Table 5.6(a), (b) and(c) list the moisture concentration at location B using different JEDEC standard pre-conditioning and the times needed to reach to the corresponding moisture concentration at 85ºC/85%RH pre-conditioning. It can be see that the moisture concentation is 6.47 [10^{-3}mg/mm^3] after 696 hours of pre-conditioning at 30ºC/60%RH. However, If 85ºC/85%RH pre conditioning is used instead, only 40 hours are needed to reach the above moisture concentration. If local moisture concentrations are considered, moisture diffusion time is decreased to a factor of around 2 to 17 depending on MSL. Apart from the high acceleration factor, another advantages of this method is the need for only one moisture diffusion chamber and it will also speed up the whole processes. All the MSL levels can be characterized simultanteously.

Table 5.6(a) Moisture concentrations at location B in SiP package for MSL1

30ºC/85%RH [hours]	unlimited
C[10^{-3}mg/mm^3] at 30ºC/85%RH	9.24
85/85%RH [hours]	84
C[10^{-3}mg/mm^3] at 85ºC/85%RH	9.24

Table 5.6(b) Moisture concentrations at location B in SiP package for MSL2

85ºC/60%RH [hours]	168 hours
C[10^{-3}mg/mm^3] at 85ºC/60%RH	7.73
85/85%RH [hours]	52
C[10^{-3}mg/mm^3] at 85ºC/85%RH	7.73
Acceleration factor	2.9

Table 5.6(c) Moisture concentrations at location B in SiP package for MSL2a to 5a

time for 30ºC/60%RH [hours]	696	192	96	72	48
30ºC/60%RH[10^{-3}mg/mm^3]	6.47	4.48	2.26	1.46	0.65
time for 85ºC/85%RH [hours]	40	27	16.5	12.5	8
85ºC/85%RH[10^{-3}mg/mm^3]	6.47	4.48	2.26	1.46	0.65

Acceleration factor	17.4	7.1	5.8	5.8	6.0

Table 5.7 Moisture concentrations at location B in SiP package

time for 60ºC/60%RH [hours]	168	52	24	20	13
60ºC/60%RH[10^{-3}mg/mm^3]	6.76	3.29	1.34	0.99	0.44
time for 85ºC/85%RH[hours]	41	19.5	12	10.5	7
85ºC/85%RH[10^{-3}mg/mm^3]	6.76	3.29	1.34	0.99	0.44
Acceleration factor	4	2.7	2	1.9	1.9

Table 5.7 lists the moisture concentration at location B after 60ºC/60%RH acceleration and the times needed to reach to the corresponding moisture concentration for 85ºC/85%RH pre conditioning. Comparing Table 5.6(c) and Table 5.7, it can be observed that the moisture concentration after 168 hours of 60ºC/60%RH accelerated test is higher than that of 30ºC/60%RH with 696 hours pre-conditioning. Therefore, it can be seen that if the moisture concentration at a certain critical location is considered, the duration needed for pre-conditioning time can be very different.

For the accelerated test, simulation at 85ºC/85%RH condition is performed. From Table 5.6 and Table 5.7, it can be seen that, the time needed to reach the concentration of level 2a can be shortened from 696 hours to 40 hours, by a factor of 17 if 85ºC/85%RH is used.

In order to have a better correlation with the accelerated test, cross sectioning are performed after the sample are subjected three reflows (reflow peak temperature is 260ºC) after 15 hours of pre-conditioning at 85ºC/85%RH and 192 hours at 30ºC/60%RH (Fig. 5.7(a) and 5.7(b)). No delaminations are found at these critical locations.

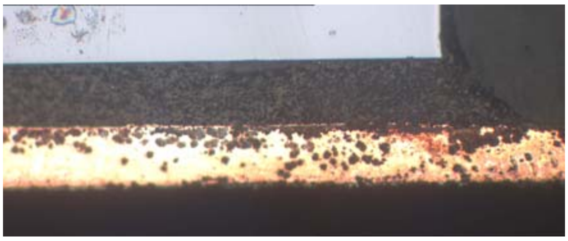

Fig. 5.7(a) Pre conditioning at 85ºC/85%RH for 15 hours + 3 reflows

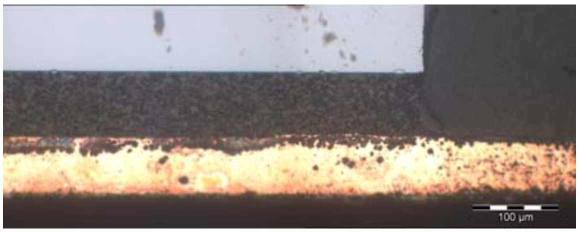

Fig. 5.7(b) Pre conditioning at 30ºC/60%RH for 192 hours + 3 reflows

In conclusion, significant acceleration has been achieved with our methods. Depending on the moisture sensitivity level, moisture absorption time is decreased by a factor of around 16 to 112 if only weight gain is used as the qualifying criterion. If local moisture concentrations are considered, moisture diffusion time is decreased by a factor of around 2 to 17. Hence, this method enables faster reliability qualification time and more simpified reliability pre-conditioning since only one condition of 85ºC/85%RH is needed.

5.3 Fast thermal cycling qualification

5.3.1 Thermal cycling method

Thermal cycling tests are performed to determine the ability of components and solder interconnects to withstand mechanical stresses induced by cycling between temperature extremes. Beside the common failure mechanism such as thermal shrinkage, embitterment of the polymer during cool down and solder ball failure, permanent changes in electrical and/or physical characteristics can also be resulted from these mechanical stresses [Zhang, 2006, Tee, 2004].

Temperature cycling test conditions (soaking mode)

Table 5.8 shows the different temperature cycling test conditions outlined by the standard, Temperature Cycling JEDEC 22-A104C [22-A104C, 2005]. Ts/(max) and Ts/(min) in table 5.8 are the maximum or minimum nominal temperatures of a specific test condition and hence test condition C (-65 to 150ºC) have the largest thermal cycling range and temperature extremes.

Soak time

Soak times, according to JEDEC 22-A104C [22-A104C, 2005], are the time duration at which the components are exposed to the temperature extremes in each cycle, see Table 5.8. The typical JEDEC mode 1, 2, 3 and 4 has a soaking time of 1, 5, 10, 15 minutes respectively.

Ramp rates

Ramp rate is the rate at which temperature increases and decreases between the thermal cycling extremes. Although ramp rate is not critical for most components testing, JEDEC 22-A104C [22-A104C, 2005] still prescribes the typical ramp as shown in Table 5.8 (second column).

Table 5.8 Thermal Cycling conditions (including soaking times/ramp rates)

Conditions (Ts/(min) →Ts/(max)[ºC]	Typical Cycles/[hour]	soaking time [min]
A (-55→85)	2-3	1,5 or 10
B (-55→125)	2-3	1 or 5
C (-65→150)	2	1 or 5
G (-40→125)	< 1-2	1, 5, 10 or 15
H (-55→150)	2	1 or 5
I (-40→115)	1-2	1, 5, 10 or 15
J (-0→100)	1-3	1, 5, 10 or 15
K (-0→125)	1-3	1, 5, 10 or 15
L (-55→110)	1-3	1, 5, 10 or 15
M (-40→150)	1-3	1, 5, 10 or 15
N (-40→85)	1-3	1,5 or 10

In order to compare simulation and experimental results, similar thermal cycling condition is needed for both simulation and experimental as per outlined in JESD 22-A104C, see section 5.5.3.

5.3.2 Package delamination modelling and measurement

The same package in the moisture diffusion analysis is used in this analysis with the only difference of having cohesive zone elements inserted between die attach (glue layer) and copper die pad (pink layer), see Fig. 5.8.

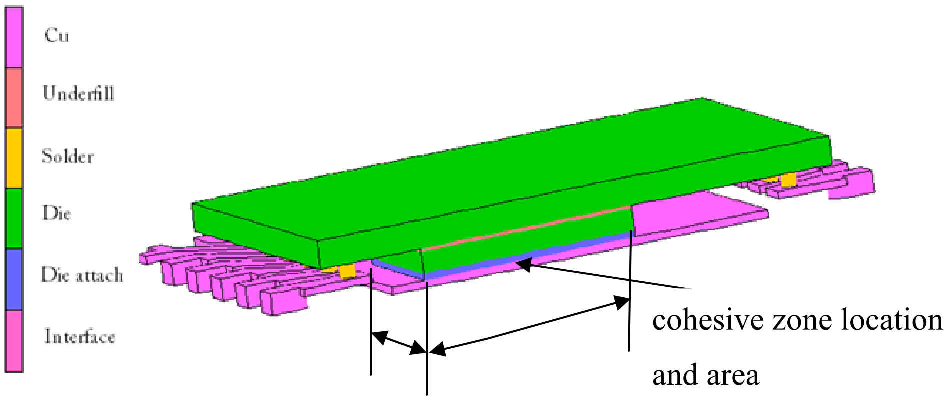

cohesive zone location and area

Fig. 5.8 QFN model with cohesive zone

The main material properties are listed in the Table 5.9

Table 5.9 Material properties in the SiP package [NXP]

Materials	E[GPa]	ν[-]	T_g[ºC]	CTE[ppm/ºC]
EMC	Visco-elastic	0.25	110	8 < Tg, 32 > Tg
Die	169	0.23		3
Underfill	visco-elastic	0.3	140	32 < Tg, 120 > Tg
Die attach	visco-elastic	0.3	-64	69 < Tg ,152 > Tg
Solder balls	35	0.4		21
Leadframe/die pad	120	0.33		17.5

Thermal temperature profile

For this analysis, thermal cycling temperature profile as shown in Fig. 5.9 is modelled. Again, the residual stresses due to the moulding process are included in the analysis in order to mimic the true stress that the package experiences during thermal cycling. This can be achieved by exposing the package to a temperature from 175ºC to 25ºC in 100 seconds before it is subjected to thermal cycling. The two temperature extremes of the thermal cycle adopted for this research are -65 and 150ºC respectively. The soaking time is 15 minutes.

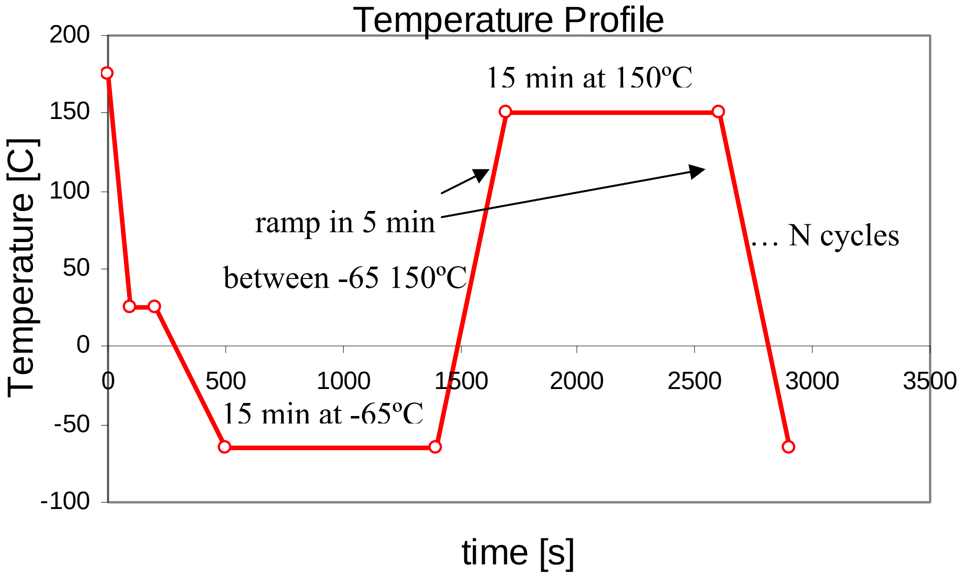

Fig. 5.9 Thermal temperature profile for simulation

Boundary conditions

The boundary conditions are shown in the Fig. 5.10. Due to the symmetry, only half of the package is modelled. Furthermore, node A is fixed in x, y and z directions and node B is fixed in x and y directions in order to prevent rigid body, see Fig. 5.10. All nodes in the symmetric plane are fixed in x direction. The delamination lengths at critical locations L and M in Fig 5.11 are measured after 10 cycles and 150 cycles.

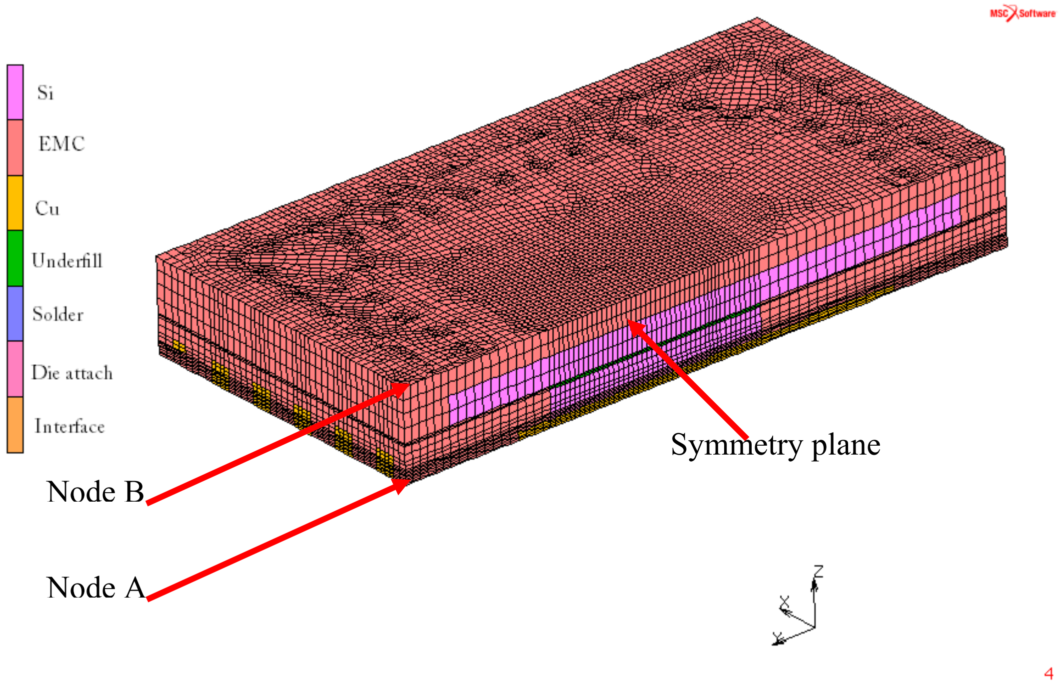

Fig. 5.10 Displacement boundary conditions of packaging model

Delamination measurements results

Since the simulation is supposed to mimic the experiment, the same experimental condition is adopted for our simulation.

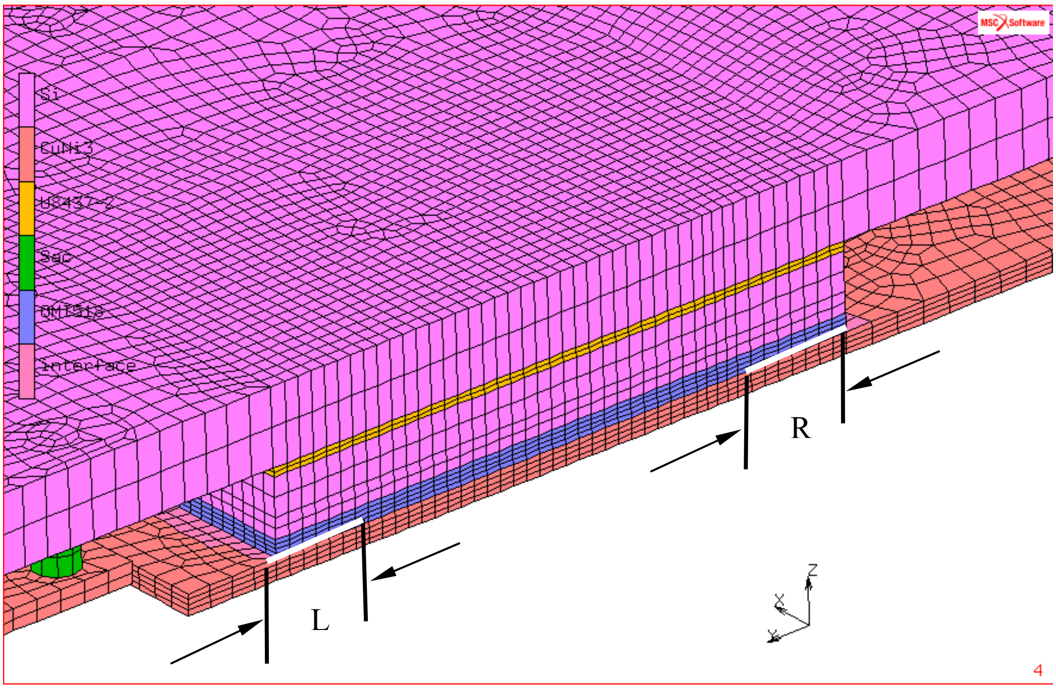

Fig. 5.11 Critical delamination locations

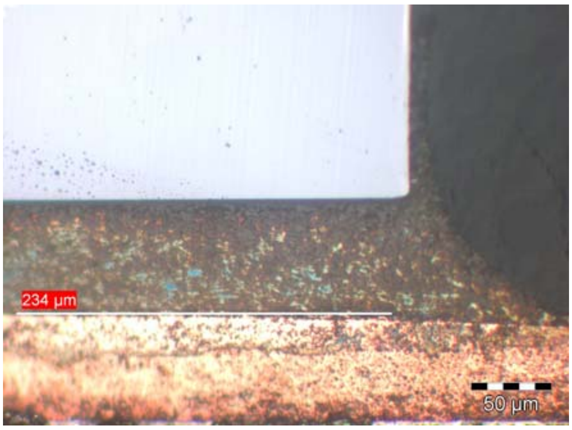

Fig. 5.12 Cross section corresponding Fig. 5.11 R location after 10 thermal cycles [Charles, 2010]

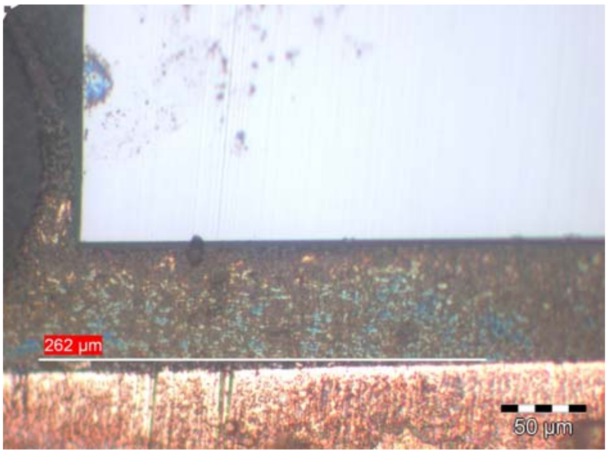

Fig. 5.13 Cross section corresponding Fig. 5.11 L location right side after 150 cycles

Experiment shows that the delamination length of sample A along the interface between die pad and die attach is around 234µm after 10 thermal cycles, see Fig. 5.12 (right side, length R) whereas the delamination length of sample B is around 263µm after 150 cycles, see Fig. 5.13 (left side length L). This is consistent with our experimental data since cross sections confirmed similar the delamination lengths after 10 and 150 cycles [Regards, C., 2010].

Simulation results

The temperature dependent interface toughness, $G_{c,}$ used in our model is characterized from the four point bending test outlines in Chapter 3. However, the critical opening is assumed to be constant and temperature independent in this research since critical opening value is only characterized at room temperature. In order to address the validity of this assumption, sensitivity study of the critical opening values on the damage values is performed. Furthermore, four point bending sample and the package may have different mode angles. This discrepancy needs to be addressed.

Fig. 5.14 shows the simulation results for different critical opening (V_c) after one thermal cycle. Firstly, this result shows that the damage profiles are sensitive to the critical opening value with small critical opening values resulting in larger damage value. Furthermore, the delamination lengths are computed to be around 180 to 300µm on the left side, and around 100 to 120µm on the right side, as shown in location L and R respectively in Fig. 5.11 when critical opening value is assumed 1µm. Hence, the corresponding damage values are between 0 and 0.1. Similarly, when critical opening value is assumed to be 0.5µm, the delamination lengths are computed to be around 200 to 700µm on the left side and around 120 to 550µm on the right side. These values are more consistent with the experimental measurements. Since the corresponding damage values are found to be between 0 and 0.6, these results suggest that experimentally observed delamination might already occur at damage values below 1.0.

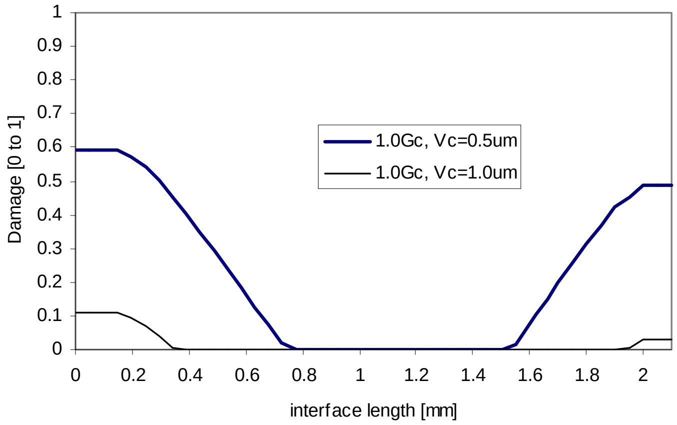

Fig. 5.14 Damage profiles with measured critical opening values

In order to investigate the sensitivity of the interface damage on interface toughness, simulations with G_c, between $0.9G_c$ and $1.1G_c$ but same critical opening values after one thermal cycle are performed, see Fig. 5.15. These results show that damage values are almost equal and this validates the assumption that the value of mode angle is not critical in our simulation.

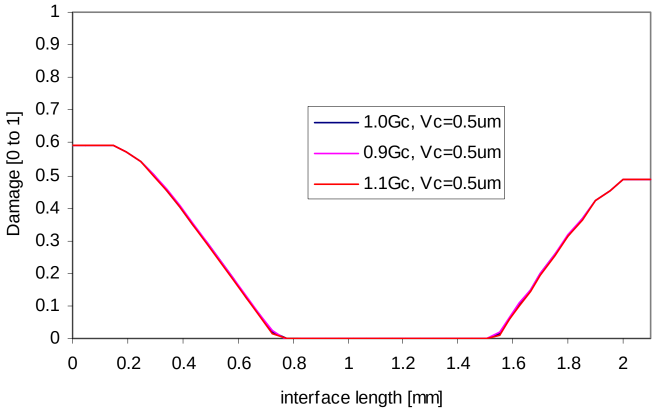

Fig. 5.15 Damage profiles as function of G_c

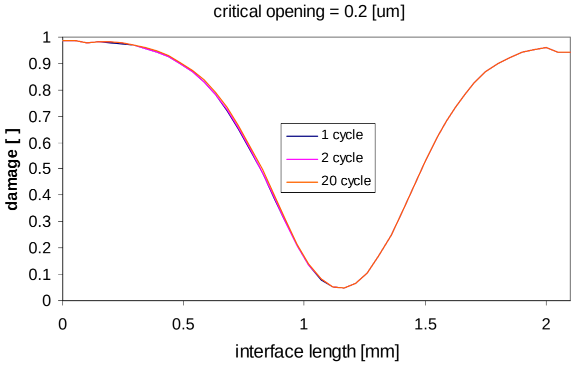

Fig. 5.16 Damage value along interface length

Fig. 5.16 shows simulation results at different thermal cycles. When critical opening value is assumed to be 0.2μm, damage value almost reaches 1. Also it can be seen that the damage curves are almost independent of thermal cycling numbers since only a little difference exists among these different thermal cycles damage curves. This is consistent with our package cross section measurements.

According to Charalambides [Charalambides, 1989], mode angle in four point bending test is depending on the ratio of E_1/E_2, delamination length/I and h_2/h_1, see Fig. 3.19. Hence, this suggests that although the estimated mode angle is around 45° to 48° in our four bending test at room temperature, this may not be right input value for package and thus a different value of G_c might be needed. Luckily this is not the case for our carrier. Fig. 5.15 confirms that the damage profiles do not change significantly. Damage may be independent of mode angle in certain ranges.

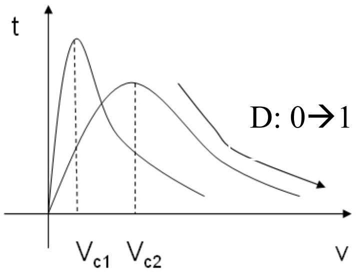

Fig. 5.16 Relation between G_c and V_c

It can be seen from Fig. 5.16 that damage can be easily achieved for small V_c at a given G_c since damage starts when V_c is reached. Furthermore, it is known that if the damage value reaches 1, the maximum interface separation will be about 6xV_c. This damage (including location and length) was confirmed at the cross section location and agrees with the results of simulations.

5.3.3 Fast thermal cycling qualification method

To do fast thermal cycling qualification, thermal cycling conditions, failure modes and the knowledge for predicting this failure are needed.

As discussed earlier, the major factors for thermal cycling conditions are the extreme temperatures, the dwell time at the temperature extremes and ramp rate. The extreme temperatures (temperature cycling test conditions) are chosen according to the users' requirements. For example, the extreme temperatures are selected to be between -65 and 150ºC if it is used for automotive application. Temperature ramp rate and the dwell time are also selected according to the standard or users' requirements.

Humidity acceleration is not considered due to minimal moisture effect on interface toughness although thermal cycling and moisture absorption method is used in JEDEC STANDARD JESD22-A100C. Using above information, fast thermal cycling can be used to predict failure.

5.4 Conclusions

Knowledge based fast qualification framework is proposed and validated for fast moisture sensitivity qualification test and fast thermal cycling qualification test.

Fast moisture sensitivity qualification tests

From the simulations and experiments conducted in this study, it has been found that the high temperature and high relative humidity acceleration method is suitable for fast moisture sensitivity analysis and significant acceleration can be achieved using these conditions as long as care is taken to ensure that no new failure modes are introduced. For example, depending on the moisture sensitivity level, moisture absorption time needed is decreased by a factor of around 16 to 112 if weight gain is used as the qualifying criterion. Furthermore, moisture diffusion time can still be decreased by a factor of around 2 to 17 even though the more stringent conditions of similar local moisture concentrations are considered. Hence, this method enables faster reliability qualification and more simpified reliability pre-conditioning since only one condition of 85ºC/85%RH is needed.

Fast thermal cycling qualification tests

Thermal cycling analysis is also performed in this research using 3D FE model and the interface properties characterized in Chapter 2. Good agreement has been observed between the predictions and experiments in our studies, such as delamination locations, delamination lengths. Furthermore, extreme temperatures are found to have the biggest effects on delamination whereas the dwell time and ramp rate have no effects on the interface delamination for package. Delamination length remains constant after 20 thermal cycles, which is consistent with the cross section measurement.

References

Charalambides, P.G., et al., A test specimen for determinining the fracture resistance of bimaterial interface, Journal of Applied Mechanics, Vol. 56, pp:77-82, 1989.

Ferguson, T., and Qu, J.M., Effect of moisture on the interface adhesion of the underfill/soder mask Interface, Journal of Electronic Packaging, Vol. 124(2), pp:106-110, 2002.

IPC/JEDEC J-STD-020D, 2007, Moisture/reflow sensitivity classification for nonhermetic solid state surface mount devices.

JEDEC22-A104C (2005) Temperature Cycling, JEDEC STANDARD

JEDEC STANDARD JESD22-A100C Cycled Temperature Humidity Bias Life Test 2007

Ma, X.S., Jansen, K.M.B., Ernst, L.J., van Driel, W.D., van der Sluis, O., Zhang, G.Q., Regard, C., Gautier, C., and Frémont, H., “Moisture Diffusion Model Verification of Packaging Materials,” Proceedings of International Conference on Electronic Packaging Technology & High Density Packaging, Bi, K.Y., and Xiao, F., pp:380-384, 2008.

Ma, X.S., Jansen, K.M.B., Ernst, L.J., van Driel, W.D., van der Sluis, O., Zhang, G.Q., “A New Method to measure the Moisture Expansion in Plastic Packaging Materials” ECTC2009, pp:1271-1276, 2009.

JESD22-A120A, 2001, Test method for the measurement of moisture diffusivity and water solubility in oganic materials used in electronic devices.

Nogueira, P., Ramirez, C., et al., Effects of Water Sorption on the Structure and Mechanical properties of an Epoxy Resin System, Journal of Applied Polymer Science, 80(1), pp:71-80, 2000.

Stellrecht, E., Han, B., and Petch, M.G., “Characterization of Hygroswelling Behaviour of Molding Compounds and Plastic Packages, IEEE Transactions on Component and Packaging Technologies, Vol. 27(3), pp:499-506, 2004.

Regard, C., Ph.D thesis, Fast qualification of SiP componants, 2010.

Regard, C., Gautier, C., Frémont, H., Ma, X.S., Jansen, K.M.B., “Fast Reliability Qualification of SiP Products,” Microelectronics Reliability, Vol. 49(9-11), pp:958-926, 2009.

Tee, T.Y., and Zhong, Z.W., Integrated Vapor Pressure, Hygroswelling, and Thermo-mechanical Stress Modelling of QFN Packaging during Reflow with Interfacial Fracture Mechanics Analysis, Microelectronics Reliability, Vol. 44(1), pp:105-114, 2004.

Wong, E.H., Rajoo, R., Koh, S.W., and Lim, T.B., The Mechanics and Impact of Hygroscopic Swelling of Polymer Materials in Electronic Packaging, Journal of Electronic Packaging, 124(2), pp:122-126, 2002.

Zhang, G.Q., van Driel, W.D., and Fan, X.J., 2006, Mechanics of Microelectronics, Springer, The Netherlands, pp:311-320, 2006.

Zhou, J., Lahoti, S., and Sitlani, M., 2005, “Investigation of Non-uniform Moisture Distribution on Determination of the Hygroscopic Swelling Coefficient and Finite Element Modeling for a Flip Chip Package,” Proceedings of EuroSime2005, Ernst, L.J., et al., eds., pp. 112-119.

Chapter 6

Conclusions

6.1 General conclusions

The aim of this thesis is to develop knowledge based fast reliability qualification methods that ensure the consistency of the failure modes during acceleration. Moisture and thermal-mechanical related qualification tests, or more specifically Moisture sensitivity levels analysis (MSLA) and thermal cycling, are selected for this work since moisture and thermo mechanical related degradation account for most of the failures in the electronic packages. A QFN system in package (SiP) is chosen as the research carrier.

This thesis has presented the research results in three main aspects:

1. A knowledge based fast qualification method has been proposed and verified.
2. More efficient moisture properties characterization methods have been developed
    - A step-RH moisture diffusion characterization method which not only significantly shortens the duration needed to perform characterization, but also produced an accurate result has been implemented.
    - A more efficient moisture induced expansion measurement method has been developed.
3. Interface properties between die attach and copper die pad have been determined by using both experiments and numerical simulations. Further, in depth understanding of these properties is conducted so that these interface properties can be used in the thermal cycling simulations.

6.1.1 Conclusions concerning knowledge based fast qualification methods

A knowledge based fast qualification method which can significantly shorten the qualification time has been developed in this research. Since only one 85ºC/85%RH accelerated pre-conditioning has been needed for this method, only one oven setting is required as compared to need for three different setting for the traditional MSL test. Furthermore, since all the MSL tests can start concurrently, further reduction of characterization duration can be achieved.

A 3D finite element model for performing moisture diffusion has been implemented into the FE MSC.Menta/Marc code to determine the time duration required to achieve equal moisture weight gain for different MSL conditions. Very high acceleration factor, ranging from 16 to 112, is achieved using the assumption of equal weight gain and 85ºC/85%RH pre-conditioning. Furthermore, even if the more stringent assumption of equal local concentration at the critical region is used, high acceleration factor of 2 to 17 can be achieved using this method.

Cohesive zone method has been employed successfully to model the delamination of the packages during thermal cycling which is essential for the thermal cycling qualification test. Using the interfacial properties characterized in this research, the FE simulation employed in this research is able to predict, in agreement with our experimental data, the delamination location and the crack length. Sensitivity study performed in this research show that damage value is insensitive to compute G_c between $0.9G_c$ to $1.1G_{c.}$ Since the rule of thumb suggests that damage values are insensitive to mode angle if damage value is comparable for ± $10\%G_c$, this implies that the mode angle effects on the damage value are very limited which this is consistent with our assumption in our cohesive zone method. However, damage values are found to be very sensitive to the critical opening value and this has to be taken into account during modelling. For example, critical opening values of 1.0 and 0.5μm will induce maximum damage values of around 0.1 and 0.6 respectively. Using the above discussion, FE result show that delamination length stabilises after only just 20 thermal cycles (which is consistent with experimental observations on cross sections) during the thermal cycling qualification test. Therefore, again, very high accelerated factor can be achieved using the proposed method since the number of thermal cycling needed for thermal cycling qualification test has now reduced from up to1500 cycles to 20 cycles.

6.1.2 Conclusions concerning new characterization methods of moisture related properties

Compared with traditional moisture property characterization methods, the new relative humidity stepwise method provides more reliable moisture diffusion properties due to the in-situ nature of the measurements. Hence, this method removes the need to manually remove the test sample from the controlled environment during measurement which could induce some uncertainty in the measured data. Another improvement of this technique over the traditional method is that it could significantly shorten the time needed to measure the moisture properties. This is because the traditional method requires a single test for each applied temperature and relative humidity level whereas the proposed stepwise method can characterize the properties of different conditions in just one test. This is important since each moisture properties models required the knowledge of moisture diffusion properties at least two different temperature and relative humidity.

With the stepwise method, moisture diffusion coefficient and moisture saturation content models for commercial EMC, underfill and die have been established. Validation the moisture diffusion model is conducted and these results show good agreement between the FE prediction and experimental results in weight gain.

6.1.3 Conclusion concerning cohesive zone interface properties

The cohesive zone interfacial properties in terms of G_c (interface toughness) and V_c (critical opening) between copper and die attach are characterized using both experiments and numerical simulations. Four point bending tests show that the critical delamination force decreases from 4.1N to 0.71N with increasing temperature from 25ºC to 150ºC. Using these critical delamination force, the calculated interface toughness (G_c) decreases from 26.5 (J/m^2) at 25ºC to 1.9 (J/m^2) at 150ºC. This implies that the interface toughness decreases significantly with increasing temperature. On the other hand, moisture does not have any effect on the interface toughness. This is mainly due to the “hydrophobic” nature of the binder BIM (bismaleimide) resin used in die attach.

6.2 Limitations and recommendations

1. Due to the limitation of testing equipment used in this research, the interfacial toughness is characterized only from 25 to 150ºC whereas the thermal cycling range

is between -65 to 150ºC in the actual qualification test. Since the accuracy of our simulation is highly dependent on the characterized cohesive zone interface toughness and critical opening, there is a need to characterize material properties in the temperature range that is similar to the actual qualification test.

2. Since the camera system used in this research could not be installed in the oven, crack opening is only characterized at room temperature in this research. This may not be sufficient as our simulation shows that the damage values are very sensitive to critical opening values. Therefore, this critical opening value should be measured at different temperatures to improve the accuracy of our model.
3. Mode angle dependency should be taken into account in other application. Even mode angle dependency is minimal in this carrier, this is not always true and this dependency needs to be characterized. Furthermore, due to the mode angle differences between characterization and the actual package interface, the characterized interface toughness values might be different.

Summary

This research aims at developing a knowledge based fast qualification method for moisture or thermally induced failure in microelectronic packages. Driven by the market competition and the need for shorter time to market, fast qualification tests are becoming more and more important for the industry. Qualifications are tests which are used in the industry to estimate the lifetime reliability of an electronic package and their ability to fulfil their engineering requirement. Since the traditional trial-and-error method is still commonly used during product and process development for design and qualification, these qualification tests are too time consuming and will result in long design cycles.

Moisture and thermal-mechanical related qualification tests are selected for this work since they are responsible for the most of the failures in the electronic packages. More specifically moisture sensitivity level analysis (MSLA) and thermal cycling, which are related to the moisture and thermal-mechanical qualification tests, are chosen in this research. Although MSLA tests consist of two stages: moisture diffusion and reflow (heating to maximum of 260ºC at solder reflow condition), only moisture diffusion is studied for MSLA as the moisture diffusion stage accounts for almost all of the duration needed for MSLA test. Furthermore, since it has been known that moisture diffusion rate increases significantly with increasing temperature and humidity, an accelerated condition of 85ºC/85%RH pre-conditioning is chosen. This corresponds to the worst condition in the JEDEC standard J-STD-020D and hence the highest acceleration. Furthermore, two different qualifying criterions are used in this research to quantify the accelerated condition. They are equal weight gain and equal local moisture concentration and significant acceleration factor has been achieved with these criterions. Compared with the traditional and 60ºC/60%RH pre-conditioning, the moisture absorption time for equal moisture weight gain is shortened by a factor of 16 to 112 if only moisture weight gain is used as a qualifying criterion. Although not as high, the acceleration factor of 2 to 17 can be achieved even if a more stringent criterion of the local moisture concentration is considered. Another advantage of using only one accelerated condition is such that it minimizes the need to maintain different humidity chambers for different MSL. This not only simplify the testing

procedures but additional time could be reduced since all the test at their level can be performed together.

Another aspect of this research is to develop advanced characterization technique that is need to support the moisture and thermal mechanical simulation. This is critical as it will not only speed up the characterization processes which is normally very time consuming, it is able to increases their accuracy too. For example, RH% steps at constant temperature methodology developed in this research could not only reduce the time duration needed for moisture diffusion characterization, it is also able to produce a much more accurate result. At least four days can be shortened using this method to characterize the moisture properties needed for fast moisture diffusion. Furthermore, the DMA plus moisture generator method is found to be more efficient than that of traditional TGA/TMA method used to determine moisture induced expansion. Compared to the regular TGA/TMA method, the CME characterization time is shortened from 210 hours to 42 hours.

Thermal cycling qualification is a test to determine the ability of the package to withstand mechanical stresses induced by cycling between two temperature extremes. Traditionally, these thermal cycling qualification test is very time consuming since it requires up to a few thousands of thermal cycles depending on the engineering requirements. In order to shorten the thermal cycling cycles, a knowledge based thermal cycling fast qualification method is also developed. For thermally induced failure, faster thermal cycling qualification can be obtained with the aid of simulations.

In this research, delamination between die attach and copper die pad is identified as the dominant failure mode during thermal cycling test. A transient delamination simulation based on cohesive zone method is implemented to predict the number of cycles needed for delamination. However, as with any simulation, meaningful delamination prediction can only be achieved with accurate input properties. Hence, interface properties (interface toughness and critical opening) between copper die pad and die attach where the delamination occur is investigated in this research. The die attach-copper interface toughness as function of temperature is characterized by using both four point bending experiments and numerical simulations and the result shows that the interface toughness decreases significantly with increasing temperature. Lastly, the critical opening value at room temperature is determined in this research using experimental results and cohesive zone simulations.

Our simulation result shows that delamination occurs at a early stage in their fatigue life but these delamination cracks will stabilize at around 20 cycles. This is consistent with our experimental measurement performed using sample cross sectioning technique. Furthermore, good agreements on delamination location and length have been also observed between the prediction and experimental measurement. The study shows the cycles needed for delamination is reduced from up to1500 cycles to 20 cycles with this qualification strategy.

In conclusion, this research provides a framework in developing a knowledge based fast qualification method which can shorten qualification time and design cycles for different electronic packages. Moisture diffusion time can be largely shortened if this method is used whereas our thermal cycling qualification can be significantly shorten our test duration.

Samenvatting

Het doel van dit onderzoek is het ontwikkelen van een op kennis gebaseerde kwalificatie methode voor door vocht of temperatuur veroorzaakt falen in micro-electronische verpakkingen. Gedreven door handelscompetitie en de marktintroductietijd, worden snelle kwalificatie tests steeds belangrijker voor de industrie. Kwalificaties zijn tests welke gebruikt worden in de industrie voor het toetsen van de betrouwbaarheid van elektronische verpakkingen. De traditionele trial-and-error methode wordt nog steeds uitvoerig gebruikt tijdens product en proces ontwikkeling voor ontwerp en kwalificatie. Deze traditionele kwalificatie tests nemen veel tijd in beslag, met als gevolg lange ontwerp cycli.

Vocht en thermo-mechanische gerelateerde tests zijn bestudeerd in dit onderzoek omdat zij verantwoordelijk zijn voor het falen van een groot gedeelte van elektronische verpakkingen. Met name zijn vocht gevoeligheid niveau analyses (VGNA) en thermische wisselingen in dit proefschrift onderzocht. VGNA tests bestaan uit twee stadia: vocht diffusie en reflow (verhitten naar 260 °C voor de condities welke nodig zijn voor het vloeien van het soldeer). In dit onderzoek is echter alleen vocht diffusie bestudeerd. Het is bekend dat de snelheid van vocht diffusie significant toeneemt met toenemende temperatuur en vochtigheid. Hierom is een versnellende conditie van 85 °C/85%RH gekozen als voorbehandeling. Dit komt overeen met het slechtse scenario in de JEDEC standaard J-STD-020D en vandaar de hoogste versnelling. Bovendien zijn twee verschillende kwalificatie criteria gebruikt in dit onderzoek om the versnelde conditie te kwantificeren. De equivalente massa toename en locale vocht concentratie en versnellende factor zijn bereikt met deze criteria. Vergeleken met de traditionele 60 °C/60%RH voorbehandeling, wordt de vochtabsorptietijd verkort met een factor 16 tot 112 als massa toename gebruikt wordt als kwalificatie criterium. Een versnellende factor van 2 tot 17 kan bereikt worden als een meer strikt criterium van de lokale vochtconcentratie wordt beschouwt. Een ander voordeel van het gebruik van aleen een versnelle conditie is dat het de noodzaak vermindert om verschillende klimaatkamers te onderhouden. Het versimpelt dus niet alleen de testmethode maar tevens kan tijdwinst worden verkregen.

Een ander aspect van dit onderzoek is het ontwikkelen van een geavanceerde karakterisatie techniek die gebruikt kan worden om vocht en thermische simulaties te ondersteunen. Deze

techniek versnelt het karakterisatieproces die normaal gesproken erg tijdrovend is. Tevens neemt de nauwkeurigheid van karakteriseren toe. De ontwikkelde methode waarbij stappen in RH% gebruikt worden bij constante temperatuur bleken in staat te zijn de tijdsduur voor vochtdiffusie te verminderen en tot een nauwkeuriger resultaat te leiden. De nieuwe karakterisatie methode verkort de benodigde testtijd met minstens vier dagen. Bovendien is de methode waarbij de DMA in combinatie met een vochtgenerator efficiënter gebleken dan de traditionele GA/TMA methode die gebruikt wordt om de door vocht veroorzaakte expansie te meten. Vergeleken met de traditionele TGA/TMA methode is de karakterisatie tijd afgenomen van 210 naar 42 uur.

De thermische cyclische kwalificatie test wordt gebruikt voor het bepalen van de weerstand die een verpakking kan bieden tegen de mechanische spanningen veroorzaakt door de alternerende hoge en lage temperatuursbelasting. Voor de traditionale thermisch cyclische kwalificatie, kunnen enkele duizenden cycli nodig zijn om te voldoen aan bepaalde ontwerp eisen, welke veel tijd kosten. Een op kennis gebaseerde thermische cyclische snelle kwalificatie methode wordt voorgesteld om het aantal benodigde cycli te verkorten. Snellere thermisch cylische kwalificatie kan worden versnelt door met behulp van simulaties.

In dit onderzoek is delaminatie tussen die attach en een koperen frame geidentificeerd als de dominante faal mode gedurende een thermisch cyclische test. Een tijdsafhankelijk delaminatie simulatie gebaseerd op een cohesive zone model is gebruikt om het aantal cycli te voorspellen dat nodig is om delaminatie te veroorzaken. Zoals met iedere simulatie, kan een betekenisvolle voorspelling alleen verkrgen worden met accurate invoer gegevens. Hierom zijn de interface eigenschappen (interface taaiheid en kritische opening) tussen koper en die attach onderzocht in dit onderzoek. De die attach-koper interface taaiheid als functie van temperatuur is gekarakteriseerd door gebruik te maken van vierpunts buigproeven en numerieke simulaties. De aldus verkregen resultaten laten zien dat de interface taaiheid significant afneemt met toenemende temperatuur. Ten slotte is de kritische opening bepaald bij temperatuur door gebruik te maken van experimentele resultaen en cohesive zone simulaties.

Onze simulaties laten zien dat delaminatie ontstaat in een vroeg stadium van de vermoeings levensduur en dat de breuken stabiliseren na ongeveer twintig cycles. Dit is consistent met metingen op de doorsnede van onze monsters. Een goede overeenkomst tussen de delaminatie locatie, lengte en breedte is gevonden tussen experimentele metingen en simulatie voorspellingen. Het onderzoek laat zien dat het aantal benodigde cycli voor delaminatie is gereduceerd van tot 1500 naar 20 cycli met de voorgestelde kwalificatie strategie.

Concluderende, dit onderzoek geeft een raamwerk voor het ontwikkelen van een op kennis gebaseerde snelle kwalificatie methode, welke de kwalificatie tijd en ontwerp cycli verkort voor verschillende elektronische verpakkingen. Vocht diffusie tijd kan vermindert worden bij gebruik van deze methode. Tevens kan thermische cycli kwalificatie verkort worden bij gebruik van de voorgestelde methode.

Acknowledgements

At this point it is traditional to thank those people who have contributed to this thesis in one way or another. I particularly remember all the valuable discussion and the pleasant contact with everybody I shared with. I would like to take this opportunity to express my thanks to all of them. In particular I would like to express my special appreciation:

My deepest gratitude and respect is expressed to my promoter Prof. G.Q. Zhang for giving me the opportunity to conduct this PhD project. The dissertation can not completed without his excellent scientific guidance, valuable suggestions, stimulating discussions and various critic supports during the whole period in the Netherlands.

I would like to express cordially gratitude to my co-promoter Dr. K.M.B. Jansen for excellent scientific support, daily supervision, especially valuable suggestions and comments during every stage of my research.

My special appreciations would like to express to Dr. Olaf van der Sluis, Prof. L.J. Ernst, Dr. Willem van Driel, for your valuable suggestions, specially in FE simulation, technique supports and friendship.

I am specially express my gratitude to our France team, H. Frémont, C. Gautier and C. Regards. I appreciate all valuable discussions and comments during our team meetings, telephone meeting, especially package validation cooperation job done by C.Regards.

I also want to express my thanks to Sau Koh and Kit Wong for their valuable support and discussions.

The experimental characterization of moisture diffusion and interface properties were conducted at the Laboratory for Engineering Mechanics. My sincere thanks are expressed to Jos van Driel, Rob Luttjeboer, Harry Jansen and Patrick van Holst for their outstanding technical support and assistance.

Special thank goes to my colleague Rene Poelma and Jan de Vreugd for his friendship and translation the summary and propositions into Dutch.

I also want to express my thanks to Daoguo Yang, Jeroen Zaal, Jan de Vreugd, Suman Nakka, Lingen Wang, Stanley Leung for valuable discussions.

I also take this opportunity to express my appreciation to my wife Yun Zhang, my son Yukun, my parents, sisters and brothers to support me to complete this Ph.D. thesis.

Last, but definitely not least, I would like to express my appreciations to all friends who make my life in Holland enjoyable. I can not possibly thank everyone individually, but I trust that all of you will accept this acknowledgement as a token of my appreciation.

About the Author

The author, Xiaosong Ma was born in Qiqihaer, Heilongjiang province in China on Oct. 18, 1963. He received his B.Sc. degree in Engineering from Guilin University of Electronic Technology in 1984 and M.Sc. degree in Engineering from Shanghai University for Science and Technology in 1999, China.

Since July 1984, he worked as assistant, lecturer and associate professor in the Faculty of Mechanical Engineering, Guilin University of Electronic Technology, China. During the years he worked as deputy dean in mechanical faculty in GUET, he did a major contribution to the establishment of the first Surface Mount Technology specialization and experimental SMT assembly line in the all nation in GUET.

In May 2005 he came to the Netherlands as a visiting researcher in the group of Mechanics of Materials, Faculty of Mechanical, Maritime and Material Engineering, Delft University of Technology, the Netherlands. Since Dec. 2006, he started his Ph.D. research under the supervision of Prof. G.Q. Zhang and associate Prof. K.B.M. Jansen. The research topics is " Fast Qualification Methods for Microelectronic Packages."

LIST OF PUBLICATIONS

Journal papers:

[1]. Ma, X.S., Jansen, K.M.B., Ernst, L.J., van Driel, W.D., van der Sluis. O. and Zhang, G.Q., "Characterization of moisture properties of polymers for IC packaging," Microelectronics Reliability, Vol. 47, 2007, pp: 1685-1689.

[2]. Ma, X.S., Jansen, K.M.B., Zhang, G.Q., van Driel, W.D., van der Sluis. O., Ernst, L.J., Regards, C., Guitier, C., and Frémont, H., "A fast moisture sensitivity qualification method," Microelectronics Reliability, Vol. 50, 2010, pp: 1654-1660.

Conference paper:

[1]. Ma, X.S., Jansen, K.M.B., Ernst, L.J., van Driel, W.D., van der Sluis. O., Zhang, G.Q., Regards, C., Guitier, C., and Frémont, H., "Die attach Interface Property Characterization as Function of Temperature Using Cohesive Zone Modelling Method," International Conf. on Thermal, mechanical and multiphysics simulation and experiments in Micro-Electronics and Micro-Systems, EuroSime2010, 2010, pp: 647-654.

[2]. Ma, X.S., Jansen, K.M.B., Ernst, L.J., van Driel, W.D., van der Sluis. O. and Zhang, G.Q., "A New Method to Measure the Moisture Expansion in Plastic Packaging Materials," Electronic Component and Technology Conference, ECTC2009, 2009 pp: 1271-1276.

[3]. Ma, X.S., Jansen, K.M.B., Ernst, L.J., van Driel, W.D., van der Sluis. O., Zhang, G.Q., Regards, C., Guitier, C., and Frémont, H., "Fast Qualification Using Thermal Shock Combined with Moisture Absorption," International Conference on Electronic Packaging Technology & High Density Packaging, ICEPT-HDP 2009, 2009.

[4]. Ma, X.S., Jansen, K.M.B., Ernst, L.J., van Driel, W.D., van der Sluis. O. and Zhang, G.Q., "Moisture effects on a system in Package Carrier," International Conf. on Thermal, mechanical and multiphysics simulation and experiments in Micro-Electronics and Micro-Systems, *EuroSimE2009*, 2009, pp:379-383.

[5]. Ma, X.S., Jansen, K.M.B., Ernst, L.J., van Driel, W.D., van der Sluis. O., Zhang, G.Q., Regards, C., Guitier, C., and Frémont, H., "Effect of aging of packaging materials on die crack of a SiP carrier," International Conf. on Thermal, mechanical and multiphysics simulation and experiments in Micro-Electronics and Micro-Systems, EuroSime2008, 2008 pp:361-364.

[6]. Ma, X.S., Jansen, K.M.B., Ernst, L.J., van Driel, W.D., van der Sluis. O., Zhang, G.Q., Regards, C., Guitier, C., and Frémont, H., "Moisture diffusion Model Verification of Packaging Materials," International Conference on Electronic Packaging Technology & High Density Packaging, ICEPT-HDP 2008, 2008, pp:636-640.

[7]. Ma, X.S., Jansen, K.M.B., Ernst, L.J., van Driel, W.D., van der Sluis. O., and Zhang, G.Q., "Characterization and modelling of moisture absorption of underfill for IC packaging," International Conference on Electronic Packaging Technology, ICEPT 2007, 2007, pp:380-384.

[8]. Ma, X.S., Jansen, K.M.B., Ernst, L.J., and Zhang, G.Q., "Filler contents effects on the moisture absorption and viscoelasticity of thermosetting IC packaging polymer," International Conference on Electronic Packaging Technology, ICEPT 2006, 2006, pp:161-165.

[9]. Ma, X.S., Jansen, K.M.B., Ernst, L.J., and Zhang, G.Q., "Hygroscopic effects on swelling and viscoelasticity of electronic packaging epoxy," International Conference on Electronic Packaging Technology, ICEPT 2006, 2006, pp:262-266.